PASSIVE VECTOR TURBULENCE

HEIKKI ARPONEN

Academic dissertation

To be presented, with the permission of the Faculty of Science of the University of Helsinki, for public criticism in Auditorium XII, University Main Building, on June 6th, 2009, at 10 a.m.

Department of Mathematics and Statistics
Faculty of Science
University of Helsinki
2009

ISBN 978-952-92-5602-0 (Paperback)
ISBN 978-952-10-5595-9 (PDF)
http://ethesis.helsinki.fi

Helsinki University Print
Helsinki 2009

Acknowledgements

I would like to thank my supervisor Antti Kupiainen for his guidance, support and the possibility of finishing this work in his research group. I am also deeply grateful to Paolo Muratore-Ginanneschi for his help and insight in all the "passive" matters concerning this work. I would also like to convey my gratitude to the prereaders Juha Honkonen and Nikolai Antonov for fulfilling their parts despite the rather tight schedule.

I would also like to thank my family and especially my parents (my father posthumously) for their at least partially successful efforts in my upbringing, despite the odds. Heartfelt thanks also to to Jonna for her patience during the writing of this thesis. Just a couple more minutes and the computer is yours!

This work was facilitated by the financial support from Academy of Finland, TEKES, Helsinki University and the Vilho, Yrjö and Kalle Väisälä foundation.

Heikki Arponen,
April 2009
Helsinki

List of included articles

This thesis consists of the following three articles:

(I) **Dynamo effect in the Kraichnan magnetohydrodynamic turbulence**
Heikki Arponen, Peter Horvai
J. Stat. Phys., **129**(2):205-239, Oct 2007

(II) **Anomalous scaling and anisotropy in models of passively advected vector fields**
Heikki Arponen
Phys. Rev. E, **79** (4):056303,2009

(III) **Steady state existence of passive vector fields under the Kraichnan model**
Heikki Arponen
Prepared manuscript

Contents

1

1. Introduction

Traces of turbulence can be observed in several everyday situations, ranging from large scale behavior such as storms and windy weather, to smaller scales such as a beverage inside a shaken bottle, or flow of water from a tap. As opposed to smooth, slowly varying behavior of near equilibrium systems, turbulent phenomena are better described by chaos, complexity and disorder. It seems however reasonable to expect turbulent systems to be described by some general laws of fluid mechanics, although it is quite obvious even to the naked eye that a turbulent flow cannot be represented by some well behaved solution of a partial differential equation.

The scientific problem of turbulence is often said to be the last great unsolved problem of classical physics, having puzzled scientist for centuries. The reason for its obscurity is not because we don't know the underlying physical laws that describe it, but because we do not know how to interpret them. Indeed, the equations that are supposed to describe turbulence have been known since the 19th century after the works of C-L. Navier and G.G. Stokes, yet their solution is in general unknown.

It is the purpose of this introductory section to clarify this apparent discrepancy, and to explain the modest contribution of the present author in it's understanding.

The behavior of constant density fluid and gas flow is adequately described by the incompressible Navier-Stokes equations,

$$\begin{aligned} \partial_t \bar{v}(t,\bar{x}) + \bar{v}(t,\bar{x}) \cdot \nabla \bar{v}(t,\bar{x}) - \nu \Delta \bar{v}(t,\bar{x}) + \nabla p(t,\bar{x}) &= 0 \\ \nabla \cdot \bar{v}(t,\bar{x}) &= 0, \end{aligned} \tag{1}$$

which is to be solved for the vector field $\bar{v}(t,\bar{x})$. The scalar field $p(t,\bar{x})$, denoting the pressure, can be solved in terms of $\bar{v}$ by the using the latter incompressibility equation. The parameter ν is the kinematic viscosity of the fluid. The vector field $\bar{v}$ then describes the velocity of an infinitesimal fluid element at time t and at position $\bar{x}$.

Using the equations and some characteristics of the system under consideration, one can derive a number quantifying the flow behavior, known as the Reynolds number,

$$Re = \frac{LV}{\nu}.$$

Here L stands for the general size of the system, V is the average speed of the fluid and ν is the kinematic viscosity. The laminar and turbulent flows correspond respectively to small and large Reynolds numbers. Perhaps the most familiar everyday example of the two cases can be observed in running water from a tap: open the tap a little and the flow is smooth, calm and transparent, but as the tap is opened to its fullest, the flow becomes very complicated and opaque. Indeed, it seems that in the turbulent regime (almost) all predictability is lost. On the mathematical side, the Navier-Stokes equations are notoriously difficult to handle. In three dimensions even the existence of solutions at all times is poorly understood.[1]

The differences between laminar (or nearly laminar) and turbulent flows can also be described by injecting dye into the fluid, or by dropping a test particle in it and observing its motion, as depicted in Fig. 1. In science literature these methods are known as the passive scalar and passive tracer, respectively. In a laminar flow the test particle is seen to follow a rather smooth and predictable path, whereas in a turbulent flow the path seems almost completely random: even if the particles start very close to each other, they quickly disperse away from each other. This is typical to what is known in science as chaotic dynamics. Corresponding behavior can also be observed in the behavior of the dye. In a laminar flow, the dye flows smoothly and decays slowly due to thermal diffusion. In a turbulent flow the dye is mixed and stirred into a mess with no discernible features. All this might lead one to conclude that we have failed in one of the two main goals of theoretical physics: to predict behavior of physical systems under known laws of nature.

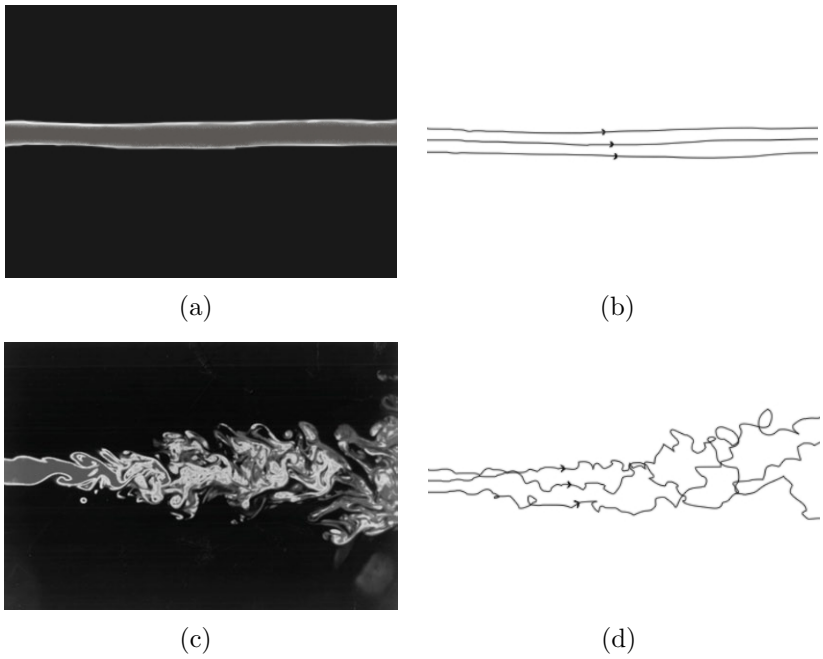

FIGURE 1. Comparison of laminar and turbulent flows. (a) shows a passive scalar in a laminar flow and in (b) a few paths of a tracer particles are sketched. Figures (c) (Prasad and Sreenivasan) and (d) show the same but in a turbulent flow.

The apparent randomness in turbulent flows quite naturally leads to the hypothesis that perhaps in some way it *is* random. We may compare the situation to a much more simple case of a small test particle suspended in a fluid that is in equilibrium. The particle seems to undergo apparently random motion due to collisions of the fluid molecules. Such behavior was observed and documented by a Scottish botanist Robert Brown in the beginning of the 19th century, after whom the mathematical description of *Brownian motion* was named. Although seemingly random, the molecules in the fluid certainly follow the Newtonian laws of mechanics. It's just that there are so many of them that it is quite difficult to describe the behavior of the test particle, starting from first principles. We may in fact fare much better by assuming the collisions to occur at random, prescribed by some probability distribution. So although we are unable to predict exactly the motion of the particle, the probabilistic theory tells us it's exact *statistical* properties. For example in Brownian motion, the average distance squared of a particle grows linearly in time, i.e. $\langle \bar{r}(t)^2 \rangle \propto t$. All the other average quantities

FIGURE 2. A trajectory of a Brownian motion.

can be expressed similarly. Considering the apparent randomness of test particle paths in turbulent fluids, it seems reasonable to attempt to formulate the problem in a completely statistical manner as with Brownian motion, at least in the case of fully developed turbulence in the limit $Re \to \infty$. Keeping L and V fixed, this amounts to the limit of vanishing viscosity ν. One attempt in this direction is to add a random forcing term in the Navier-Stokes equations, describing e.g. shaking of the fluid container, and by trying to describe the behavior of the velocity field $\bar{v}$ by trying to compute its averages. We can for example ask what is the average value of the velocity field $\bar{v}$ in a given position x at time t. We show in Fig. (3) a typical snapshot of a turbulent fluid where the arrows depict the velocity field $\bar{v}$. In practice we can do this by calculating a time average $\frac{1}{T}\int_0^T \bar{v}(t+s,\bar{x})ds$ over some sufficiently long time interval T. It is a rather general property of chaotic behavior that such time averages equal averages over some probability distributions, in which case we equate the time averages with *ensemble* averages, $\frac{1}{T}\int_0^T \bar{v}(t+s,\bar{x})ds = \langle \bar{v}(t,\bar{x})\rangle$. This relies on the assumption of a *statistical steady state*, which roughly speaking means that the time averages taken e.g. a few hours apart yield the same results. We can also consider conditional probabilities by asking what is the probability

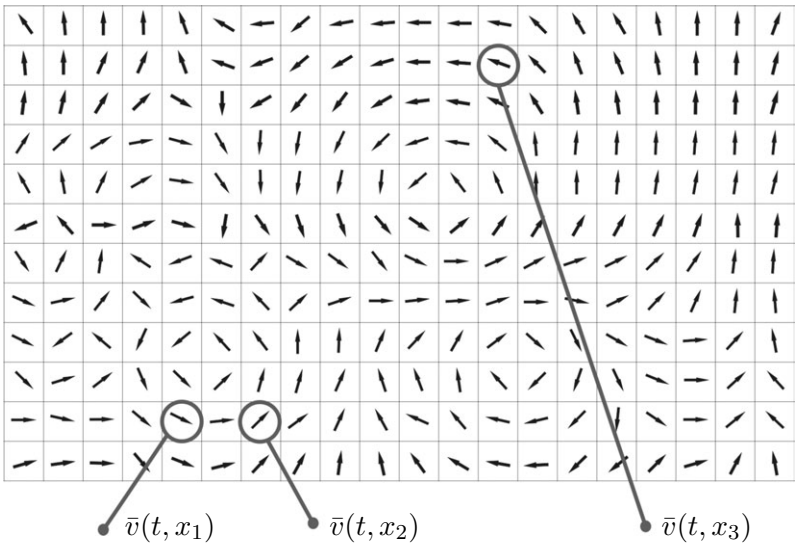

FIGURE 3. A typical snapshot of a velocity field configuration at a time t (approximated as a lattice). Fields close to each other (at x_1 and x_2) are more strongly correlated than faraway vector fields (x_1 or x_2 and x_3).

distribution of $\bar{v}(t, \bar{x}')$, given the statistics of $\bar{v}(t, \bar{x})$, which is connected to the pair correlation function $\langle \bar{v}(t, \bar{x}) \bar{v}(t, \bar{x}') \rangle$.[1] This construction is naturally generalized to the n -point correlation functions of n vector fields. Knowing all the correlation functions amounts to knowing the exact statistics of the problem. Usually one is however satisfied in understanding the properties of the so called (longitudinal) structure functions, defined as

$$S_n(r) = \langle [(\bar{v}(t, \bar{x} + \bar{r}) - \bar{v}(t, \bar{x})) \cdot \hat{r}]^n \rangle. \tag{2}$$

Note that the structure function is assumed to depend of the distance between the fields alone. It relies on the subtle assumptions that far away from the boundaries of the physical system, the behavior is homogeneous and isotropic, i.e. there is no preferred direction or place inside the flow. This is a general manifestation of a symmetry of the system: we say that the flow is invariant under translations and rotations if the laws remain the same at different locations and directions. In the limit of vanishing viscosity $\nu \to 0$, the Navier-Stokes equations are also believed to be scale invariant at scales much smaller than the characteristic forcing scale L_f: if $\bar{v}(t, \bar{x})$ is a solution to the equation, then so is $\tilde{v}(t, \bar{x}) \doteq \lambda^{-\zeta} \bar{v}(\lambda^{1+\zeta} t, \lambda \bar{x})$, where λ is a scaling parameter

[1] Of course, this could be generalized to non equal times as well.

and ζ is some unknown scaling exponent. Applying this blindly to the structure function would give

$$S_n(r) = C_n r^{n\zeta} \tag{3}$$

with some n dependent constant factor C_n. Of course, this is not going to be very helpful until we find out a way to determine the scaling exponent α.

The modern study of turbulence is considered to have begun in 1941 after the works of Andrey Nikolaevich Kolmogorov in his seminal paper [2], where he obtained the exact result for the $n = 3$ structure function, implying that the scaling exponent is $\zeta = 1/3$. However this is true only for the $n = 3$ case. Indeed, it has been observed in experiments and in numerical simulations that the scaling exponent actually grows slower than linearly as a function of n. This peculiar scaling property is broadly defined as *anomalous scaling*[2], and its study is at the center stage of contemporary turbulence research. The reason for the anomaly is that the limits $\nu \to 0$ and $L_f \to \infty$ are singular, and therefore require a more sophisticated analysis. These aspects will however not be further pursued here. Suffice it to say that the problem is far from being solved despite a multitude of more or less successful attempts.

It seems reasonable to expect that anomalous scaling of the velocity correlation functions should also manifest as anomalous scaling of the passive scalar and tracer correlation functions. What is not at all obvious is the fact that these passive quantities exhibit anomalous scaling even for nonanomalous velocity statistics, as observed by Robert Kraichnan in the sixties [3]. Kraichnan studied the anomalous scaling problem via the passive scalar equation (to be defined below), where the velocity statistics were prescribed as a mean zero, gaussian velocity field determined via the pair correlation function

$$\langle v_i(t, \bar{x} + \bar{r}) v_j(t', \bar{x}) \rangle = \delta(t - t') D_{ij}(\bar{r}, L), \tag{4}$$

where $\delta(t)$ is the Dirac delta function and D_{ij} is a divergence free tensor field that scales as $\propto r^{\xi}$ with ξ between zero and two.[3] The model incorporates an "integral scale" L, which describes the size of the system. This model can hardly be deemed a realistic model of fully developed turbulence because 1) it is Gaussian, 2) it is completely decorrelated in time due to the Dirac delta function and 3) because (in three dimensions) it is not even a steady state for physical values of ξ, as will be

[2]It should be pointed out that usually the term "anomalous scaling" is used to describe noncanonical scaling, and the different scaling exponents of different structure functions is known as multiscaling.

[3]More exactly, the structure function exhibits this scaling in the limit $L \to \infty$.

discovered in the last of the papers in the present thesis. It will however provide us with important insight on the physical mechanism of anomalous scaling.

The passive scalar equation is

$$\partial_t \theta(t,\bar{x}) + \bar{v}(t,\bar{x}) \cdot \theta(t,\bar{x}) - \kappa \Delta \theta(t,\bar{x}) = f_L(t,\bar{x}), \tag{5}$$

where κ is a small molecular diffusion constant due to thermal noise, and f_L is a (Gaussian) pumping term acting on a characteristic length scale L_f, designed to counter the eventual dissipation of the scalar. Considering the inertial range asymptotic behavior with $l_\kappa < r < L$ amounts to sending $l_\kappa \to 0$ and $L \to \infty$, (where l_κ is a length scale depending on κ). We still have the finite forcing length scale L_f, which will either be sent to infinity in the case of large scale forcing, or to zero in the case of small scale forcing. The problem is then exactly solvable [4], and one can show that in certain situations, the passive scalar structure functions exhibit anomalous scaling (for $n > 2$) [5, 6, 7, 8]. The existence of anomalous scaling for large scale forcing was traced to the existence of "zero modes", which are certain statistical integrals of motion of the passive scalar. They arise by applying the passive scalar equations of motion (5) to the correlation functions, and by requiring them to be constant in time. Similar phenomena was observed also for the small scale forcing [9], i.e. when $L_f \ll r$. Curiously, it was also observed in [10] that in the case of a small scale forcing, the isotropy hypothesis does not hold for a general class of physically realistic forcings: there are now anomalous scaling exponents of the anisotropic sectors that dominate the large scale behavior over the isotropic exponents.

Inspired by the success of the passive scalar problem, it was natural to extend the study of Kraichnan advected passive quantities to vector fields. The advantage of the passive vector problem is that already the pair correlation function is anomalous. These models include e.g. the magnetohydrodynamic model (see e.g. [11]), the linear pressure model a.k.a the passive vector (see e.g. [12, 13, 14]) and the linearized Navier-Stokes equations. In [15] a specific model dubbed the $\mathcal{A}$ -model, was conceived, that incorporates all of the above models via a parameter $\mathcal{A}$.

It is the central theme of the present thesis to study various aspects of the $\mathcal{A}$ model (starting by demoting $\mathcal{A}$ to a). The first paper is concerned with the so called "dynamo effect" of magnetohydrodynamic turbulence. The purpose of the paper is to study the circumstances under which the steady state assumption is not valid, which manifests as an unbounded growth of the pair correlation function, and to obtain the growth rate at which the dynamo grows. The problem was considered in the limits of zero and infinite Prandtl numbers, where the Prandtl

number describes the relative strengths of magnetic vs. thermal diffusion effects. The dynamo effect has been studied before in the context of the Kraichnan model, although the results have in the end been numerical. The purpose of the paper was to present an analytical solution to the problem, although the scheme used was rather approximative in nature. The problem was also extended to arbitrary dimension, and it was observed that the existence of the dynamo depends on the space dimension.

The second paper consists of a study of the pair correlation function steady state for general values of a. Both small and large scale forcings are considered with the goal of uncovering the possible anomalous behavior. We also considered anisotropic forcing in the hopes of finding traces of anisotropy dominance, as in the large scale passive scalar problem. The small scale problem has been studied before in several cases (see the references above and in the paper), although not much has been done in the case of the linearized Navier-Stokes equation. The large scale results are completely new, and although the large scales are in general anomalous, the anisotropy dominance in these models was found out to be rather an exception than a rule. One should note that a simple zero mode analysis is not enough to obtain such results, but instead one must genuinely invert the zero mode operator. In other words, one also needs to determine whether a zero mode is actually present in a particular solution or not, which in turn depends on the forcing. In this sense all the passive vector findings are also new, as previous studies have been content with only finding the zero modes.

The third paper is concerned with the important question of existence of the steady state solution, without which all the steady state results would only have conjectural value. Methods similar to the previous paper were employed to find a critical value of the roughness exponent ξ below which the steady state exists in any dimension d. Previously the existence problem has only been addressed in the magnetohydrodynamic and linear pressure model cases only. The iteration formulae presented in the paper also seems to be an efficient tool for a more general study of nonlocal linear partial differential equations.

References

[1] C. L. Fefferman. Existence and smoothness of the navier-stokes equation. `http://www.claymath.org/millennium/Navier-Stokes_Equations/navierstokes.pdf`.

[2] A. N. Kolmogorov. The local structure of turbulence in incompressible viscous fluid for very large reynolds numbers. *Proc. USSR Acad. Sci.*, 30:299–303, 1941.

[3] R. H. Kraichnan. Small-scale structure of a scalar field convected by turbulence. *Phys. Fluids*, 11:945, 1968.

[4] K. Gawędzki and A. Kupiainen. Universality in turbulence: an exactly soluble model. `http://arxiv.org/abs/chao-dyn/9504002`.

[5] Robert H. Kraichnan. Anomalous scaling of a randomly advected passive scalar. *Phys. Rev. Lett.*, 72(7):1016–1019, Feb 1994.

[6] K. Gawędzki and A. Kupiainen. Anomalous scaling of the passive scalar. *Phys. Rev. Lett.*, 75(21):3834–3837, Nov 1995.

[7] B. Shraiman and E. Siggia. Anomalous scaling of a passive scalar in turbulent flow. *C.R. Acad. Sci.*, 321:279–284, 1995.

[8] M. Chertkov, G. Falkovich, I. Kolokolov, and V. Lebedev. Normal and anomalous scaling of the fourth-order correlation function of a randomly advected scalar. *Phys. Rev. E*, 52:4924–4941, 1995.

[9] G. Falkovich and A. Fouxon. Anomalous scaling of a passive scalar in turbulence and in equilibrium. *Phys. Rev. Lett.*, 94(21):214502, 2005.

[10] A. Celani and A. Seminara. Large-scale anisotropy in scalar turbulence. *Phys. Rev. Lett.*, 96(18):184501, 2006.

[11] H. Arponen and P. Horvai. Dynamo effect in the kraichnan magnetohydrodynamic turbulence. *J. Stat. Phys.*, 129(2):205–239, Oct 2007.

[12] L. Ts. Adzhemyan, N. V. Antonov, and A. V. Runov. Anomalous scaling, nonlocality, and anisotropy in a model of the passively advected vector field. *Phys. Rev. E*, 64(4):046310, Sep 2001.

[13] Itai Arad and Itamar Procaccia. Spectrum of anisotropic exponents in hydrodynamic systems with pressure. *Phys. Rev. E*, 63(5):056302, Apr 2001.

[14] R. Benzi, L. Biferale, and F. Toschi. Universality in passively advected hydrodynamic fields: the case of a passive vector with pressure. *The European Physical Journal B*, 24:125, 2001.

[15] L. Ts. Adzhemyan, N. V. Antonov, A. Mazzino, P. Muratore-Ginanneschi, and A. V. Runov. Pressure and intermittency in passive vector turbulence. *EPL (Europhysics Letters)*, 55(6):801–806, 2001.

2. Dynamo effect in the Kraichnan magnetohydrodynamic turbulence

2

J Stat Phys (2007) 129: 205–239
DOI 10.1007/s10955-007-9399-5

Dynamo Effect in the Kraichnan Magnetohydrodynamic Turbulence

Heikki Arponen · Peter Horvai

Received: 26 October 2006 / Accepted: 9 August 2007 / Published online: 28 September 2007

Abstract The existence of a dynamo effect in a simplified magnetohydrodynamic model of turbulence is considered when the magnetic Prandtl number approaches zero or infinity. The magnetic field is interacting with an incompressible Kraichnan-Kazantsev model velocity field which incorporates also a viscous cutoff scale. An approximate system of equations in the different scaling ranges can be formulated and solved, so that the solution tends to the exact one when the viscous and magnetic-diffusive cutoffs approach zero. In this approximation we are able to determine analytically the conditions for the existence of a dynamo effect and give an estimate of the dynamo growth rate. Among other things we show that in the large magnetic Prandtl number case the dynamo effect is always present. Our analytical estimates are in good agreement with previous numerical studies of the Kraichnan-Kazantsev dynamo by Vincenzi (J. Stat. Phys. 106:1073–1091, 2002).

Keywords Dynamo · Magnetohydrodynamic · Turbulence · Kraichnan-Kazantsev

1 Introduction

The study of the dynamo effect in short time correlated velocity fields was initiated by Kazantsev in [15], where he derived a Schrödinger equation for the pair correlation function of the magnetic field. However, that equation was still quite difficult to analyze except in some special cases. The large magnetic Prandtl number Batchelor regime was studied by Chertkov et al. [5], with methods of Lagrangian path analysis of [4, 21]. However this approach is valid only for limited time (until the finiteness of the velocity field's viscous scale becomes relevant) even for infinitesimal magnetic fields. For the problem involving the full inertial range of the advecting velocity field, Vergassola [22] has obtained the zero

H. Arponen (✉)
Department of Mathematics and Statistics, Helsinki University, P.O. Box 68, 00014 Helsinki, Finland
e-mail: heikki.arponen@helsinki.fi

P. Horvai
Science & Finance, Capital Fund Management, 6-8 Bd Haussmann, 75009 Paris, France

mode exponents in the inertial range (and hence a criterion for presence of the dynamo). Vincenzi [23] obtained numerically (in three dimensional space) the dynamo growth rate at finite magnetic Reynolds and Prandtl numbers. However, until now, an analytical method to obtain the dynamo growth rate was lacking.

Our objective in this paper is to exhibit such a method, derived from the work in [11]. This allows us to better understand the dynamo effect. Last but not least we obtain good approximations to the numerical computation results of Vincenzi.

1.1 From Full MHD to the Kraichnan-Kazantsev Model

Magnetohydrodynamics (MHD) is usually described by the Navier-Stokes equations for a conducting fluid coupled to the magnetic field in the following way:

$$\partial_t \boldsymbol{v} + (\boldsymbol{v}\cdot\nabla)\boldsymbol{v} - \frac{1}{\mu_f \rho_f}(\boldsymbol{B}\cdot\nabla)\boldsymbol{B} + \frac{1}{2\mu_f\rho_f}\nabla(|\boldsymbol{B}|^2) + \frac{1}{\rho_f}\nabla p = \nu_f \Delta \boldsymbol{v} + \boldsymbol{F}, \quad (1.1)$$

$$\partial_t \boldsymbol{B} + (\boldsymbol{v}\cdot\nabla)\boldsymbol{B} - (\boldsymbol{B}\cdot\nabla)\boldsymbol{v} = \frac{1}{\mu_f\sigma_f}\Delta \boldsymbol{B}, \quad (1.2)$$

$$\nabla\cdot\boldsymbol{v} = 0, \quad (1.3)$$

$$\nabla\cdot\boldsymbol{B}, = 0, \quad (1.4)$$

where $\boldsymbol{v}$ and $\boldsymbol{B}$ are the fluid velocity and magnetic (induction) fields respectively, ρ_f is the density of the fluid, μ_f is its magnetic permeability, σ_f its conductivity and ν_f its viscosity, p is the pressure and $\boldsymbol{F}$ may be some externally imposed volume force acting on the fluid. These equations already take into account the so called MHD approximation, whereby the fluid is supposed to be locally charge neutral everywhere, the displacement current is supposed negligible.

In the current paper we will be interested by the growth of an initial seed magnetic field, so we can suppose $\boldsymbol{B}$ to be infinitesimal above. Hence the terms involving $\boldsymbol{B}$ in (1.1) may be neglected (all the more so that they are quadratic). This turns the problem into a passive advection one for the magnetic field (i.e. the magnetic field doesn't influence the evolution of the velocity field), while the velocity field evolves according to the Navier-Stokes equations with some external forcing (independent of the magnetic field).

Since in the passive advection case the velocity field evolves autonomously, one can define for it as usual the Reynolds number $Re = L_v V/\nu_f$, where L_v is the integral scale (scale of largest wavelength excited mode) of the velocity field and V is the typical velocity magnitude at these scales. One can also define a magnetic Reynolds number as $Re_M = VL_v/\kappa$, where $\kappa = 1/(\mu_f\sigma_f)$ is the magnetic diffusivity. Note that L_v is the integral scale of the *velocity* field and V is the *velocity* at such a scale. We will be mostly working in the case where both Reynolds numbers are very large, more specifically in the case when L_v is sent to infinity.

To give an intuitive idea of the dynamo effect, note that, for low values of the magnetic diffusivity (low in the sense that the magnetic Reynolds number based on it is high), the magnetic field lines are approximately frozen into the fluid and they are typically stretched by the flow, due to the term $\boldsymbol{B}\cdot\nabla\boldsymbol{v}$ appearing in (1.2). This process may lead to an exponential growth in time of the magnetic field. If there is such a growth then we talk about turbulent dynamo. If the seed magnetic field is unable to grow, and instead it decays, then we say that there is no dynamo. We point out that this definition is based merely on a linear stability analysis, and does not exclude the possibility of persistent magnetic fields starting from a finite size perturbation, even if the system doesn't show dynamo effect for infinitesimal magnetic fields (reminiscent of the case of hydrodynamic turbulence in a pipe flow).

In addition, we wish to study the situation where the velocity field is turbulent, or in other terms the Reynolds number Re is high. Then, using real solutions of the Navier-Stokes equations is only possible for numerical computations.

To deal analyitically with the passive advection problem, a typical way is to resort to some statistical model of the velocity field. We choose here to use the Kraichnan-Kazantsev model [15, 16], because it readily yields to analytical treatment of passive advection [9] and is well understood (see e.g. [3, 8] for a general review, or [1, 12, 22, 23] dealing specifically with the passive turbulent dynamo).

Our problem is now reduced to studying the evolution of $\boldsymbol{B}$ described by

$$\partial_t \boldsymbol{B} + \boldsymbol{v} \cdot \nabla \boldsymbol{B} - \boldsymbol{B} \cdot \nabla \boldsymbol{v} = \kappa \Delta \boldsymbol{B}, \tag{1.5}$$

$$\nabla \cdot \boldsymbol{B} = 0, \tag{1.6}$$

where $\boldsymbol{v}$ is given according to the Kraichnan-Kasantsev model presented below. We will derive an equation for the pair correlation function

$$\left\langle B_i(t, \boldsymbol{r}) B_j(t, \boldsymbol{r}') \right\rangle \tag{1.7}$$

averaged over the velocity statistics, and attempt to solve it using a certain approximation scheme, which will be explained at the end of this introduction.

The possible unbounded growth—as we shall see—of the magnetic field's pair correlation function, depending on the roughness parameter ξ (to be defined below) of the velocity field and the magnetic Prandtl number, is in contrast with the passive scalar case, where in the absence of external forcing the dynamics was always dissipative [10, 14, 18].

1.2 Definition of Kraichnan Model

The Kraichnan model is defined as a Gaussian, mean zero, random velocity field, with pair correlation function

$$\begin{aligned} \left\langle v_i(t, \boldsymbol{r}) v_j(t', \boldsymbol{r}') \right\rangle &= \delta(t - t') D_0 \int \mathrm{d}\!\!^{-}\boldsymbol{k} \frac{e^{i\boldsymbol{k}\cdot(\boldsymbol{r}-\boldsymbol{r}')}}{|\boldsymbol{k}|^{d+\xi}} f(l_v|\boldsymbol{k}|) P_{ij}(\boldsymbol{k}) \\ &=: \delta(t - t') D_{ij}(\boldsymbol{r} - \boldsymbol{r}'; l_v), \end{aligned} \tag{1.8}$$

with $\mathrm{d}\!\!^{-}\boldsymbol{k} := \frac{d^d k}{(2\pi)^d}$ and

$$P_{ij}(\boldsymbol{k}) = \delta_{ij} - \frac{k_i k_j}{k^2} \tag{1.9}$$

to guarantee incompressibility. It is evident that D_{ij} is homogenous and isotropic. We briefly discuss below the meanings of ξ, l_v and f.

The parameter ξ, such that $0 \leq \xi \leq 2$, describes the roughness of the velocity field. The choice of $\xi = 4/3$ would correspond to the Kolmogorov scaling of equal-time velocity structure functions. However there is no evident prescription for ξ that would best reproduce a real turbulent velocity field, and even for the case under study of passive advection of a magnetic field, it is not clear what ξ should be considered.

The function f is an ultraviolet cutoff, which simulates the effects of viscosity. It decays faster than exponentially at large k, while $f(0) = 1$ and $f'(0) = 0$. For example we could choose $f(l_v k) = \exp(-l_v^2 k^2)$, although the explicit form of the function is not needed below.

In the usual case without the cutoff function f the velocity correlation function behaves as a constant plus a term $\propto r^{\xi}$, but in this case we have an additional scaling range for $r \ll l_\nu$ where it scales as $\propto r^2$. The length scale l_ν can be used to define a viscosity ν or alternatively one can use κ to define a length scale l_κ. We can then define the Prandtl number[1] measuring the relative effects of viscosity and diffusivity as $P = \nu/\kappa$. Note that the integral scale was assumed to be infinite, i.e. there is no IR cutoff.

1.3 Plan of the Paper

The goal of the present paper is to extend previous considerations by introducing a set of approximate equations, which admit an exact analytical solution. The analysis proceeds along the same lines as in a previous paper for a different problem by one of us [11]. The problem in the analysis can be traced to existence of length scales dividing the equation in different scaling ranges. In our case there are two such length scales, one arising from the diffusivity κ and the other from the UV cutoff in the velocity correlation function. As will be seen in Appendix 1, what one actually needs in the analysis is the velocity *structure* function defined as

$$\begin{aligned}
&\frac{1}{2}\big\langle (v_i(t,\boldsymbol{r}) - v_i(t,\boldsymbol{r}'))(v_j(t',\boldsymbol{r}) - v_j(t',\boldsymbol{r}'))\big\rangle \\
&\quad = \delta(t-t')D_0 \int \mathrm{d}\boldsymbol{k}\, \frac{1 - e^{i\boldsymbol{k}\cdot(\boldsymbol{r}-\boldsymbol{r}')}}{|\boldsymbol{k}|^{d+\xi}} f(l_\nu|\boldsymbol{k}|) P_{ij}(\boldsymbol{k}) \\
&\quad =: \delta(t-t') d_{ij}(\boldsymbol{r}-\boldsymbol{r}'; l_\nu).
\end{aligned} \tag{1.10}$$

This is all one needs to derive a partial differential equation for the pair correlation function of $\boldsymbol{B}$, but it will still be very difficult to analyze. Hence the approximation, which proceeds as follows:

(1) Consider the asymptotic cases where r is far from the length scales l_κ and l_ν with the separation of the length scales large as well. There are therefore three ranges where the equation is simplified into a much more manageable form. The equations are of the form $\partial_t H - \mathcal{M}H = 0$, where $\mathcal{M}$ is a second order differential operator with respect to the radial variable. We then consider the eigenvalue problem $\mathcal{M}H = zH$.
(2) By a suitable choice of constant parameters in terms of the length scales, we can adjust the differential equations to match in different regions as closely as possible. Solving the equations, we obtain two independent solutions in all ranges.
(3) We match the solutions by requiring continuity and differentiability at the scales l_ν and l_κ. Also appropriate boundary conditions are applied.
(4) According to standard physical lore, the form of cutoffs do not affect the results when the cutoffs are removed. In addition to l_ν, we can interpret l_κ as a cutoff. Therefore we conjecture that the solution approaches the exact one for small cutoffs. We also expect the qualitative results, such as the existence of the dynamo effect, to apply for finite cutoffs as well.

For concreteness, suppose that $\mathcal{M}$ is of the form

$$\mathcal{M} = a(l_\nu, l_\kappa, r)\partial_r^2 + b(l_\nu, l_\kappa, r)\partial_r + c(l_\nu, l_\kappa, r). \tag{1.11}$$

[1] We choose to write the Prandtl number as P instead of the usual Pr since it appears so frequently in formulae.

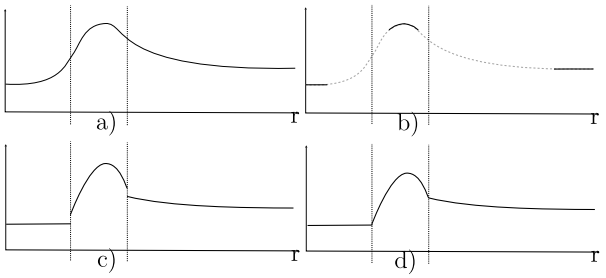

Fig. 1 A sketch of the procedure of approximating the example equation. The *dashed vertical lines* correspond to either one of the length scales l_ν and l_κ with pictures (**a**), a plot of the "real" coefficient, which depends of the cutoff function (and is really unknown), (**b**) an approximate form obtained by taking r far from the length scales (*dotted parts of the lines* are dropped), (**c**) the approximations extended to cover all $r \in \mathbb{R}$, and (**d**) adjusting the coefficients to match at the scales l_ν and l_κ. For r much larger than the cutoffs, the error due to the approximation is lost

The coefficients are some functions of the length scales l_ν and l_κ and the radial variable r. In general, solving the eigenvalue problem for such a differential equation is not possible except numerically. However, we can approximate the coefficients in the asymptotic regions when r is far from the length scales. The asymptotic coefficients are all power laws and solving the equations becomes much easier. Figure 1 illustrates this procedure corresponding to steps (1) and (2) for any of the coefficients.

After some preparations, we begin by writing down the equation for the pair correlation function of the magnetic field using the Itô formula. The derivation can be found in Appendix 1. The equation is of third order in the radial variable, but it can be manipulated into a second order equation by using the incompressibility condition. In Sect. 2 the approximate equations will be derived when $\nu \ll \kappa$ and $\kappa \ll \nu$, or Prandtl number small or large, respectively. We use adimensional variables for sake of convenience and clarity. The focus of the paper is mainly on the existence of the dynamo effect and its growth rate. Therefore we consider the spectrum of $\mathcal{M}$. By a spectral mapping theorem, we relate the spectra of $\mathcal{M}$ and the corresponding semigroup $e^{t\mathcal{M}}$. It is then evident that if the spectrum of $\mathcal{M}$ contains a positive part, there is exponential growth, i.e. a dynamo effect.

1.4 Structure Function Asymptotics

Due to the viscous scale l_ν in the structure function (1.10), there are two extreme scaling ranges $r \gg l_\nu$ (inertial range) and $r \ll l_\nu$. For $r \gg l_\nu$ we can set $l_\nu = 0$ in (1.10) and obtain

$$d_{ij}^{>}(\boldsymbol{r}) := D_1 r^\xi \left((d+\xi-1)\delta_{ij} - \xi \frac{r_i r_j}{r^2} \right), \tag{1.12}$$

where

$$D_1 = \frac{D_0 C_\infty}{(d-1)(d+2)}, \quad C_\infty = \frac{\Gamma(1-\xi/2)}{2^{d+\xi-2}\pi^{d/2}\Gamma(d/2+\xi/2)}. \tag{1.13}$$

The second case corresponds to the viscous range, which is to leading order in r:

$$d_{ij}^{<}(\boldsymbol{r}) := D_2 l_\nu^{\xi-2} r^2 \left((d+1)\delta_{ij} - 2\frac{r_i r_j}{r^2} \right), \tag{1.14}$$

where

$$D_2 = \frac{D_0 C_0}{(d-1)(d+2)}, \quad C_0 = \int \mathrm{d}\boldsymbol{k} \frac{f(k)}{k^{d+\xi-2}}. \tag{1.15}$$

We see that the viscous range form (1.14) can be obtained from (1.12) by a replacement $\xi \to 2$ and $D_1 \to D_2 l_\nu^{\xi-2}$. Note that by adjusting the cutoff function f we can also adjust D_2/D_1.

1.5 Incompressibility Condition

Due to rotation and translation invariance, the equal-time correlation function of $\boldsymbol{B}$ must be of the form

$$G_{ij}(t, |\boldsymbol{x} - \boldsymbol{x}'|) := \langle B_i(t, \boldsymbol{x}) B_j(t, \boldsymbol{x}') \rangle = G_1(t, r)\delta_{ij} + G_2(t, r)\frac{r_i r_j}{r^2}, \tag{1.16}$$

where $r = |\boldsymbol{x} - \boldsymbol{x}'|$. Additional simplification arises from the incompressibility condition $\partial_i G_{ij}(t, r) = 0$:

$$\partial_r G_1(t, r) = -\frac{1}{r^{d-1}} \partial_r (r^{d-1} G_2(t, r)). \tag{1.17}$$

The general solution of the incompressibility condition can be written as

$$\begin{cases} G_1(t, r) = r\partial_r H(t, r) + (d-1)H(t, r), \\ G_2(t, r) = -r\partial_r H(t, r). \end{cases} \tag{1.18}$$

In terms of a so far arbitrary function H. Alternatively, adding the above equations we may write

$$H(t, r) = \frac{1}{d-1} \left(G_1(t, r) + G_2(t, r) \right). \tag{1.19}$$

This observation leads to a considerable simplification in the differential equation for the correlation function: whereas the equations for G_1 and G_2 are of third order in r, we can use the above result to obtain a second order equation for H. Then we would get back to G through (1.18); for example we have for the trace of G:

$$G_{ii}(t, r) = (d-1) \left(r\partial_r H(t, r) + d H(t, r) \right), \tag{1.20}$$

although we refrain from doing this since H has the same spectral properties as G_{ii}.

2 Equations of Motion

The equation of motion for the pair correlation function is derived in Appendix 1:

$$\partial_t G_{ij} = 2\kappa \Delta G_{ij} + d_{\alpha\beta} G_{ij,\alpha\beta} - d_{\alpha j,\beta} G_{i\beta,\alpha} - d_{i\beta,\alpha} G_{\alpha j,\beta} + d_{ij,\alpha\beta} G_{\alpha\beta}. \tag{2.1}$$

The indices after commas are used to denote partial derivatives and we use the Einstein summation. For derivatives with respect to the radial variable r we will simply denote ∂_r. We will also try to avoid writing any arguments, unless it may cause confusion. By taking $r \gg l_\nu$

and $r \ll l_\nu$ we can use the approximations (1.12) and (1.14) to write the equation in the corresponding ranges. This is done for the quantity $H = (G_1 + G_2)/(d-1)$ in Appendix 1 as well, resulting in the equations

$$\partial_t H = \xi(d-1)(d+\xi)D_1 r^{\xi-2}H + \left[2(d+1)\kappa + (d^2-1+2\xi)D_1 r^\xi\right]\frac{1}{r}\partial_r H + \left[2\kappa + (d-1)D_1 r^\xi\right]\partial_r^2 H, \quad r \gg l_\nu, \tag{2.2}$$

and

$$\partial_t H = 2(d-1)(d+2)D_2 l_\nu^{\xi-2}H + \left[2(d+1)\kappa + (d^2+3)D_2 l_\nu^{\xi-2}r^2\right]\frac{1}{r}\partial_r H + \left[2\kappa + (d-1)D_2 l_\nu^{\xi-2}r^2\right]\partial_r^2 H, \quad r \ll l_\nu. \tag{2.3}$$

Simple dimensional analysis leads to the observation

$$[\kappa] = [D_1 r^\xi] = [D_2 l_\nu^{\xi-2} r^2], \tag{2.4}$$

where the brackets denote the scaling dimension of the quantities. We define the length scale l_κ as the scale below which the diffusive effects of κ become important. This will be done explicitly below for different Prandtl number cases. In general, one can write $\kappa = D_1 l_\nu^{\xi-p} l_\kappa^p$ for some $p \in (0, 2]$. Now one just needs to identify the dominant terms in the three scales divided by l_ν and l_κ. For sake of clarity, we choose to write these equations in adimensional variables. This can be done for example by defining $r = l\rho$ and $t = l^{2-\xi}\tau/D_1$ with l being a length scale. It turns out to be convenient to choose the larger of l_κ and l_ν as l. Since we deal with a stochastic velocity field with no intrinsic dynamics, we cannot, in principle, talk about viscosity. However, it is convenient to define a viscosity ν (of dimension length squared divided by time) by dimensional analysis from the length scale l_ν and the dimensional velocity magnitude D_1, giving a relationship between ν, l_ν and D_1 similar to what we would get in a dynamical model. We therefore define

$$\nu := D_1 l_\nu^\xi. \tag{2.5}$$

This permits us to define the Prandtl number in the standard manner as $P = \nu/\kappa$. We then consider the cases $P \ll 1$ and $P \gg 1$.

2.1 Small Prandtl Number

Now $\nu \ll \kappa$, and we choose as adimensional variables

$$\begin{cases} r = l_\kappa \rho, \\ t = \frac{l_\kappa^{2-\xi}}{D_1}\tau. \end{cases} \tag{2.6}$$

Note that the relation between l_κ and κ has not yet been determined. In these variables, (2.2) and (2.3) become

$$\partial_\tau H = \xi(d-1)(d+\xi)\rho^{-2+\xi}H + \left[2(d+1)\frac{\kappa}{D_1 l_\kappa^\xi} + (d^2-1+2\xi)\rho^\xi\right]\frac{1}{\rho}\partial_\rho H + \left[2\frac{\kappa}{D_1 l_\kappa^\xi} + (d-1)\rho^\xi\right]\partial_\rho^2 H, \quad \rho \gg l_\nu/l_\kappa \tag{2.7}$$

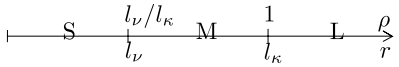

Fig. 2 Sketch of the scaling ranges at small Prandtl number

and

$$\begin{aligned}\partial_\tau H &= 2(d-1)(d+2)\frac{D_2}{D_1}\left(\frac{l_v}{l_\kappa}\right)^{\xi-2} H \\ &+ \left[2(d+1)\frac{\kappa}{D_1 l_\kappa^\xi} + (d^2+3)\frac{D_2}{D_1}\left(\frac{l_v}{l_\kappa}\right)^{\xi-2}\rho^2\right]\frac{1}{\rho}\partial_\rho H \\ &+ \left[2\frac{\kappa}{D_1 l_\kappa^\xi} + (d-1)\frac{D_2}{D_1}\left(\frac{l_v}{l_\kappa}\right)^{\xi-2}\rho^2\right]\partial_\rho^2 H, \quad \rho \ll l_v/l_\kappa. \end{aligned} \tag{2.8}$$

As mentioned above, we also consider $r \ll l_\kappa$ and $r \gg l_\kappa$, that is $\rho \ll 1$ and $\rho \gg 1$, respectively. There are now three regions in ρ, divided by l_v/l_κ and 1, with $l_v/l_\kappa \ll 1$. The regions, solutions and various other quantities will be labelled by S, M and L, corresponding to $\rho \ll l_v/l_\kappa$, $l_v/l_\kappa \ll \rho \ll 1$ and $1 \ll \rho$. See Fig. 2 for quick reference. Therefore the short range equation will be derived from (2.8) and the two others from (2.7). Consider for example explicitly the coefficients of $\partial_\rho^2 H$:

$$\begin{aligned} L:&\quad 2\frac{\kappa}{D_1 l_\kappa^\xi} + (d-1)\rho^\xi, \\ M:&\quad 2\frac{\kappa}{D_1 l_\kappa^\xi} + (d-1)\rho^\xi, \\ S:&\quad 2\frac{\kappa}{D_1 l_\kappa^\xi} + (d-1)\frac{D_2}{D_1}\left(\frac{l_v}{l_\kappa}\right)^{\xi-2}\rho^2. \end{aligned} \tag{2.9}$$

By definition of the length scale l_κ, in the region L the diffusivity is negligible and in the region M it is dominant, as it is in the region S since in there ρ approaches zero. The coefficients are then approximately

$$\begin{aligned} L:&\quad (d-1)\rho^\xi, \\ M:&\quad 2\frac{\kappa}{D_1 l_\kappa^\xi}, \\ S:&\quad 2\frac{\kappa}{D_1 l_\kappa^\xi}. \end{aligned} \tag{2.10}$$

Matching the coefficients of L, M at $\rho = 1$ provides us with a condition (matching between S and M gives nothing new)

$$d - 1 = 2\frac{\kappa}{D_1 l_\kappa^\xi}. \tag{2.11}$$

This is used as a definition of κ as $\kappa = \frac{1}{2}(d-1)D_1 l_\kappa^\xi$. Writing down the short range equation with the above approximations,

$$\partial_\tau H_S = 2(d-1)(d+2)\frac{D_2}{D_1}\left(\frac{l_v}{l_\kappa}\right)^{\xi-2} H_S + (d^2-1)\frac{1}{\rho}\partial_\rho H_S + (d-1)\partial_\rho^2 H_S, \tag{2.12}$$

by using the derived expression for the Prandtl number,

$$P = \frac{\nu}{\kappa} = \frac{2}{d-1}\left(\frac{l_\nu}{l_\kappa}\right)^\xi, \tag{2.13}$$

and by defining

$$\frac{D_2}{D_1} = \left(\frac{2}{d-1}\right)^{1-2/\xi} \tag{2.14}$$

(remember that D_2 could be adjusted by a choice of the cutoff function f, see (1.14) and below) a more neat expression is obtained for the short range equation. We can now write down all the equations:

$$\partial_\tau H_S = 2(d-1)(d+2)P^{1-2/\xi}H_S + (d^2-1)\frac{1}{\rho}\partial_\rho H_S + (d-1)\partial_\rho^2 H_S, \tag{2.15a}$$

$$\partial_\tau H_M = \xi(d-1)(d+\xi)\rho^{-2+\xi}H_M + (d^2-1)\frac{1}{\rho}\partial_\rho H_M + (d-1)\partial_\rho^2 H_M, \tag{2.15b}$$

$$\partial_\tau H_L = \xi(d-1)(d+\xi)\rho^{-2+\xi}H_L + (d^2-1+2\xi)\rho^{\xi-1}\partial_\rho H_L + (d-1)\rho^\xi\partial_\rho^2 H_L. \tag{2.15c}$$

2.2 Large Prandtl Number

Now $\nu \gg \kappa$, and we choose

$$\begin{cases} r = l_\nu \rho, \\ t = \frac{l_\nu^{2-\xi}}{D_1}\tau. \end{cases} \tag{2.16}$$

Then (2.2) and (2.3) for $r \gg l_\nu$ and $r \ll l_\nu$ become in the new variables

$$\partial_\tau H = \xi(d-1)(d+\xi)\rho^{-2+\xi}H + \left[2(d+1)\frac{\kappa}{D_1 l_\nu^\xi} + (d^2-1+2\xi)\rho^\xi\right]\frac{1}{\rho}\partial_\rho H + \left[2\frac{\kappa}{D_1 l_\nu^\xi} + (d-1)\rho^\xi\right]\partial_\rho^2 H, \quad \rho \gg 1 \tag{2.17}$$

and

$$\partial_\tau H = 2(d-1)(d+2)\frac{D_2}{D_1}H + \left[2(d+1)\frac{\kappa}{D_1 l_\nu^\xi} + (d^2+3)\frac{D_2}{D_1}\rho^2\right]\frac{1}{\rho}\partial_\rho H + \left[2\frac{\kappa}{D_1 l_\nu^\xi} + (d-1)\frac{D_2}{D_1}\rho^2\right]\partial_\rho^2 H, \quad \rho \ll 1. \tag{2.18}$$

The ranges S, M and L now correspond to $\rho \ll l_\kappa/l_\nu$, $l_\kappa/l_\nu \ll \rho \ll 1$ and $1 \ll \rho$, see Fig. 3. Note that equations in both S and M are now derived from (2.18). As before, we consider again the coefficients of $\partial_\rho^2 H$ and drop the terms $\propto \kappa$ in L and $\propto \rho^2$ in S. The diffusive effects are not dominant in the region M since $r \gg l_\kappa$, so we drop the $\propto \kappa$ term in M too.

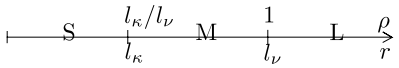

Fig. 3 Sketch of the scaling ranges at large Prandtl number

The approximative coefficients are then

$$\begin{aligned} L:&\quad (d-1)\rho^{\xi},\\ M:&\quad (d-1)\frac{D_2}{D_1}\rho^2,\\ S:&\quad 2\frac{\kappa}{D_1 l_\nu^{\xi}}. \end{aligned} \tag{2.19}$$

We then obtain two equations by matching the coefficient of L with M at $\rho = 1$ and of M with S at l_κ/l_ν:

$$\begin{aligned} &\frac{D_2}{D_1}(d-1) = (d-1),\\ &(d-1)\frac{D_2}{D_1}\left(\frac{l_\kappa}{l_\nu}\right)^2 = 2\frac{\kappa}{D_1 l_\nu^{\xi}}, \end{aligned} \tag{2.20}$$

with solutions

$$\begin{aligned} &D_2 = D_1,\\ &\kappa = \frac{d-1}{2} D_1 l_\kappa^2 l_\nu^{\xi-2}. \end{aligned} \tag{2.21}$$

The Prandtl number is in this case

$$P = \frac{2}{d-1}\left(\frac{l_\nu}{l_\kappa}\right)^2. \tag{2.22}$$

Note that one can obtain this from the small Prandtl number equation (2.13) by replacing $\xi \to 2$. This is a reflection of a more subtle observation that the large Prandtl number case for *any* ξ is similar to the small Prandtl number case with $\xi = 2$. We collect the equations using the above approximations,

$$\partial_\tau H_S = 2(d-1)(d+2)H_S + 2\frac{d+1}{P}\frac{1}{\rho}\partial_\rho H_S + \frac{2}{P}\partial_\rho^2 H_S, \tag{2.23a}$$

$$\partial_\tau H_M = 2(d-1)(d+2)H_M + (d^2+3)\rho\partial_\rho H_M + (d-1)\rho^2\partial_\rho^2 H_M, \tag{2.23b}$$

$$\partial_\tau H_L = \xi(d-1)(d+\xi)\rho^{-2+\xi}H_L + (d^2-1+2\xi)\rho^{\xi-1}\partial_\rho H_L + (d-1)\rho^{\xi}\partial_\rho^2 H_L. \tag{2.23c}$$

Note that the short and long range equations are somewhat similar to the respective small Prandtl number ones, (2.15a) and (2.15c). However, the equation in the medium range above is scale invariant in ρ, unlike the corresponding small Prandtl number one (2.15b).

3 Resolvent

In the preceding section we have reduced the evolution of the two-point function of the magnetic field to a parabolic partial differential equation (PDE) of the form $\partial_\tau H = \mathcal{M}H$, where $\mathcal{M}$ is an elliptic operator on the positive half-line.

We are now concerned with finding the fastest possible long time asymptotic growth rate of a solution H. If that maximal growth rate is positive then we say that there is dynamo effect with that growth rate.

In mathematical terminology, the operator $\mathcal{M}$ is the generator of a time evolution semigroup acting on (the space of the) H and the maximum growth rate is the maximum real part of the spectrum of the evolution semigroup. We expose below how the spectrum of the semigroup is related to that of its generator, and then study the spectrum of $\mathcal{M}$.

3.1 General Considerations

Given a differential operator $\mathcal{M}$ with a domain $D(\mathcal{M})$, we define the resolvent

$$R(z,\mathcal{M}) := (z-\mathcal{M})^{-1} \tag{3.1}$$

and the resolvent set as

$$\varrho(\mathcal{M}) := \{z \in \mathbb{C} | z-\mathcal{M} : D(\mathcal{M}) \to \mathrm{X} \text{ is bijective}\}. \tag{3.2}$$

The complement of the resolvent set, denoted by $\sigma(\mathcal{M})$, is the spectrum of $\mathcal{M}$.

According to the well known Hille-Yosida theorems (see e.g. [7]), if $(\mathcal{M}, D(\mathcal{M}))$ is closed and densely defined and if there exists $z_0 \in \mathbb{R}$ such that for each $z \in \mathbb{C}$ with $\Re z > z_0$ we have $z \in \varrho(\mathcal{M})$, and additionally the resolvent estimate $\|R(z,\mathcal{M})\| \leq 1/(\Re z - z_0)$ holds, then $\mathcal{M}$ is the generator of a strongly continuous semigroup $T(t)$ satisfying $\|T(t)\| \leq e^{z_0 t}$. However the last inequality gives only an upper bound on the growth rate of the semigroup, and this bound is not necessarily strict, so it is not possible to say exactly how fast grows the norm of the vector which is fastest stretched under the action of the semigroup.

Therefore we shall need in our analysis the somewhat stronger property of spectral mapping, relating the spectrum of the generator to that of the semigroup:

$$\sigma\left(T(t)\right) = \{0\} \cup e^{t\sigma(\mathcal{M})}. \tag{3.3}$$

This is the case in particular if $\mathcal{M}$ is a so called sectorial operator, meaning that its spectrum is contained in some angular sector $\{z \in \mathbb{C} : |\arg(z-z_0)| > \alpha > \pi/2\}$ and that outside this sector the resolvent satisfies the (stronger) estimate

$$\|R(z,\mathcal{M})\| \leq \frac{C}{|z-z_0|}. \tag{3.4}$$

Under these hypotheses $\mathcal{M}$ generates an analytic semigroup, for which the spectral mapping property (3.3) holds.

We take a moment to remind the reader that analytic semigroups are those to which physicists are used, for example one can use for them the Cauchy integral formula:

$$T(t) := e^{t\mathcal{M}} = \frac{1}{2\pi i}\int_{\mathcal{C}} dz e^{zt} R(z,\mathcal{M}), \tag{3.5}$$

where the contour surrounds the spectrum $\sigma(\mathcal{M})$. However all strongly continuous semigroups are not analytic.

We do not prove in the present work that $\mathcal{M}$ is sectorial, however we refer the interested reader to the general mathematical theory in [19] where it is explained and substantiated

that strongly elliptic operators are, under quite general assumption, sectorial generators, on a wide range of Banach spaces (e.g. L^p and C^1 spaces to name but a few).

According to the above discussion, in order to explain the existence of the dynamo effect and its growth rate, we only need to find the spectrum of $\mathcal{M}$ via the resolvent set $\varrho(\mathcal{M})$. Note that we are interested only in the positive part of the spectrum, since we want to determine the existence of the dynamo effect only.

3.2 The Resolvent Equations

The operator $\mathcal{M}$ in our case is cut up as the operators $\mathcal{M}_L$, $\mathcal{M}_M$ and $\mathcal{M}_S$ in the corresponding ranges, obtained from (2.15a) and (2.23). The resolvent is found from the equation

$$(z - \mathcal{M})\, R(z, \mathcal{M})(\rho, \rho') = \delta(\rho - \rho'). \tag{3.6}$$

Since we are primarily interested in the long range (L) behavior $\rho > 1$, we let ρ' stay in the region L at all times. This results in three equations

$$\begin{cases} (z - \mathcal{M}_L)\, R_L(\rho, \rho') = \delta(\rho - \rho'), \\ (z - \mathcal{M}_M)\, R_M(\rho, \rho') = 0, \\ (z - \mathcal{M}_S)\, R_S(\rho, \rho') = 0, \end{cases} \tag{3.7}$$

where $R_L(\rho, \rho')$ is the expression of the resolvent for $\rho \in L$ (the large scale range) and $\rho' \in \mathbb{R}_+$ and similarly R_M and R_S are valid when ρ is in the middle and small scale ranges respectively. We require the following boundary conditions from the resolvents: for small ρ we are in the diffusion dominated range, so we require smooth behavior at $\rho \to 0$. For large ρ we eventually cross the integral scale (although we haven't defined it explicitly) above which the velocity field behaves like the $\xi = 0$ Kraichnan model, leading to diffusive behavior at the largest scales for which the appropriate condition on the resolvent is exponential decay at infinity.

3.3 Piecewise Solutions of the Resolvent Equations

Assuming $\rho \neq \rho'$, we solve (3.7) with the corresponding operators $\mathcal{M}$.

The operator $\mathcal{M}_L$ does not depend on the Prandtl number. So in the region L, we get from e.g. (2.23c) (we use lowercase letters $h^{\pm}$ to denote the independent solutions)

$$h_L^{\pm}(\rho) = \rho^{-d/2 - \frac{\xi}{d-1}}\, \tilde{Z}_\lambda^{\pm}(w\rho^{1-\xi/2}), \tag{3.8}$$

where $\tilde{Z}_\lambda^{+} \equiv I_\lambda$ and $\tilde{Z}_\lambda^{-} \equiv K_\lambda$ are modified Bessel functions of the first and second kind respectively, and we have introduced w related to z by

$$w = \frac{2}{2-\xi}\sqrt{\frac{z}{(d-1)}} \quad \text{and} \quad z = (d-1)\left(\frac{2-\xi}{2}w\right)^2, \tag{3.9}$$

and the order parameter λ is

$$\lambda = \frac{\sqrt{d[2(d-1)^3 - (d-2)(2\xi + d - 1)^2]}}{(2-\xi)(d-1)}. \tag{3.10}$$

Because the range S is always in the diffusive region, we require smoothness of the solution at zero. Only one of the solutions satisfies this, so we get from (2.15a) and (2.23a)

$$h_{S,1}(\rho) = \rho^{-d/2}\, I_{d/2}\left(\sqrt{\frac{z}{d-1} - 2(d+2)P^{1-2/\xi}}\,\rho\right) \tag{3.11}$$

and

$$h_{S,2}(\rho) = \rho^{-d/2}\, I_{d/2}\left(\sqrt{\frac{z}{2} - (d-1)(d+2)\sqrt{P}}\;\rho\right), \tag{3.12}$$

where the subindex 1 refers to $P \ll 1$ (small Prandtl number) and 2 to $P \gg 1$. We will use this notation in other objects as well.

In the range M, when $P \gg 1$ we have the scale invariant equation in (2.23b) with power law solutions

$$h^{\pm}_{M,2}(\rho) = \rho^{-d/2-\frac{2}{d-1}\pm\zeta}, \tag{3.13}$$

where

$$\zeta = \sqrt{\frac{z - z_2}{d-1}}, \tag{3.14}$$

with

$$z_2 = -\frac{d-1}{4}[(2-\xi)\lambda]^2|_{\xi=2} = -\frac{d}{4(d-1)}(d^3 - 10d^2 + 9d + 16). \tag{3.15}$$

The medium range equation for $P \ll 1$ cannot be solved exactly, but we can consider it in two different asymptotic cases. From (2.15b) we get

$$\left(\xi(d+\xi)\rho^{-2+\xi} - \frac{z}{d-1}\right) R_M + (d+1)\frac{1}{\rho}\partial_\rho R_M + \partial^2_\rho R_M = 0 \tag{3.16}$$

and note that since by definition of the medium range $l_v/l_\kappa \ll \rho \ll 1$, implying $1 < \rho^{-2+\xi} < (l_\kappa/l_v)^{2-\xi}$ (the $\ll$ was replaced by $<$, so that things remain valid even as $\xi \to 2$), the term $\propto \rho^{-2+\xi}$ can be dropped if we assume that

$$|z| \gg (l_\kappa/l_v)^{2-\xi} \approx P^{-\frac{2-\xi}{\xi}}. \tag{3.17}$$

If on the other hand we have

$$|z| \ll 1, \tag{3.18}$$

then z can be neglected in the equation.

The solution for large z is similar to the short range solutions,

$$h^{\pm}_{M,1}(\rho) = \rho^{-d/2}\tilde{Z}^{\pm}_{d/2}\left(\sqrt{\frac{z}{d-1}}\rho\right), \quad |z| \gg (l_\kappa/l_v)^{2-\xi}, \tag{3.19}$$

where we denoted the $P \ll 1$ case by a subscript 1. For small z we have instead

$$h^{\pm}_{M,1} = \rho^{-d/2} Z^{\pm}_{d/\xi}(2\sqrt{d/\xi + 1}\,\rho^{\xi/2}), \quad |z| \ll 1, \tag{3.20}$$

where $Z^+_{d/\xi} \equiv J_{d/\xi}$ and $Z^-_{d/\xi} \equiv Y_{d/\xi}$ are Bessel functions of the first and second kind respectively. It turns out however that the explicit form of the above solutions affects only a specific numerical multiplier and has no effect on the presence of the dynamo. Because of this we in fact derive a lower bound for the growth rate which in view of the present approximation provides a more reliable result.

3.4 Matching of the Solutions

Consider equations (3.7). We denote the long range regions $\rho < \rho'$ and $\rho > \rho'$ as $L_<$ and $L_>$. The boundary conditions for the resolvent demanded finiteness at $\rho = 0$, but in general the resolvent must be in $L_2(\mathbb{R}_+)$. We therefore have in the region $L_>$ only the h^-_L solution, since it decays as a stretched exponential at infinity (the other one grows as a stretched exponential). We also drop the subscripts labelling the different Prandtl number cases for now. The full solutions are written as follows:

$$\begin{cases} R_S(z|\rho,\rho') = \alpha h_S(\rho), \\ R_M(z|\rho,\rho') = C^+_M h^+_M(\rho) + C^-_M h^-_M(\rho), \\ R_{L_<}(z|\rho,\rho') = C^+_L h^+_L(\rho) + C^-_L h^-_L(\rho), \\ R_{L_>}(z|\rho,\rho') = \beta h^-_L(\rho). \end{cases} \tag{3.21}$$

We denote the matching point between the short and medium ranges by a_i, i.e.

$$\begin{cases} a_1 = l_\nu / l_\kappa, \\ a_2 = l_\kappa / l_\nu. \end{cases} \tag{3.22}$$

The other matching points are $\rho = 1$ and $\rho = \rho'$ in both cases. There are six coefficients to be determined, α, $C^\pm_M$, $C^\pm_L$ and β, and in total six conditions, four from the continuity and differentiability at $\rho = a_i$ and $\rho = 1$ and two conditions at $\rho = \rho'$ around the delta function, so all coefficients will be determined from these. They will then depend on the variables z and ρ'. The C^1 conditions at $\rho = 1$ are

$$C^+_L h^+_L + C^-_L h^-_L(1) = C^+_M h^+_M(1) + C^-_M h^-_M(1) \tag{3.23}$$

and

$$C^+_L \partial h^+_L(1) + C^-_L \partial h^-_L(1) = C^+_M \partial h^+_M(1) + C^-_M \partial h^-_M(1), \tag{3.24}$$

where we denoted $\partial h(1) = \partial_\rho h(\rho)|_{\rho=1}$. This can be expressed conveniently as

$$\begin{pmatrix} h^+_L & h^-_L \\ \partial h^+_L & \partial h^-_L \end{pmatrix}_1 \begin{pmatrix} C^+_L \\ C^-_L \end{pmatrix} = \begin{pmatrix} h^+_M & h^-_M \\ \partial h^+_M & \partial h^-_M \end{pmatrix}_1 \begin{pmatrix} C^+_M \\ C^-_M \end{pmatrix}, \tag{3.25}$$

where the matrix subindex refers to evaluation of the matrix elements at $\rho = 1$. Since we have only one solution at short range, we get similarly at a_i

$$\begin{pmatrix} h^+_M & h^-_M \\ \partial h^+_M & \partial h^-_M \end{pmatrix}_{a_i} \begin{pmatrix} C^+_M \\ C^-_M \end{pmatrix} = \alpha \begin{pmatrix} h_S \\ \partial h_S \end{pmatrix}_{a_i}, \tag{3.26}$$

where again the matrix subindex indicates the point where matrix elements are to be evaluated. We can solve these for $C^\pm_L$,

$$\begin{pmatrix} C^+_L \\ C^-_L \end{pmatrix} = \mathcal{J}' \begin{pmatrix} \partial h^-_L & -h^-_L \\ -\partial h^+_L & h^+_L \end{pmatrix}_1 \begin{pmatrix} h^+_M & h^-_M \\ \partial h^+_M & \partial h^-_M \end{pmatrix}_1 \begin{pmatrix} \partial h^-_M & -h^-_M \\ -\partial h^+_M & h^+_M \end{pmatrix}_{a_i} \begin{pmatrix} h_S \\ \partial h_S \end{pmatrix}_{a_i}. \tag{3.27}$$

The numeric constant $\mathcal{J}'$ above contains the determinants of the inverted matrices and α. It is certainly nonsingular due to the linear independence of the solutions. We have decided not to explicitly write it down since, as we will see below, we only need the fraction C_L^-/C_L^+. Now we have piecewise the resolvents

$$\begin{cases} R_{L_<}(z|\rho,\rho') = C_L^+(h_L^+(\rho) + \frac{C_L^-}{C_L^+}h_L^-(\rho)), \\ R_{L_>}(z|\rho,\rho') = \beta h_L^-(\rho), \end{cases} \tag{3.28}$$

and we still need to use the first equation of (3.7) for C_L^+ and β. The continuity condition is

$$C_L^+\left(h_L^+(z,\rho') + \frac{C_L^-}{C_L^+}h_L^-(z,\rho')\right) = \beta h_L^-(z,\rho'). \tag{3.29}$$

The other condition is obtained by integrating the equation with respect to ρ over a small interval and then shrinking the interval to zero:

$$C_L^+\left(\partial h_L^+(\rho') + \frac{C_L^-}{C_L^+}\partial h_L^-(\rho')\right) - \beta\partial h_L^-(\rho') = 1. \tag{3.30}$$

These can be solved to yield

$$C_L^+ = \frac{h_L^-(\rho')}{\mathcal{W}(h_L^+, h_L^-)(\rho')} \tag{3.31}$$

and

$$\beta = \frac{C_L^+h_L^+(\rho') + C_L^-h_L^-(\rho')}{C_L^+\mathcal{W}(h_L^+, h_L^-)(\rho')}, \tag{3.32}$$

where $\mathcal{W}$ is the Wronskian, $\mathcal{W}(f,g) = fg' - f'g$. Explicitly from (3.8),

$$\mathcal{W}(h_L^+, h_L^-)(z,\rho') = (\rho')^{-d-\frac{2\xi}{d-1}}\mathcal{W}(I_\lambda, K_\lambda) = -(1-\xi/2)(\rho')^{-d-1-\frac{2\xi}{d-1}}. \tag{3.33}$$

Using the above obtained expressions of C_L^+, β and $\mathcal{W}$ in (3.28) we thus have the solutions

$$\begin{cases} R_{L_<}(z|\rho,\rho') = -\frac{(\rho')^{d+1+2\xi/(d-1)}}{1-\xi/2}(h_L^+(\rho)h_L^-(\rho') + (\frac{C_L^-}{C_L^+})h_L^-(\rho)h_L^-(\rho')), \\ R_{L_>}(z|\rho,\rho') = -\frac{(\rho')^{d+1+2\xi/(d-1)}}{1-\xi/2}(h_L^-(\rho)h_L^+(\rho') + (\frac{C_L^-}{C_L^+})h_L^-(\rho)h_L^-(\rho')), \end{cases} \tag{3.34}$$

with C_L^-/C_L^+ obtained from (3.27). We have calculated in Appendix 2 the asymptotic expression for C_L^-/C_L^+ for the two Prandtl number cases $P \ll 1$ and $P \gg 1$,

$$\frac{C_L^-}{C_L^+} = -\frac{\partial h_L^+(1) - \Lambda_L h_L^+(1)}{\partial h_L^-(1) - \Lambda_L h_L^-(1)}, \tag{3.35}$$

with leading order contribution to Λ_L as

$$\Lambda_L = \frac{\partial h_M^\pm(1)}{h_M^\pm(1)}, \tag{3.36}$$

with either the $+$ or the $-$ solution understood, the choice depending on the Prandtl number.

4 Dynamo Effect

The mean field dynamo effect for the 2-point function of the magnetic field corresponds to the case when the evolution operator $\mathcal{M}$ has positive (possibly generalized) eigenvalues. Eigenvalues correspond to poles, in z, of the resolvent given in (3.34) and generalized eigenvalues to branch cuts. The z dependence is not seen explicitly in (3.34), but recall from (3.8) that the $h_L^{\pm}$ depend on z, and we see from (3.35) and matter in Appendix 2 that there is further dependence through C_L^-/C_L^+.

The $h_L^{\pm}$ (see (3.8)) depend on the square root of z, and since the Bessel functions are analytic on the complex right half-plane, this square root dependence leads directly to a branch cut along the negative real axis in the z dependence of the resolvent. This corresponds to a heat equation like continuum spectrum of decaying modes, these modes don't contribute to the dynamo effect.

Any other possible contributions to the spectrum come from the fraction C_L^-/C_L^+. An expression for the latter is given in (3.35), with Λ_L computed in Appendix 2. Equation (3.35) can be simplified by noting that (using (3.8) and (3.9))

$$\partial h_L^{\pm}(1) = -\left(\frac{d}{2} + \frac{\xi}{d-1}\right)\tilde{Z}_\lambda^{\pm}(w) + (1-\xi/2)\partial_w \tilde{Z}_\lambda^{\pm}(w). \tag{4.1}$$

Then we can write

$$\frac{C_L^-}{C_L^+} = -\frac{(1-\xi/2)wI_\lambda'(w) - [\frac{d}{2} + \frac{\xi}{d-1} + \Lambda_L]I_\lambda(w)}{(1-\xi/2)wK_\lambda'(w) - [\frac{d}{2} + \frac{\xi}{d-1} + \Lambda_L]K_\lambda(w)}\,. \tag{4.2}$$

We underline again that w depends on the square root of z, so the complex plane minus the negative real line for z corresponds to the $\Re w > 0$ half-plane for w. Since Bessel functions are analytical on this half-plane, the new singularities introduced by C_L^-/C_L^+ may come either from singularities of Λ_L or zeros of the denominator C_L^+. Let us introduce

$$\tilde{\Lambda}_L = \frac{2}{2-\xi}\left[\frac{d}{2} + \frac{\xi}{d-1} + \Lambda_L\right]. \tag{4.3}$$

Then the condition $C_L^+ = 0$ may be written

$$w\frac{K_\lambda'(w)}{K_\lambda(w)} = \tilde{\Lambda}_L. \tag{4.4}$$

Finally we remind the reader that z corresponds to the growth rate with respect to the reduced time τ rather than real time t, and the real growth rate is thus $(\tau/t)z$, where for the $P \to 0$ case from (2.6) we have $\tau/t = D_1 l_\kappa^{\xi-2}$ and for the $P \to \infty$ case from (2.16) we have $\tau/t = D_1 l_\nu^{\xi-2}$.

4.1 Prandtl Number $P \to 0$

In Appendix 3.1.2 it is shown that Λ_L does not introduce new singularities in the small Prandtl case, so we only need to solve in w (4.4). In particular we are interested in the largest solution of that equation, since that will give the growth rate of the fastest growing mode of the two-point function of the magnetic field, and that is what we call the dynamo growth rate. In this aim we first study the large and small w asymptotics of the two sides of (4.4) and then, based on that, we derive estimates for its largest solution.

4.1.1 Asymptotics of $\tilde{\Lambda}_L$

As shown in Appendix 2.1, (8.18), in the limit of vanishing Prandtl number and for large z,—or equivalently large w,—from the medium range solutions of (3.19) we get

$$\Lambda_L = (1-\xi/2)w\frac{I_{1+d/2}\left((1-\xi/2)w\right)}{I_{d/2}\left((1-\xi/2)w\right)}. \tag{4.5}$$

For large w we deduce from the asymptotic properties of Bessel functions [13] that $\Lambda_L \sim (1-\xi/2)w$.

As shown in Appendix 2.1, (8.21), in the limit of vanishing Prandtl number and for small z,—or equivalently small w,—from the medium range solutions of (3.20) we get

$$\Lambda_L = -\xi\sqrt{d/\xi+1}\frac{J_{d/\xi+1}(2\sqrt{d/\xi+1})}{J_{d/\xi}(2\sqrt{d/\xi+1})}, \tag{4.6}$$

which is obviously independent of w, so it is in fact the $w \to 0$ limit of Λ_L, which we shall denote by $\Lambda_L(0)$.

4.1.2 Asymptotics of $wK'_\lambda(w)/K_\lambda(w)$

From the asymptotic properties of Bessel functions [13] we deduce that, when w goes to infinity, $K'_\lambda(w)/K_\lambda(w) \sim -w$.

However, except for the above large w asymptotics, the behaviour of $wK'_\lambda(w)/K_\lambda(w)$ is very different according to weather λ is real or pure imaginary. Based on its definition in (3.10), λ is pure imaginary if

$$\xi > \xi^* := (d-1)\left(\sqrt{\frac{d-1}{2(d-2)}} - \frac{1}{2}\right) \tag{4.7}$$

and it is real otherwise, and indeed positive (possibly infinite) since we take $\xi \leq 2$ and $d \geq 1$. We study separately the two cases below.

Pure Imaginary λ For λ pure imaginary, $K_\lambda(w)$ has an infinity of positive zeros (may be seen from its small w development), accumulating at $w = 0$, and $wK'_\lambda(w)/K_\lambda(w)$ has a pole at each of those zeros. Importantly for us, $K_\lambda(w)$ has a largest positive zero (may be seen from its large w asymptotics), which we shall denote by w_0.

Since for large w, asymptotically $K_\lambda(w) \sim (\pi/2w)^{1/2}\exp(-w) > 0$, we must have $K'_\lambda(w_0) > 0$ (note that we can exclude $K_\lambda(w_0) = K'_\lambda(w_0) = 0$, since the Bessel function is the solution of a second order homogeneous differential equation). Hence the pole of $wK'_\lambda(w)/K_\lambda(w)$ at w_0 has a positive coefficient.

Real Positive λ Using the integral representation of the modified Bessel function of the second kind,

$$K_\lambda(w) = \int_0^\infty dt e^{-w\cosh(t)}\cosh(\lambda t), \tag{4.8}$$

we see that when $\lambda \in \mathbb{R}$ and $w > 0$, then $K_\lambda(w) > 0$.

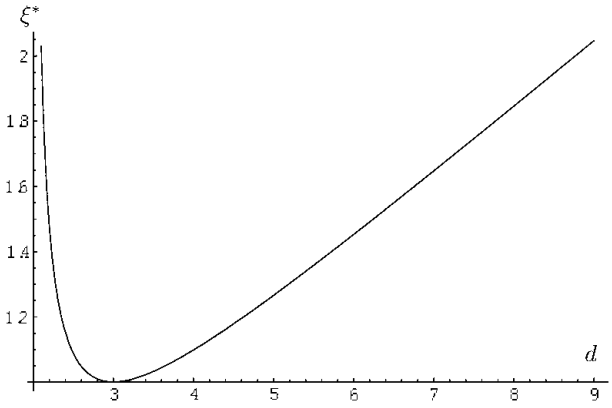

Fig. 4 Plot of the critical value ξ^* as a function of d

On the other hand using the recurrence relation $K'_\lambda(w) = -K_{\lambda-1}(w) - \lambda K_\lambda(w)/w$ we get $wK'_\lambda(w)/K_\lambda(w) = -\lambda - wK_{\lambda-1}(w)/K_\lambda(w)$, and since $K_\lambda(w)$ and $K_{\lambda-1}(w)$ are both positive, we deduce

$$w\frac{K'_\lambda(w)}{K_\lambda(w)} \leq -\lambda. \tag{4.9}$$

Using the power series development of Bessel functions we also get that $wK'_\lambda(w)/K_\lambda(w) \to -\lambda$ as $w \to 0$.

4.1.3 Presence of Dynamo at $\xi > \xi^*$ and Bounds on Growth Rate

We are now going to use the above characterized asymptotic behaviours of the two side of (4.4) to derive estimates on its largest solution. We start with the case of ξ above the critical value ξ^*, which is equivalent to λ being pure imaginary. Note that since $\xi \leq 2$ necessarily, this case is only meaningful if $\xi^* < 2$, which we shall suppose here. The plot in Fig. 4 shows that this is the case for $d_{\min} < d < d_{\max}$, with $d_{\min} \approx 2.1$ and $d_{\max} \approx 8.8$.

Lower Bound We have shown above that for large w the l.h.s. of (4.4) behaves as $-w$ while the r.h.s. behaves as $(1 - \xi/2)w$, furthermore that the l.h.s. has a rightmost pole at $w_0 > 0$ and that this pole has a positive coefficient. Using continuity of the two sides we deduce—see also Fig. 5—that (4.4) admits a solution which is larger than w_0. Hence, there is a dynamo and its growth rate is bounded from below by $z(w_0)$ (cf. (3.9) for the relation between z and w).

One can also obtain upper bounds on the dynamo growth rate. Of course we hope to find one of the same order of magnitude as the lower bound w_0, so that we could use w_0 not just a lower bound but as a convenient estimate of the largest solution of (4.4). We show below the existence of such an upper bound near $\xi = \xi^*$ and near $\xi = 2$, without succeeding to do this for intermediate values of ξ.

We still believe that w_0 is not just a lower bound for the dynamo growth rate but in fact a rather good *estimate* of it. To corroborate this claim, we have plotted in Fig. 6 the value of w_0 as a function of ξ for the $d = 3$ dimensional case, and it indeed compares well with the numerical results for the dynamo growth rate obtained in [23]. The agreement is all the more remarkable that the numerical results are based on the exact evolution equation for the two-point function of the magnetic field, whereas we started our analysis by deriving the approximating system (2.15).

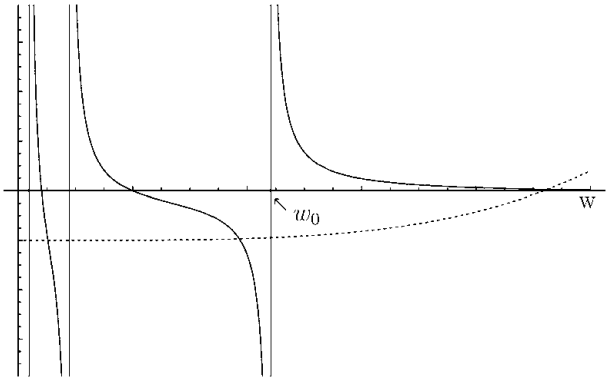

Fig. 5 Based on the asymptotic properties of the left and right hand sides of (4.4), when λ is pure imaginary and $K_\lambda(w)$ has a largest zero w_0, the latter has to be a lower bound on the largest solution of (4.4). The *dashed line* depicts the right hand side of the equation and the *solid line* the left hand side

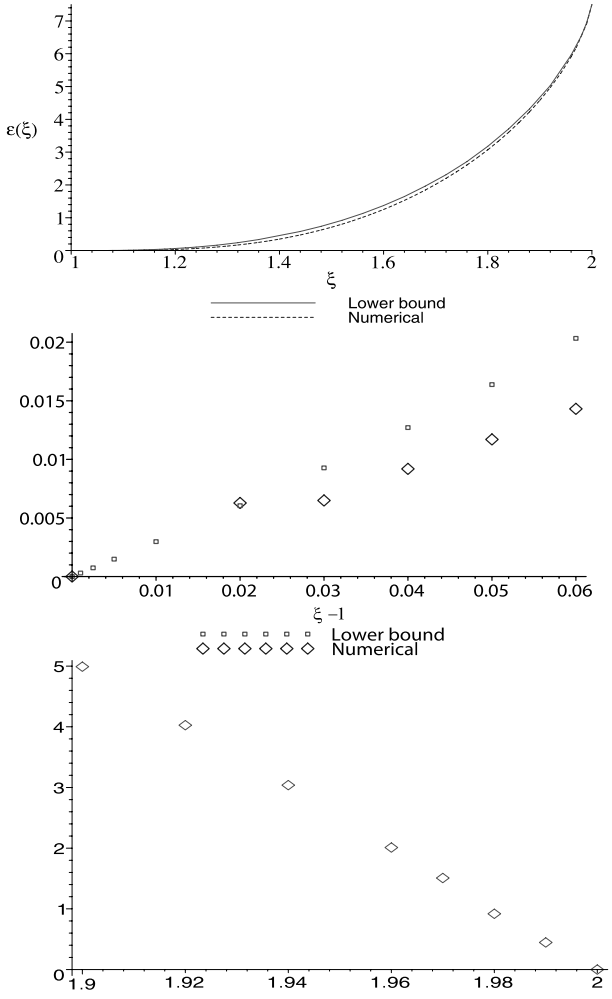

Fig. 6 In the above figure we have plotted the lower bound w_0 with the numerical results of [23]. The middle figure shows plots of both data with $1/\log(\epsilon(\xi))^2$ on the y-axis. The lower bound data shows linear behavior consistent with the asymptotics in (4.12). We note that there seems to be a numerical error in the data of [23] for $\xi = 1.02$. In the *lowest figure* we have also plotted the numerical data in [23] near $\xi = 2$ for $(15/2 - \epsilon(\xi))^{3/2}$ showing linear behavior as expected in (4.13). The plots in other dimensions look similar, except that they begin from the critical value $\xi^* > 1$

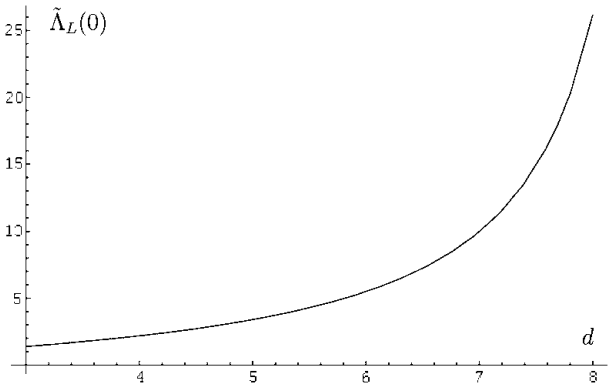

Fig. 7 Plot of $\tilde{\Lambda}_L(0)$ as a function of $\xi^*(d)$ with d taking values between 3 and 8

Upper Bound First we note that, as shown in Appendix 3.1.2, Λ_L is increasing. The small w (equivalently, small z) asymptotics of Λ_L is given in (4.6). It will be now convenient to write out explicitly the dependence of $\tilde{\Lambda}_L$ on w, by employing the notation $\tilde{\Lambda}_L(w)$. The special case $\tilde{\Lambda}_L(0)$ is taken to mean the $w \to 0$ limit of $\tilde{\Lambda}_L(w)$, and this is coherent with the previous use of the symbol.

Two cases are distinguished, depending on the sign of $\tilde{\Lambda}_L(0)$. If $\tilde{\Lambda}_L(0) \geq 0$, then we have the upper bound w_0', where w_0' is the largest zero of K_λ'. This is a good upper bound in the sense that it is always of the same order as the lower bound w_0.

In the contrary case of $\tilde{\Lambda}_L(0) < 0$ we use $\partial_w(wK_\lambda'(w)/K_\lambda(w)) < -1$ from Appendix 3.2 and get the upper bound $w_1 = w_0' + |\tilde{\Lambda}_L(0)|$. However, this upper bound is not as good as just w_0', because it cannot be directly compared to the lower bound w_0.

The asymptotic estimates computed in Sect. 4.1.5 rely on the stronger upper bound w_0', at least for ξ in some neighbourhood of ξ^* and 2 respectively.

For $\xi = \xi^*$ we have $\tilde{\Lambda}_L(0) > 0$, as shown in Fig. 7, where $\tilde{\Lambda}_L$ comes from (4.3) and $\Lambda_L(0)$ is taken from (4.6). By continuity, we still have $\tilde{\Lambda}_L(0) > 0$ on some neighbourhood of ξ^*, and by the above w_0' is a valid upper bound there.

The situation for the $\xi \to 2$ asymptotics is more complicated but in Appendix 2.1.3 it is explained why near $\xi = 2$ we may use the upper bound w_0': although $\tilde{\Lambda}_L(0) < 0$, we can justify $\tilde{\Lambda}_L(w) > 0$ for w corresponding to the dynamo growth rate.

4.1.4 Absence of Dynamo at $\xi \leq \xi^*$

So far we have dealt with the case when $\xi^* < \xi \leq 2$, and we were able to show the existence of a dynamo effect and give bounds for the dynamo growth rate. We are now going to argue that in all other situations there is no dynamo effect. Note that the absence of dynamo for $\xi \leq \xi^*$ (i.e. λ real) can be shown outside of our approximation scheme (2.15), as shown in Appendix 4. Here we show that the absence of dynamo for $\xi \leq \xi^*$ holds also for the approximate system (though much less obviously), thus further validating the scheme.

First we study the case of $d \geq 3$ and distinguish two situations. For $3 \leq d \leq 8$ the critical ξ^* takes values between 1 and 2, in particular for $d = 3$ we get $\xi^* = 1$ as expected [15, 22, 23]. For $d \geq 9$ we get $\xi^* > 2$ so necessarily $\xi < \xi^*$ since $\xi \leq 2$. We are going to show below that for ξ such that

$$0 \leq \xi \leq \min(\xi^*, 2), \tag{4.10}$$

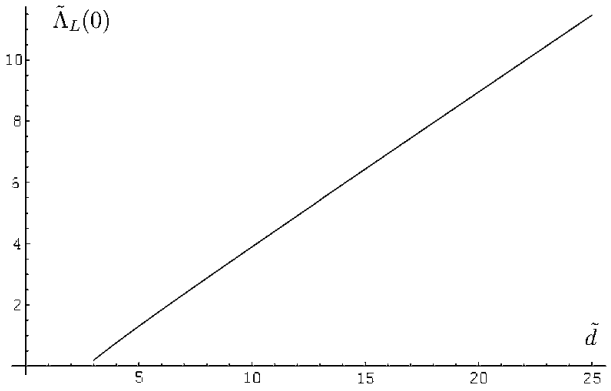

Fig. 8 Plot of the bracketed part of $\tilde{\Lambda}_L(0)$ as a function of $\tilde{d} \in (3 \ldots 25)$

we have $\tilde{\Lambda}_L(0) > 0$, whence (recall that $\tilde{\Lambda}_L(w)$ increases with w) the r.h.s. of (4.4) is always positive. On the other hand for the l.h.s. of (4.4) we have the estimate (4.9). Hence there can be no solutions of (4.4), hence no dynamo.

To prove $\tilde{\Lambda}_L(0) > 0$ as claimed above, we first write, based on (4.4), the estimate

$$\tilde{\Lambda}_L \geq \frac{2\xi}{2-\xi}\left[\frac{d}{2\xi} + \frac{\Lambda_L}{\xi}\right].$$

In particular for $w = 0$ one may use the value of $\Lambda_L(0)$ from (4.6). Using the parameter $\tilde{d} = d/\xi$, we can write then

$$\tilde{\Lambda}_L(0) \geq \frac{2\xi}{2-\xi}\left[\frac{\tilde{d}}{2} - \sqrt{\tilde{d}+1}\,\frac{J_{\tilde{d}+1}(2\sqrt{\tilde{d}+1})}{J_{\tilde{d}}(2\sqrt{\tilde{d}+1})}\right]. \tag{4.11}$$

From (4.10) and $d \geq 3$ we have $\tilde{d} \geq d/\min(\xi^*, 2)$, and using additionally (4.7) we may obtain $\tilde{d} \geq 3$. Now a plot in Fig. 8 of the term inside brackets in (4.11) and the fact that asymptotically the bracketed term behaves as $\tilde{d}/2 - \sqrt{\tilde{d}/2+1}$ can convince us that it is positive for $\tilde{d} \geq 3$, and hence that $\tilde{\Lambda}_L(0) > 0$ as claimed.

For $d = 2$ one readily verifies that $\xi^* = +\infty$, so necessarily $\xi < \xi^*$ since $\xi \leq 2$. We may again use the estimate (4.9) for the l.h.s. of (4.4), however the r.h.s. is not anymore positive. But the plot in Fig. 9 shows that $\tilde{\Lambda}_L(0) > -\lambda$ and we have shown that $\tilde{\Lambda}_L(w)$ grows with w. This excludes the presence of solutions to (4.4).

We have thus found that in dimensions $3 \leq d \leq 8$ a critical value $1 \leq \xi^* < 2$ exists above which the dynamo is present and below which we don't expect it to be present. In other (integer) dimensions we expect no dynamo for any value of ξ.

4.1.5 Asymptotics for ξ Near ξ^* and 2

We now proceed to give estimates of the growth rate of the dynamo in the cases when ξ is near the critical value ξ^* above which dynamo is present, and when ξ is near its maximum possible value 2. What we need is an estimate of the largest solution w of (4.4), from which the corresponding growth rate z is immediately deduced through (3.9). We have argued in Sect. 4.1.3 that, as an order of magnitude estimate for the solution, we may take the largest zero w_0 of $K_\lambda(w)$, at least in some regions around $\xi = \xi^*$ and $\xi = 2$ respectively. Here we are going to derive the asymptotic behavior of w_0 for ξ near ξ^* and 2, and see that it predicts correctly the behaviour of the exact dynamo growth rate obtained numerically in [23].

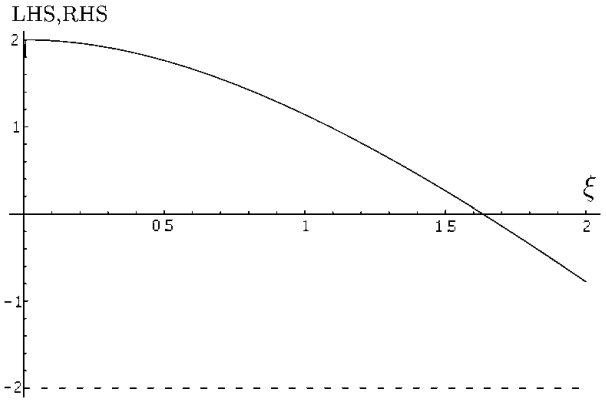

Fig. 9 Plot of $\tilde{\Lambda}_L(0)$ vs. $-\lambda$, multiplied by $2-\xi$, as functions of ξ. *Solid line* represents the left hand side ($\tilde{\Lambda}_L(0)$) and the *dashed line* is the right hand side which at two dimensions is -2

ξ Near ξ^* The case $\xi \searrow \xi^*$, corresponding to $\lambda \to 0$ along the imaginary axis, is somewhat simpler, it can be dealt with starting from the integral representation (4.8). Since $\xi > \xi^*$, the parameter λ is imaginary and we write $\lambda = i\tilde{\lambda}$ with $\tilde{\lambda} \in \mathbb{R}$, hence $K_{i\tilde{\lambda}}(w) = \int_0^\infty dt \exp(-w\cosh(t))\cos(\tilde{\lambda}t)$. Now $\cos(\tilde{\lambda}t)$ is positive near $t = 0$ and it becomes negative for the first time only for $t > \pi/(2\tilde{\lambda})$. On the other hand the term $\exp(-w\cosh(t))$ is basically a double exponential and decays very fast for $w\cosh(t) > 1$. So in order to get for the previous integral a non-positive result, we need $w_0\cosh(\pi/(2\tilde{\lambda})) \sim 1$ implying $w_0 \sim \exp(-\pi/(2\tilde{\lambda}))$. Through (3.9) one deduces the behaviour $\ln z \sim c/\tilde{\lambda}$, and since $\tilde{\lambda} \propto (\xi - \xi^*)^{1/2}$ near ξ^* (the term under the square root in (3.10) is expected to have a simple root at $\xi = \xi^*$), we finally have

$$\ln z \propto (\xi - \xi^*)^{-1/2} \tag{4.12}$$

near ξ^*.

ξ Near 2 We now pass to the asymptotics of the case $\xi \to 2$. Under this limit λ diverges as $(2-\xi)^{-1}$, along the imaginary axis. The largest zero w_0 of $K_\lambda(w)$ is known [2, 6] to behave asymptotically for large purely imaginary λ as $w_0 = |\lambda|(1 + 2^{-1/3}A_1|\lambda|^{-2/3} + O(|\lambda|^{-4/3}))$ where $A_1 \approx -2.34$ is the first (smallest absolute value) negative zero of the Airy function Ai. Combining this with (3.9) and (3.10) we get

$$z \approx z_2 - c(2-\xi)^{2/3}, \quad c = |A_1|(d-1)^{1/3}z_2^{2/3} \tag{4.13}$$

valid for ξ near 2, where $c > 0$ is some constant of order unity and z_2 was introduced in (3.15).

4.2 Prandtl Number $P \to \infty$

For large Prandtl number the analysis proceeds exactly as in the previous section, except that we have a different Λ_L. From (8.30) and (8.27) we have, using the definition of ζ from (3.14),

$$\Lambda_L = \zeta - \frac{2}{d-1} - \frac{d}{2}. \tag{4.14}$$

There is now a branch cut originating from z_2 (defined in (3.15)) extending to infinity along the negative real axis. When $3 \leq d \leq 8$, z_2 is positive and the branch cut extends up to the positive value z_2 along the positive real axis, i.e. the spectrum has a continuous positive part for *all* $\xi \in [0, 2]$. Another major difference when comparing to the small Prandtl number case is that the spectrum is continuous also in the positive part.

We conclude that the dynamo is present for all ξ for large Prandtl numbers.

5 Some Remarks

5.1 Connection to the Schrödinger Operator Formalism

Here we would like to make a few comments regarding the large Prandtl number case, addressed principally to the reader familiar with the paper by Vincenzi [23] and the Schrödinger operator formalism used therein. For the definitions of ψ, U and m we refer the reader to that paper.

We note that same kind of piecewise analysis we have accomplished in the present work would have been possible also if we had first passed to the Schrödinger equation formalism. In that setup the existence of the dynamo would depend on whether the eigenvalues of the Schrödinger operator are negative or not. It may be explained heuristically why for a sufficiently large Prandtl number there is always a negative energy bounded state. Consider the zero energy Schrödinger equation

$$\psi''(r) = V(r)\psi(r), \tag{5.1}$$

where $V(r) = m(r)U(r)$ is the effective potential. The potential V behaves as $2/r^2$ at very short and long scales, but as $-4/r^2$ at the medium range, where the ranges correspond to the ones in this paper. The medium range solutions are $\sin(\sqrt{15}/2\log(r))$ and $\cos(\sqrt{15}/2\log(r))$. When the Prandtl number is increased, the medium range region is stretched, and it is clear that for sufficiently large Prandtl numbers the solutions cross zero an increasing number of times (see Fig. 10). According to a well known theorem, such a solution cannot be a ground state (see e.g. [20], pp. 90). In fact, the number of zeros of the solution (with nonzero derivative and excluding the zero at $r = 0$) is the number of negative energy states, which implies the existence of unbounded growth.

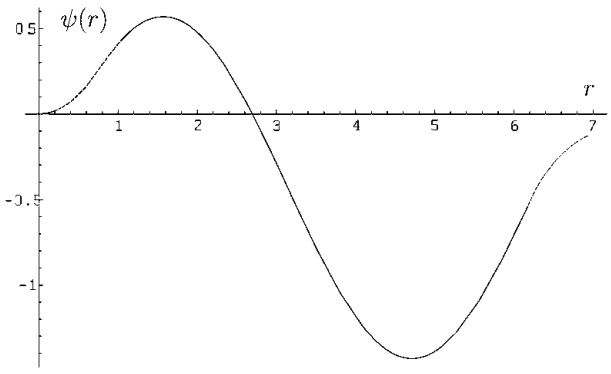

Fig. 10 Sketchy plot of the medium range zero energy solution $\sin(\sqrt{15}/2\log(r))$ crossing zero, implying the existence of a negative energy state. The *dashed lines* correspond to regions outside the medium range. As the range grows when increasing the Prandtl number, more zeros will emerge

5.2 Finite Magnetic Reynolds Number Effects

Let us finally touch upon some questions not discussed in the text. Our method allows us in principle, without further complications, to estimate the critical magnetic Reynolds number (dependent on velocity roughness exponent ξ and space dimension d) at which dynamo effect sets in, and the growth of the dynamo exponent with Reynolds number. However we get only a logarithmic estimate whose uncertainty is at least an order of magnitude or even two, which makes it not too useful. Notwithstanding, we would like to mention that the estimates we would obtain this way are hardly compatible with numerical results of [23], our thresholds being significantly lower. This issue is currently clarified with D. Vincenzi.

5.3 Exceptional Solutions

An other issue is that of the existence of "exceptional" dynamos. It seems to us that the "typical" dynamo (note that we consider here only the infinite magnetic Reynolds number case) corresponds to the situation when our $\xi > \xi^*$, in which case there is an infinite discrete spectrum of growing modes. However our equations do not exclude *a priori* the possibility of a single growing mode at some $\xi < \xi^*$. In fact, if we take for example, at a formal level, $d = 2.125$ then $\xi^* \approx 1.82$ and for $\xi' \leq \xi < \xi^*$ (where ξ' is some value of which we only need to know here that $\xi' < 1.77$), (4.4) will have, in what we have called the small z approximation (cf. (3.18)), a single solution $w_0 > 0$. If we take $\xi = 1.77$ then $w_0 \approx 0.077$ and $z \approx 8.8 \cdot 10^{-5} \ll 1$ in a self-consistent manner. However it remains to be known if such a solution is not just an artefact of our resolution method, and if not, then to see if one can construct a model where such solutions occur for the more physical value of $d = 3$.

A partial answer to these concerns is given in Appendix 4, where it is shown that for the system (2.7), (2.8), without the approximation (2.15), the absence of dynamo is quite straightforward, independently of the value of d, and doesn't require the finer analysis of Sect. 4.1.4.

6 Conclusions

The mean-field dynamo problem was considered in arbitrary space dimensions. We have shown that, to obtain the spectrum of the dynamo problem, (4.4) has to be solved for w, from which the growth rate z can be expressed through (3.9). The quantity Λ_L appearing in (4.4) is given, for small magnetic Prandtl numbers, by either (4.5) or (4.6), depending on which of the self-consistent conditions (3.17) or (3.18) is verified (note that this leaves a gap between, with no explicit formula). For large magnetic Prandtl number we have to use (4.14) instead.

It was observed that, in our model, the dynamo can only exist when $3 \leq d \leq 8$. The results for small Prandtl numbers were shown to confirm previous results [15, 23] obtained in three dimensions. For $d > 3$ a critical value for ξ was found, above which the dynamo is present, which is larger than the three dimensional critical value $\xi^* = 1$. Furthermore, in the vanishing Prandlt number limit we have obtained the asymptotic estimates (4.12) and (4.13), which are in good qualitative agreement with numerical simulations of [23].

For large Prandtl numbers it was shown that the dynamo exists for *all* ξ and that the spectrum is continuous. We hope our work will contribute to clarifying this somewhat controversial issue. The physical idea behind our explanations is that at large magnetic Prandtl number the magnetic field can feel the smooth scales of the fluid flow (they are not "wiped

out" by magnetic diffusivity), and correlations in the velocity field above the viscous scale l_ν won't do more harm to the dynamo than if we had a Batchelor type flow with no correlations of velocity at scales significantly larger than l_ν.

Our methods were based on approximating piecewise the evolution operator of the two-point function of the magnetic field. This approximation introduces inaccuracies and one may ask how these influence the fine details of our reasoning, which relied on non-trivial estimates. We think that the general picture sketched up should be valid for the exact problem also, based on the good agreement with available numerical data from the literature. Since for $\xi = \xi^*$ and $\xi = 2$ one can find the fastest growing mode explicitly, it should also be possible to do a perturbation theory around these points for the exact evolution operator, this is however left for future work.

Acknowledgements H.A. would like to thank P. Muratore-Ginanneschi and A. Kupiainen for useful comments, suggestions and discussions related to the problem at hand. P.H. would like to thank A. Kupiainen for inviting him to work at the Mathematics Department of Helsinki University, where most of this work has been done. The work of H.A. was partly supported by the Vilho, Yrjö and Kalle Väisälä foundation. We would also like to thank Dario Vincenzi for discussing his results with us and providing data from his simulations.

Appendix 1: PDE for the 2-Point Function of $\boldsymbol{B}$

We rewrite (1.5) as an Itô type SPDE (following the formalism of [17], Sect. 5)

$$dB_i + d\boldsymbol{w}\cdot\nabla B_i - \boldsymbol{B}\cdot\nabla dw_i - \kappa'\Delta B_i dt = 0, \tag{7.1}$$

where $\kappa' = \kappa + D/2$ with D defined as

$$D_{ij}(0) = D\delta_{ij}. \tag{7.2}$$

The new diffusion term in κ' emerges by advecting the magnetic field along the particle trajectories similarly as in the passive scalar case by using the Itô formula. It will cancel out eventually, as it should. We can express the above equation more conveniently by defining

$$db_i(t,\boldsymbol{x}) = -\mathcal{D}^x_{ijk}(B_j(t,\boldsymbol{x})dw_k(t,\boldsymbol{x})), \tag{7.3}$$

where $\mathcal{D}^x_{ijk} = \delta_{ij}\partial^x_k - \delta_{ik}\partial^x_j$.[2] The equation is then simply

$$dB_i - \kappa'\Delta B_i dt = db_i. \tag{7.4}$$

For a function F of fields $\boldsymbol{B}$, we have the (generalized) Itô formula,

$$\begin{aligned} dF(\boldsymbol{B}(t,\cdot)) = &\int d^d\boldsymbol{x}\frac{\delta F}{\delta B_i(\boldsymbol{x})}[\kappa'\Delta B_i dt + db_i] \\ &+ \frac{1}{2}\int d^d\boldsymbol{x}d^d\boldsymbol{y}\frac{\delta^2 F}{\delta B_i(\boldsymbol{x})\delta B_j(\boldsymbol{y})}\boldsymbol{E}(db_i(t,\boldsymbol{x})db_j(t,\boldsymbol{y})). \end{aligned} \tag{7.5}$$

The advecting velocity field is a time derivative of a Brownian motion on some state space, that is

$$\mathbb{E}dw_i(t,\boldsymbol{x})dw_j(t,\boldsymbol{y}) = dt\,D_{ij}(\boldsymbol{x}-\boldsymbol{y}), \tag{7.6}$$

[2] This is just a rewriting of the expression $\nabla\times(\boldsymbol{B}\times\boldsymbol{v})$ for incompressible fields $\boldsymbol{B}$ and $\boldsymbol{v}$.

where D_{ij} was defined in (1.8). This means that

$$\mathbb{E}db_i(t,\boldsymbol{x})db_j(t,\boldsymbol{y}) = \mathcal{D}^x_{ikl}\mathcal{D}^y_{jmn}\left(B_k(t,\boldsymbol{x})B_m(t,\boldsymbol{y})D_{ln}(\boldsymbol{x}-\boldsymbol{y})\right)dt. \tag{7.7}$$

We apply this to $F = u_i(t,\boldsymbol{x})u_j(t,\boldsymbol{y})$, denote $G_{ij}(\boldsymbol{x}-\boldsymbol{y}) = \mathbb{E}u_i(t,\boldsymbol{x})u_j(t,\boldsymbol{y})$ and use the decomposition $D_{ij}(\boldsymbol{x}-\boldsymbol{y}) = D\delta_{ij} - d_{ij}(\boldsymbol{x}-\boldsymbol{y})$ introduced in (1.10). Noting that terms proportional to dw disappear, we obtain the equation for the two point function:

$$\partial_t G_{ij} = 2\kappa\Delta G_{ij} + \mathcal{F}_{ij}, \tag{7.8}$$

and

$$\mathcal{F}_{ij} = d_{\alpha\beta}G_{ij,\alpha\beta} - d_{\alpha j,\beta}G_{i\beta,\alpha} - d_{i\beta,\alpha}G_{\alpha j,\beta} + d_{ij,\alpha\beta}G_{\alpha\beta}, \tag{7.9}$$

where the indices after commas denote partial derivatives with respect to $\boldsymbol{r} = \boldsymbol{x}-\boldsymbol{y}$. Note that this depends only on κ, not κ', i.e. the constant part $D\delta_{ij}$ of the structure function is absent. Using the decomposition (1.16) and the explicit form of the long distance velocity structure function (1.12) we get from (7.8) two equations for G_1 and G_2,

$$\partial_t G_1 = \frac{2\kappa}{r^2}(2G_2 + (d-1)r\partial_r G_1 + r^2\partial_r^2 G_1) + \mathcal{A}, \tag{7.10}$$

and

$$\partial_t G_2 = \frac{2\kappa}{r^2}(-2dG_2 + (d-1)r\partial_r G_2 + r^2\partial_r^2 G_2) + \mathcal{B}. \tag{7.11}$$

The symbols $\mathcal{A}$ and $\mathcal{B}$ are the terms arising from the interaction with the (long distance) velocity fields. Using the relations (1.18) for G_1 and G_2 in terms of H, their explicit form is as follows:

$$\begin{aligned}\frac{\mathcal{A}}{D_1 r^{-2+\xi}} &= \xi(d-1)(d-3+\xi)H \\ &\quad + (2-d-2d^2+d^3+(-5+d+2d^2)\xi+(1+d)\xi^2)r\partial_r H \\ &\quad + (2d(d-1)+(d+1)\xi))r^2\partial_r^2 H + (d-1)r^3\partial_r^3 H,\end{aligned} \tag{7.12}$$

$$\begin{aligned}-\frac{\mathcal{B}}{D_1 r^{-2+\xi}} &= -\xi(d-1)(2-\xi)H + ((1-d^2)+(d-5+2d^2)\xi+4\xi^2-\xi^3)r\partial_r H \\ &\quad + (d+1)(d-1+\xi)r^2\partial_r^2 H + (d-1)r^3\partial_r^3 H.\end{aligned} \tag{7.13}$$

Now we can just add the equations (7.10) and (7.11), and by using $G_1 + G_2 = (d-1)H$ we get

$$\begin{aligned}\partial_t H &= \xi(d-1)(d+\xi)D_1 r^{-2+\xi}H + (2(d+1)\kappa + (d^2-1+2\xi)D_1 r^\xi)r^{-1}\partial_r H \\ &\quad + (2\kappa + (d-1)D_1 r^\xi)\partial_r^2 H.\end{aligned} \tag{7.14}$$

Appendix 2: Computation of the Fraction C_L^-/C_L^+

By evaluating the matrix multiplications on the right hand side of (3.27), we can write the fraction C_L^-/C_L^+ as

$$\frac{C_L^-}{C_L^+} = -\frac{\partial h_L^+(1) - \Lambda_L h_L^+(1)}{\partial h_L^-(1) - \Lambda_L h_L^-(1)}, \tag{8.1}$$

where (again) for the sake of conciseness we write $\partial h(1) = \partial_\rho h(\rho)|_{\rho=1}$, and Λ_L can be written as the following nested expression:

$$\begin{cases} \Lambda_L = \dfrac{\partial h_M^+(1) + \Lambda_M \partial h_M^-(1)}{h_M^+(1) + \Lambda_M h_M^-(1)}, \\ \Lambda_M = -\dfrac{\partial h_M^+(a_i) - \Lambda_S h_M^+(a_i)}{\partial h_M^-(a_i) - \Lambda_S h_M^-(a_i)}, \\ \Lambda_S = \dfrac{\partial h_S(a_i)}{h_S(a_i)}. \end{cases} \tag{8.2}$$

This follows from defining

$$\begin{pmatrix} h_S \\ \partial h_S \end{pmatrix}_{a_i} = h_S(a_i) \begin{pmatrix} 1 \\ \Lambda_S \end{pmatrix} \tag{8.3}$$

and writing (3.27) as

$$\begin{pmatrix} C_L^+ \\ C_L^- \end{pmatrix} = c \begin{pmatrix} \partial h_L^- & -h_L^- \\ -\partial h_L^+ & h_L^+ \end{pmatrix}_1 \begin{pmatrix} h_M^+ & h_M^- \\ \partial h_M^+ & \partial h_M^- \end{pmatrix}_1 \begin{pmatrix} \partial h_M^- & -h_M^- \\ -\partial h_M^+ & h_M^+ \end{pmatrix}_{a_i} \begin{pmatrix} 1 \\ \Lambda_S \end{pmatrix}, \tag{8.4}$$

where $h_S(a_i)$ is absorbed in the coefficient. We have defined above a constant c which gets cancelled in the end of computations. It will be used below as well as a generic constant that does not affect the final results. Multiplying the last matrix with the vector, we define similarly

$$\begin{pmatrix} \partial h_M^- & -h_M^- \\ -\partial h_M^+ & h_M^+ \end{pmatrix}_{a_i} \begin{pmatrix} 1 \\ \Lambda_S \end{pmatrix} = \begin{pmatrix} \partial h_M^- - \Lambda_S h_M^- \\ -\partial h_M^+ + \Lambda_S h_M^+ \end{pmatrix}_{a_i} = c \begin{pmatrix} 1 \\ \Lambda_M \end{pmatrix}, \tag{8.5}$$

that is,

$$\Lambda_M = -\frac{\partial h_M^+(a_i) - \Lambda_S h_M^+(a_i)}{\partial h_M^-(a_i) - \Lambda_S h_M^-(a_i)}. \tag{8.6}$$

Doing this again for the second matrix, we obtain similarly

$$\Lambda_L = \frac{\partial h_M^+(1) + \Lambda_M \partial h_M^-(1)}{h_M^+(1) + \Lambda_M h_M^-(1)} \tag{8.7}$$

and finally

$$\frac{C_L^-}{C_L^+} = -\frac{\partial h_L^+(1) - \Lambda_L h_L^+(1)}{\partial h_L^-(1) - \Lambda_L h_L^-(1)}. \tag{8.8}$$

We are interested in the leading order behavior of the fraction C_L^-/C_L^+ only, so we need to determine what happens to Λ_M as P approaches zero or infinity. It turns out that either $\Lambda_M \to 0$ or $\Lambda_M \to \pm\infty$, so to the leading order,

$$\Lambda_L = \frac{\partial h_M^{\pm}(1)}{h_M^{\pm}(1)} \,. \tag{8.9}$$

2.1 $P \ll 1$

Below the suspension dots denote higher order terms in powers of P (or P^{-1} for large Prandtl numbers). Recall from (3.22) and (2.13) that

$$a_1 = l_v/l_\kappa = \left(\frac{d-1}{2}P\right)^{1/\xi} . \tag{8.10}$$

The short range solution was

$$h_S(\rho) = \rho^{-d/2}\, I_{d/2}\,(\alpha\rho)\,, \tag{8.11}$$

with a temporary notation $\alpha = \sqrt{(z + 2P^{1-2/\xi}(2-d-d^2))/(d-1)}$ and note that $|\alpha|$ behaves as $P^{1/2-1/\xi}$. Using standard relations of Bessel functions [13] and using the definition for Λ_S in (8.2), we have

$$\Lambda_S = \frac{\partial h_S(a_1)}{h_S(a_1)} = \alpha \frac{I_{1+d/2}\big((\frac{d-1}{2}P)^{1/\xi}\alpha\big)}{I_{d/2}\big((\frac{d-1}{2}P)^{1/\xi}\alpha\big)}. \tag{8.12}$$

Since P is small and the arguments of the Bessel functions above scale as $P^{1/2}$, we can use the expansion

$$I_{d/2}(u) = u^{d/2}\left(\frac{2^{-d/2}}{\Gamma(1+d/2)} + \frac{2^{-2-d/2}}{\Gamma(2+d/2)}u^2 + \mathcal{O}(u^4)\right) \tag{8.13}$$

(and a corresponding one when the order parameter is $1 + d/2$) to conclude that

$$\Lambda_S = cP^{1-1/\xi} + \cdots . \tag{8.14}$$

At this point our analysis splits according to which approximation (3.19) or (3.20) we use for $h_{M,1}^{\pm}$, i.e. we treat separately the cases of small and large z. Finally when $\xi = 2$ the problem can be treated for any z.

2.1.1 Large z Case

The medium range solutions in the large z case, (3.19), are

$$h_{M,1}^{\pm}(\rho) = \rho^{-d/2}\begin{cases} I_{d/2} \\ K_{d/2} \end{cases}\left(\sqrt{\beta}\rho\right), \tag{8.15}$$

with $\beta = z/(d-1)$. The leading order behavior is

$$\begin{cases} h_M^+(a_1) = c + \cdots, \\ \partial h_M^+(a_1) = cP^{1/\xi} + \cdots, \\ h_M^-(a_1) = cP^{-d/\xi} + \cdots, \\ \partial h_M^-(a_1) = cP^{-1/\xi - d/\xi} + \cdots . \end{cases} \tag{8.16}$$

Using these on Λ_M as given by (8.6), we see that to leading order

$$\Lambda_M = cP^{d/\xi+1}, \tag{8.17}$$

which goes to zero. Therefore we have

$$\Lambda_L \sim \frac{\partial h_M^+(1)}{h_M^+(1)} = \sqrt{\frac{z}{d-1}}\frac{I_{1+d/2}\left(\sqrt{\frac{z}{d-1}}\right)}{I_{d/2}\left(\sqrt{\frac{z}{d-1}}\right)}. \tag{8.18}$$

Note that, notwithstanding the fractional powers appearing above, Λ_L is a single valued function, indeed near $z=0$ it behaves as $\Lambda_L \approx z/(d-1)$. One also notes that in the large z case Λ_L is always positive, since the Bessel functions I are positive for positive parameter and argument.

2.1.2 *Small z Case*

We may perform a similar analysis for the small z approximation, based on (3.20),

$$h_{M,1}^{\pm}(\rho) = \rho^{-d/2}\begin{cases} J_{d/\xi} \\ Y_{d/\xi} \end{cases}\left(\gamma\rho^{\xi/2}\right), \tag{8.19}$$

with $\gamma = 2\sqrt{d/\xi+1}$. The leading order behavior is

$$\begin{cases} h_M^+(a_1) = c + \cdots, \\ \partial h_M^+(a_1) = cP^{1-1/\xi} + \cdots, \\ h_M^-(a_1) = cP^{-d/\xi} + \cdots, \\ \partial h_M^-(a_1) = cP^{-1/\xi-d/\xi} + \cdots. \end{cases} \tag{8.20}$$

Using these on Λ_M (cf. (8.6)), we see that once again Λ_M behaves at leading order as given in (8.17), meaning that it goes to zero as P goes to zero. Therefore we have

$$\Lambda_L \sim \frac{\partial h_M^+(1)}{h_M^+(1)} = -\xi\sqrt{d/\xi+1}\frac{J_{d/\xi+1}(2\sqrt{d/\xi+1})}{J_{d/\xi}(2\sqrt{d/\xi+1})}. \tag{8.21}$$

2.1.3 *Case of* $\xi = 2$

In the particular case of $\xi = 2$ the medium range solution can be explicitly calculated for any z, and we have

$$h_{M,1}^{\pm}(\rho) = \rho^{-d/2}\begin{cases} J_{d/2} \\ Y_{d/2} \end{cases}\left(\sqrt{\beta}\rho\right), \tag{8.22}$$

where now $\beta = 2(d+2) - z/(d-1)$. The approximations in (8.16) or (8.20) (for $\xi = 2$ those two coincide) are valid uniformly as ξ goes to 2, so when β is of order unity, the leading order behaviour (8.17) is valid. Note that for $z = z_2$ we indeed have β of order unity. Now one deduces that $\Lambda_L = -\sqrt{\beta}J_{d/2+1}(\sqrt{\beta})/J_{d/2}(\sqrt{\beta})$, and for $z = z_2$ one finds $\sqrt{\beta} = (d^2-d+4)/4/(d-1)$. One can then verify numerically that for $\xi = 2$ and $z = z_2$ and relevant values of d (between 3 and 8 inclusive) we have $\tilde{\Lambda}_L > 0$. By continuity, positivity carries over to values of ξ close to 2 and the corresponding dynamo growth rate z. This permits us to use near $\xi = 2$ the upper bound w_0' on the largest solution of (4.4), and obtain the asymptotic behaviour of Sect. 4.1.5.

2.2 $P \gg 1$

Now we have $a_2 = ((d-1)P/2)^{-1/2}$. The short range solution is in this case

$$h_S(\rho) = \rho^{-d/2}\, I_{d/2}(\sqrt{P}\alpha'\rho), \tag{8.23}$$

with

$$\alpha' = \frac{1}{\sqrt{2}}\sqrt{z + 2(2-d-d^2)}. \tag{8.24}$$

Similarly to the $P \ll 1$ case,

$$\Lambda_S = \sqrt{P}\alpha' \frac{I_{1+d/2}(\sqrt{\frac{2}{d-1}}\alpha')}{I_{d/2}(\sqrt{\frac{2}{d-1}}\alpha')} = c\sqrt{P} + \cdots. \tag{8.25}$$

The medium range solutions are now power laws,

$$h_M^{\pm} = \rho^{-d/2-2/(d-1)\pm\delta}, \tag{8.26}$$

where

$$\delta = \frac{\sqrt{d(d^3 - 10d^2 + 9d + 16) + 4(d-1)z}}{2(d-1)}. \tag{8.27}$$

Since $\partial h_M^{\pm}(a_2) \propto \sqrt{P} h_M^{\pm}(a_2)$,

$$\partial h_M^{\pm}(a_2) - \Lambda_S h_M^{\pm}(a_2) = c\sqrt{P} h_M^{\pm}(a_2) + \cdots, \tag{8.28}$$

that is,

$$\Lambda_M = c\frac{h_M^+(a_2)}{h_M^-(a_2)} + \cdots = c\frac{1}{P} + \cdots. \tag{8.29}$$

This goes to zero as $P \to \infty$, and we have

$$\Lambda_L \to \frac{\partial h_M^+(1)}{h_M^+(1)} = \zeta - \frac{2}{d-1} - \frac{d}{2}, \tag{8.30}$$

where ζ was defined in (3.14). In fact we wouldn't have needed to worry if the limit of Λ_M was infinite or zero. The difference would only be a different sign of ζ, which doesn't affect anything since it is the presence of the branch cut alone which determines the positive part of the spectrum.

Appendix 3: Some Sturm-Liouville Theory

Consider the following general second order linear eigenvalue problem, where a, b, c are positive functions and $z \in \mathbb{R}$:

$$a(\rho)h''(\rho) + b(\rho)h'(\rho) + c(\rho)h(\rho) = zh(\rho). \tag{9.1}$$

Introduce $g = h'/h$, then g verifies the first order non-linear (Riccati) differential equation

$$g' = \frac{z - c - bg - ag^2}{a}. \tag{9.2}$$

Note that a zero of h corresponds to a pole of g, and the pole is always such that as ρ increases g goes to $-\infty$ and comes back at $+\infty$ (since if h is positive before crossing zero then its derivative must be negative and vice versa).

3.1 Monotonicity of Solutions in z

Consider for (9.1) the initial condition $h'(0) = 0$ and $h(0) > 0$ which in particular implies $g(0) = 0$. Now consider (9.1) and (9.2) for two different values of z, say z_1 and z_2, and denote the corresponding solutions by h_1, g_1 and h_2, g_2 respectively. We show that if $z_1 > z_2$, then $g_1(\rho) > g_2(\rho)$ for ρ less than the first zero of h_2.

This can be seen as follows. First, the assertion is true near $\rho = 0$ since $g_1'(0) = (z_1 - c(0))/a(0) > (z_2 - c(0))/a(0) = g_2'(0)$ while $g_1(0) = g_2(0) = 0$. Now suppose that at some point the ordering of g_1 and g_2 changes, this means that the two have to cross, i.e. for some ρ we have $g_1(\rho) = g_2(\rho) = G$. However at this point $g_1'(\rho) = (z_1 - c(\rho) - b(\rho)G - a(\rho)G^2)/a(\rho) > (z_2 - c(\rho) - b(\rho)G - a(\rho)G^2)/a(\rho) = g_2'(\rho)$, meaning that g_1 cannot cross g_2 downwards, which is a contradiction.

Below we give a few specific applications of these results to our problem. Some of these are used in the main text.

3.1.1 Position of First Zero of h Increases with z

From the above it also follows that the first zero of h_1 is larger than the first zero of h_2. Indeed h_2 has, obviously, no zero before its first zero. Thus g_2 doesn't go to $-\infty$ before that point, implying that g_1 neither since $g_1 > g_2$. But then h_1 has no zero either before the first zero of h_2.

A particularly useful application of this is to use the position of the first zero of the solution with $z = 0$ as a lower bound on the first zero of any solution for $z > 0$.

3.1.2 At small Prandtl, Λ_L is Non-Singular and Increases with z

We may apply the above to the case when (9.1) corresponds to the small Prandtl approximation (2.15b) of $\mathcal{M}_M$. For $P \to 0$ the lower (i.e. left) boundary condition for h_M becomes $h_M'(0) = 0$. The case $z = 0$ can be explicitly solved and we get $h_M^0(\rho) := h_M^{z=0}(\rho) = \rho^{-d/2} J_{d/\xi}(2\sqrt{d/\xi + 1}\rho^{\xi/2})$. What needs to be seen is that h_M^0 does not have zeros between 0 and 1, equivalent to $J_{d/\xi}$ not having zeros between 0 and $2\sqrt{d/\xi + 1}$. The latter follows from the fact that $j_{\nu,1} > 2\sqrt{\nu + 1}$ for $\nu \geq 0$ (where $j_{\nu,1}$ is the first positive zero of the Bessel function of index ν), which may be seen from the plot in Fig. 11, in conjunction with the fact that we have $j_{\nu,1} > \nu$ [24].

In view of Appendix 3.1.1 this allows us to conclude that $h_M(\rho)$ doesn't have zeros for any $z \geq 0$ for $\rho \in [0, 1]$, so $\Lambda_L = h_M'(1)/h_M(1)$ is finite and grows with z for $z \geq 0$.

Finally let us point out that h_M^0 *does* have zeros (for $\rho > 1$ though), and this is due to the presence of the term $\xi(d-1)(d+\xi)\rho^{\xi-2}h_M$ in (2.15b). Without this term we would have $h_M^0 = 1$, and obviously it wouldn't have zeros. However the term in question corresponds to the effect of the velocity field *below* the magnetic diffusive scale l_κ. Thus it is quite surprising that such a contribution makes it completely *non* self evident—or even seemingly fortuitous—that Λ_L is indeed always monotonously increasing and finite.

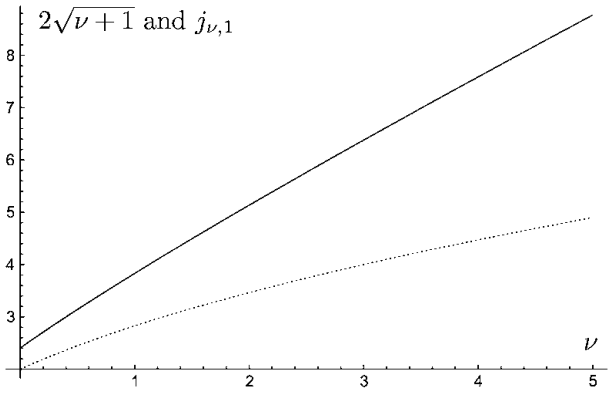

Fig. 11 Plot of $j_{\nu,1}$ (*solid line*) and $2\sqrt{\nu+1}$ (*dashed line*) for $\nu = 0 \ldots 5$. For $\nu > 5$ we have $j_{\nu,1} > \nu > 2\sqrt{\nu+1}$ by [24]

3.1.3 Nodeless Zero Mode Implies no $z > 0$ Eigenfunction

Along the same lines one can prove for our case the standard lore of Sturm-Liouville theory that if the zero mode ($z = 0$ solution) has no zeros, then there is no eigenfunction with $z > 0$.

The idea is that while the zero mode decays near infinity as a power law, any eigenfunction h_1 for $z > 0$ has to decay exponentially, so it will be below the zero mode. On the other hand, from (9.1) one deduces that $h''(0)$ grows with z, so that h_1 has to be larger than the zero mode near $\rho = 0$. This would imply that the two have to cross in the sense that h_2 comes from above and goes below the zero mode, but at the crossing point g_1 would be less than that of the zero mode, which contradicts the above said.

3.2 Consequences for Modified Bessel Function

We wish to prove here that, for pure imaginary λ, the slope of $\rho K'_\lambda(\rho)/K_\lambda(\rho)$ is bounded from above by -1 for all $\rho > 0$.

Using notation from the previous subsections, introduce $f(\rho) = \rho g(\rho)$. Then (9.2) translates to $f' = [(z-c)\rho + (a/\rho - b)f - (a/\rho)f^2]/a$. Applied to the particular case of the modified Bessel equation with parameter λ

$$\rho^2 h'' + \rho h' - \rho^2 h = \lambda^2 h,$$

i.e. when $a(\rho) = \rho^2$, $b(\rho) = \rho$, $c(\rho) = -\rho^2$ and $z = \lambda^2$, we obtain

$$f' = (\rho^2 + \lambda^2 - f^2)/\rho. \tag{9.3}$$

Solving (9.3) for $f' = -1$ gives $f^2 = s(\rho)^2$ where we define $s(\rho) = -[(\rho + 1/2)^2 + \lambda^2 - 1/4]^{1/2}$. Moreover when $f^2 > s^2$ then $f' < -1$.

We now take $f = \rho K'_\lambda(\rho)/K_\lambda(\rho)$ in the case when λ is pure imaginary. Then, for large ρ, asymptotically $f(\rho) - s(\rho) \sim -(1 - 4\lambda^2)/(16\rho^2) < 0$, the last inequality being guaranteed by the fact that we consider the case when λ is pure imaginary and hence $\lambda^2 \leq 0$. This means that for large ρ asymptotically $f < s$.

Using the fact that f is continuous, if f were to become larger than s for some finite ρ, necessarily it would pass through $f = s$, but at that point we would have $f' = -1 > s'$ (the inequality holding for λ pure imaginary), which is a contradiction to the fact that for larger ρ we should have $f < s$.

This proves that $f < s \leq 0$ when s is real, and thus $f^2 > s^2$ for all $\rho \geq 0$, whence $f' < -1$ for $\rho \geq 0$.

3.3 Real Spectrum

Though we do not consider $\mathcal{M}$ to be self-adjoint, its spectrum is always real, for the following reason.

Since $\mathcal{M}$ is a second order differential operator we may conjugate it by a multiplication operator (by a "function" which is known in the theory of diffusion processes as the speed measure) to get a symmetric operator $\tilde{\mathcal{M}}$, and taking into account the boundary conditions we have (we see that for any $z \in \mathbb{C} \setminus \mathbb{R}_-$ the solution of $\tilde{\mathcal{M}}h = zh$ which verifies the boundary conditions is a twice differentiable function with zero derivative at $\rho = 0$ and exponentially decaying as $\rho \to \infty$, so h is also in the domain of $\tilde{\mathcal{M}}^\dagger$), we can use the same trick as for self-adjoint operators: suppose $\tilde{\mathcal{M}}h = zh$ and write $\int \bar{h}\tilde{\mathcal{M}}h = z\int \bar{h}h$, now take the complex conjugate of both sides, and since $\tilde{\mathcal{M}}$ is real and symmetric, we have $\int \bar{h}\tilde{\mathcal{M}}h = \bar{z}\int \bar{h}h$, showing that $z = \bar{z}$, i.e. that z is real.

Appendix 4: Exact Results for $P = 0$

Here we want to study more rigorously the case of $P = 0$. In this case we can find exactly the zero mode of (2.7). For λ real (recall its definition from (3.10)) we show that the Appendix 3.1.3 we conclude that there is no dynamo effect in this case. On the other hand for λ pure imaginary the zero mode has an infinity of nodes.

Recalling (2.11), first we have to solve for the zero mode of the operator $[\xi(d-1)\times(d+\xi)\rho^{\xi-2} + (d^2-1+2\xi)\rho^{\xi-1}\partial_\rho + (d-1)\rho^\xi\partial_\rho^2] + [(d^2-1)\rho^{-1}\partial_\rho + (d-1)\partial_\rho^2]$. At zero Prandtl number the boundary condition is to have finite limit at $\rho = 0$. The appropriate solution is

$$(\rho^\xi + 1)^{(d-3)/(d-1)}\,{}_2F_1(a, b; c; -\rho^\xi),$$

where ${}_2F_1$ is the hypergeometric function and

$$\begin{cases} a = \dfrac{2(d-2)\xi + d(d-1) + (2-\xi)(d-1)\lambda}{2\xi(d-1)}, \\ b = \dfrac{2(d-2)\xi + d(d-1) - (2-\xi)(d-1)\lambda}{2\xi(d-1)}, \\ c = \dfrac{d+\xi}{\xi}. \end{cases} \tag{10.1}$$

Let us start with the case of λ real. Without loss of generality, we may suppose $\lambda > 0$ (or otherwise exchange a and b, since the hypergeometric function is symmetric in those arguments). Notice that $2(d-2)\xi + d(d-1) > 0$ and $[2(d-2)\xi + d(d-1)]^2 - [(2-\xi)(d-1)\lambda]^2 = 2d^2(d-1)^2 - 8\xi^2(d-2) \geq 2[d^2(d-1)^2 - 16(d-2)] > 0$, implying $b > 0$.

Notice also $2(d-1)(d+\xi) - [2(d-2)\xi + d(d-1)] = d(d-1) + 2\xi > 0$ implying $c - b > 0$.

Now write the following integral representation of the hypergeometric function:

$${}_2F_1(a, b; c; x) = \frac{\Gamma(c)}{\Gamma(b)\Gamma(c-b)}\int_0^1 \frac{t^{b-1}(1-t)^{c-b-1}}{(1-tx)^a}dt \quad (c > b > 0)$$

whence ${}_2F_1(a, b; c; x) > 0$ for any $x < 1$ and $c > b > 0$.

Since we have shown above $c > b > 0$ and since our $x < 0$, this proves that the zero mode has no zeros, and hence there cannot be a dynamo effect.

For λ pure imaginary it is possible to make a large ρ development using the so called linear transformation formula

$$
\begin{aligned}
{}_2F_1(a,b;c;-x) = {} & \frac{\Gamma(c)\Gamma(b-a)}{\Gamma(b)\Gamma(c-a)} x^{-a} {}_2F_1(a,1-c+a;1-b+a;-1/x) \\
& + \frac{\Gamma(c)\Gamma(a-b)}{\Gamma(a)\Gamma(c-b)} x^{-b} {}_2F_1(b,1-c+b;1-a+b;-1/x). \qquad (10.2)
\end{aligned}
$$

Since a and b are complex conjugates in the case of pure imaginary λ, the large x asymptotics can be written as ${}_2F_1(a,b;c;-x) \sim \Re(\frac{\Gamma(c)\Gamma(b-a)}{\Gamma(b)\Gamma(c-a)} x^{-a})$, which has an infinity of zeros since a has an imaginary part.

References

1. Adzhemyan, L.T., Antonov, N.V., Mazzino, A., Muratore-Ginanneschi, P., Runov, A.V.: Pressure and intermittency in passive vector turbulence. Europhys. Lett. **55**(6), 801 (2001). arXiv:nlin/0102017
2. Balogh, C.B.: Asymptotic expansions of the modified Bessel function of the third kind of imaginary order. SIAM J. Appl. Math. **15**(5), 1315 (1967)
3. Chaves, M., Eyink, G., Frisch, U., Vergassola, M.: Universal decay of scalar turbulence. Phys. Rev. Lett. **86**, 2305 (2001)
4. Chertkov, M., Falkovich, G., Kolokolov, I., Lebedev, V.: Statistics of a passive scalar advected by a large-scale two-dimensional velocity field: analytic solution. Phys. Rev. E **51**, 5609 (1995)
5. Chertkov, M., Falkovich, G., Kolokolov, I., Vergassola, M.: Small-scale turbulent dynamo. Phys. Rev. Lett. **83**, 4065 (1999)
6. Dunster, T.M.: Bessel functions of purely imaginary order with an application to second-order linear differential equations having a large parameter. SIAM J. Math. Anal. **21**(4), 995–1018 (1990)
7. Engel, K.-J., Nagel, R.: One-Parameter Semigroups for Linear Evolution Equations. Springer, Berlin (2000)
8. Falkovich, G., Gawedzki, K., Vergassola, M.: Particles and fields in fluid turbulence. Rev. Mod. Phys. **73**, 913–975 (2001)
9. Gawedzki, K., Kupiainen, A.: Universality in turbulence: An exactly soluble model. In: Grosse, H., Pittner, L. (eds.) Low-Dimensional Models in Statistical Physics and Quantum Field Theory, pp. 71–105. Springer, Berlin (1996). arXiv:chao-dyn/9504002
10. Gawedzki, K.: Easy turbulence. In: Saint-Aubin, Y., Vinet, L. (eds.) Theoretical Physics at the End of the Twentieth Century. Lecture Notes of the CRM Summer School, Banff, Alberta (CRM Series in Mathematical Physics). Springer, New York (2001). arXiv:chao-dyn/9907024
11. Gawedzki, K., Horvai, P.: Sticky behavior of fluid particles in the compressible Kraichnan model. J. Stat. Phys. **116**(5,6), 1247–1300(54) (2004)
12. Goldston, R.J., Rutherford, P.H.: Introduction to Plasma Physics. IOP Publishing, Bristol (1995)
13. Gradshteyn, I.S., Ryzhik, I.M.: Table of Integrals, Series and Products. Academic Press, New York (1965)
14. Hakulinen, V.: Passive advection and the degenerate elliptic operators M_n. Commun. Math. Phys. **235**(1), 1–45 (2003). arXiv:math-ph/0210001
15. Kazantsev, A.P.: Enhancement of a magnetic field by a conducting fluid flow. Sov. Phys. JETP **26**, 1031 (1968)
16. Kraichnan, R.H.: Small scale structure of a scalar field convected by turbulence. Phys. Fluids **11**, 945–953 (1968)
17. Kupiainen, A.: Statistical theories of turbulence. In: Lecture Notes from Random Media 2000. Madralin, June (2000). http://www.helsinki.fi/~ajkupiai/papers/poland.ps
18. Le Jan, Y., Raimond, O.: Integration of Brownian vector fields. Ann. Probab. **30**(2), 826–873 (2002). arXiv:math.PR/9909147
19. Lunardi, A.: Analytic Semigroups and Optimal Regularity in Parabolic Problems. Birkhäuser, Basel (1995)

20. Reed, M., Simon, B.: Methods of Modern Mathematical Physics IV: Analysis of Operators. Academic Press, London (1978)
21. Shraiman, B., Siggia, E.: Lagrangian path integrals and fluctuations in random flow. Phys. Rev. E **49**, 2912 (1994)
22. Vergassola, M.: Anomalous scaling for passively advected magnetic fields. Phys. Rev. E **53**, R3021–R3024 (1996)
23. Vincenzi, D.: The Kraichnan-Kazantsev dynamo. J. Stat. Phys. **106**, 1073–1091 (2002)
24. Watson, G.N.: In: Theory of Bessel Functions, p. 485. Cambridge University Press, Cambridge (1962)

3. Anomalous scaling and anisotropy in models of passively advected vector fields

3

Anomalous scaling and anisotropy in models of passively advected vector fields

Heikki Arponen

Helsinki University, Department of Mathematics and Statistics,

*P.O. Box 68, 00014 Helsinki (Finland)**

(Dated: April 15, 2009)

Abstract

An anisotropically forced passive vector model is analyzed at scales much smaller and larger than the forcing scale by solving exactly the equation for the pair correlation function. The model covers the cases of magnetohydrodynamic turbulence, the linear pressure model and the linearized Navier-Stokes equations by choice of a simple parameter. We determine whether or not the anisotropic injection mechanism induces dominance of the anisotropic effects at the asymptotic scaling regimes. We also show that under very broad conditions, both scaling regimes exhibit anomalous scaling due to the existence of nontrivial zero modes.

PACS numbers: 47.27.E-, 47.27.-i

*Electronic address: heikki.arponen@helsinki.fi

I. INTRODUCTION

One of the most important problems of turbulence is the observed deviation of Kolmogorov scaling in the structure functions of the randomly stirred Navier-Stokes equations in the inertial range of scales [1]. Contemporary research in turbulence has recently provided an explanation for this phenomenon in the context of passive advection models (see e.g. [2] for an introduction and further references). In the case of the passive scalar model describing the behavior of a dye concentration in a turbulent fluid, such a violation of canonical scaling behavior (henceforth referred to as anomalous scaling) has recently been traced to the existence of a type of statistical integrals of motion known as zero modes [2, 3]. The result can be obtained under some simplifying assumptions about the velocity field, namely assuming the velocity statistics to be gaussian and white noise in time, which results in a solvable hierarchy of Hopf equations for the correlation functions. Such properties are included in the so called Kraichnan model [4] of velocity statistics, which will also be utilized in the present work.

As opposed to a thermodynamical equilibrium, the passive scalar is maintained in a nonequilibrium steady state by external forcing designed to counter molecular diffusion. It was proved in [5] that even in the limit of vanishing molecular diffusivity the steady state exists and is unique. Furthermore defining the integral scale to be infinity results in an infinite inertial range, divided only by the injection scale L due to the forcing. While the above results of the passive scalar anomalous scaling were concerned with the small scale problem $r \ll L$, in [6] it was observed that one obtains anomalous scaling also at large scales, provided the forcing is of "zero charge", $q_0 \doteq \int đ^d \boldsymbol{r} C_L(\boldsymbol{r}) = 0$, where C_L is the forcing pair correlation function. Such a forcing is concentrated around finite wavenumbers $k \sim 1/L$, which behaves similarly to a zero wavenumber concentrated forcing at small scales, but is more realistic for probing scales larger than the forcing scale.

The forcing is usually taken to be statistically isotropic. Justification for this is that one usually expects the anisotropic effects to be lost anyway at scales much smaller that the forcing scale, according to a universality hypothesis by the K41 theory[1]. Nevertheless, in [7] it was discovered that even a small amount of anisotropy in the forcing (that can

never be avoided in a realistic setting) in the passive scalar equation would render the large scale behavior to be dominated by anisotropic zero modes responsible for another type of anomalous scaling. As pointed out in [7], such behavior is nontrivial also in the sense that one might expect the system to obey Gibbs statistics with exponentially decaying correlations at large scales, as indeed happens for the pair correlation function with isotropic zero charge forcing [6].

The purpose of the present work is to consider the small and large scale behavior of passive *vector* models stirred by an anisotropic forcing, and especially to determine if the phenomena of anomalous scaling and persistence of anisotopy is a general feature of passive advection models or just a curiosity of the passive scalar. The passive vector models arise as quite natural generalizations of the scalar problem and turn out to possess much richer phenomena already at the level of the pair correlation function. For example the pair correlation function of the magnetohydrodynamic equations exhibit anomalous scaling [8] whereas one needs to study the fourth and higher order structure functions of the passive scalar to see such behavior (see e.g. [9] and references therein). It has also been argued that the linear passive vector models might yield the exact scaling exponents of the full Navier-Stokes turbulence [10]. The equation under study is defined as

$$\dot{u}_i - \nu\Delta u_i + \mathbf{v}\cdot\nabla u_i - a\mathbf{u}\cdot\nabla v_i + \nabla_i P = f_i, \tag{1}$$

with a parameter $a = -1, 0$ or 1, corresponding respectively to the linearized Navier-Stokes equations (abbreviated henceforth as LNS), the so called linear pressure model (LPM) and the magnetohydrodynamic (MHD) equations. ν is a constant viscosity/diffusivity term, f_i denotes an external stirring force, v_i is a gaussian, isotropic external velocity field defined by the Kraichnan model and P is the pressure, giving rise to nonlocal interactions. The equation was introduced in [11], where the authors derived and studied a zero mode equation for the pair correlation function in the isotropic sector and found the small scale exponents numerically and to a few first orders in perturbation theory (see also [12] for a more detailed exposition). They also reported perturbative results for higher order correlation functions and anisotropic sectors using the renormalization group. Although the purpose of the present work is to consider arbitrary values of a, some cases have already been studied elsewhere. The $a = 1$ case, corresponding to magnetohydrodynamic

turbulence, has probably received the most attention[8, 13–17]. The linear pressure model (or just the passive vector model) with $a = 0$, has been studied in e.g.[12, 18, 19]. The linearized Navier-Stokes equation (see [1]), $a = -1$, was studied in [12] and numerically in [20] in two dimensions and is the least known of the above cases, although perhaps the most interesting. The above mentioned studies have been restricted to the small scale problem and rely heavily on the zero mode analysis, i.e. finding the homogeneous solutions to the pair correlation equation. For our purposes this is not enough. To capture the anomalous properties as discussed above, one needs to consider the amplitudes of the zero modes as well, as it may turn out that some amplitudes vanish. Indeed, it is exactly this sort of mechanism that is responsible for the anisotropy dominance in [7].

We provide an exact solution of the equation for the pair correlation function with anisotropic forcing and study both small and large scale behavior. It turns out that for the "zero charge" forcing as above, the large scale behavior is anomalous even in the isotropic sector for all a. The anisotropy dominance seems however rather an exception than a rule in three dimensions, as only the trace of the correlation function for the $a = 0$ model exhibits similar phenomena at large scales. Nevertheless, in two dimensions the anisotropy dominance is a more common phenomenon. Perhaps the most interesting case is the linearized Navier-Stokes equation for which $a = -1$. The field u is now considered to be a small perturbation to the steady turbulent state described by v. This case is unfortunately complicated by the fact that practically nothing is known of the existence of the steady state, although an attempt to rectify the situation is underway by the present author.

In section II we introduce the necessary tools, discuss the role of the forcing and present the equation for the pair correlation function in a Mellin transformed form. Details of it's derivation can be found in appendix A. In section III we present the solution in both isotropic and anisotropic sectors and explain the results for the passive scalar of [7] in our formalism. The next three sections are concerned with the specific cases of magnetohydrodynamic turbulence, linear pressure model and the linearized Navier-Stokes equations. Although the space dimension is arbitrary (although larger than or equal to two), we concentrate mostly on two and three dimensions. The reasons for this are the considerable differences between $d = 2$ and $d = 3$ cases and the similarities of dimensions

$d \geq 3$. Mainly one may expect some sort of logarithmic behavior in two dimensions while in higher dimensions the behavior is power law like. Also the presence of anomalous scaling is seen to be independent of dimension for $d \geq 3$, although the actual existence of the steady state may very well depend on the dimension as observed in [15]. This will be further studied in an undergoing investigation of the steady state existence problem. The last section before the conclusion attempts to shed light on the role of the parameter a as it is varied between -1 and 1. The actual results are collected and discussed in the conclusion. We also give some computational details in the appendices.

II. PRELIMINARIES AND THE EQUATION

All vector quantities in the equation (1) being divergence free results in an expression for the pressure after taking the divergence,

$$P = (1-a)\left(-\Delta\right)^{-1}\partial_i v_j \partial_j u_i. \tag{2}$$

We may then write the equation compactly as

$$\dot{u}_i - \nu\Delta u_i + \mathcal{D}_{ijk}\left(u_j v_k\right) = f_i, \tag{3}$$

with a differential operator

$$\mathcal{D}_{ijk} = \delta_{ij}\partial_k - a\delta_{ik}\partial_j + (a-1)\partial_i\partial_j\partial_k\Delta^{-1}, \tag{4}$$

where Δ^{-1} is the inverse laplacian. The equal time pair correlation is defined as

$$G_{ij}(t,\boldsymbol{r}) = \langle u_i(t,\boldsymbol{x}+\boldsymbol{r})u_j(t,\boldsymbol{x})\rangle, \tag{5}$$

where the angular brackets denote an ensemble average with respect to the forcing and the velocity field. The equation for the pair correlation function is then

$$\partial_t G_{ij} - 2\nu'\Delta G_{ij} - \mathcal{D}_{i\mu\nu}\mathcal{D}_{i\rho\sigma}\left(D_{\nu\sigma}G_{\mu\rho}\right) = C_{ij}, \tag{6}$$

where the velocity and forcing pair correlation tensors D_{ij} and C_{ij} will be defined below. The above equation should however be understood in a rather symbolic sense, as the defining equation for the field u is in fact a stochastic partial differential equation. The equation is more carefully derived in appendix A in Fourier variables using the rules of stochastic

calculus. In the present form it is also very difficult to study because of the nonlocal terms for $a \neq 1$ and the tensorial structure. We will therefore now briefly explain the structure of the calculations in a rather superficial but hopefully transparent way (see appendix A for details). Assuming that we have reached a steady state, i.e. $\partial_t G = 0$, we rewrite eq. (6) symbolically as

$$-2\nu'\Delta G + \mathcal{M}G = C, \tag{7}$$

with the effective diffusivity $\nu' = \nu - \frac{1}{2}Dm_v^{-\xi}$ and $\mathcal{M}$ is some complicated integro-differential operator. Taking the Fourier transform of the above equation would still leave us with an integral equation due to the inherent nonlocality from the pressure term. We deal with this now by taking also the Mellin transform (after dividing by p^2), which yields

$$2\nu'\bar{g}(z) + \int đz' \mathcal{M}_{z,z'}\bar{g}(z - z') = \bar{c}(z - 2) \tag{8}$$

with a rather complicated expression for $\mathcal{M}_{z,z'}$, see eq. (A12). The advantage of the above form is that various powers of m_v arise as poles in $\mathcal{M}_{z,z'} \propto m_v^{z'-\xi}$, the leading ones residing at $z' = 0$ and $z' = \xi$. Other poles produce positive powers of m_v and can therefore be safely neglected. The residue at $z' = 0$ cancels with the term in the effective diffusivity, leaving us with only the bare diffusivity ν. The remaining equation can then be written in the limit of vanishing m_v and ν as

$$-\mathcal{R}\left(\mathcal{M}_{z,z'}|z' = \xi\right)\bar{g}(z - \xi) = \bar{c}(z - 2), \tag{9}$$

where $\mathcal{R}$ denotes the residue (the minus sign arises from the clockwise contour). The equation is then simply solved by dividing by the residue term and using the Mellin transform inversion formula

$$G(\boldsymbol{r}) = \int đz |\boldsymbol{r}|^z \mathcal{A}_z \bar{g}(z), \tag{10}$$

where $\mathcal{A}_z$ is a simple z dependent function arising from the fact that we performed the Mellin transform on the Fourier transform of the equation.

A. Kraichnan model

We define the Kraichnan model as in [21] with the velocity correlation function

$$\begin{aligned}\left\langle v_i(t,\boldsymbol{r})v_j(0,0)\right\rangle &= \delta(t)\int đ^d\boldsymbol{q}\, e^{i\boldsymbol{q}\cdot\boldsymbol{r}}\widehat{D}_{m_v}(q)P_{ij}(\boldsymbol{q}) \\ &=: \delta(t)D_{ij}(\boldsymbol{r}; m_v)\end{aligned} \tag{11}$$

where we have defined the incompressibility tensor $P_{ij}(\boldsymbol{q}) = \delta_{ij} - \widehat{\boldsymbol{q}}_i\widehat{\boldsymbol{q}}_j$ and denoted $\not{d}^d\boldsymbol{q} := \frac{d^dq}{(2\pi)^d}$. Defining

$$\widehat{D}_{m_v}(q) = \frac{\xi D_0}{(\boldsymbol{q}^2 + m_v^2)^{d/2+\xi/2}} \tag{12}$$

and applying the Mellin transform (See e.g. [22] and the appendix A of [9]) we have

$$\widehat{D}^{z'}_{m_v}(\boldsymbol{q}) := \int_0^\infty \frac{dw}{w} w^{z'+d}\widehat{D}_{m_v}(wq) = \bar{d}_{m_v}(z')q^{-z'-d}, \tag{13}$$

where

$$\bar{d}_{m_v}(z') = \frac{\xi}{2}D_0 m_v^{z'-\xi}\frac{\Gamma\left(d/2 + z'/2\right)\Gamma\left(\xi/2 - z'/2\right)}{\Gamma\left(d/2+\xi/2\right)}, \tag{14}$$

and z' is constrained inside the strip of analyticity $-d < Re(z') < \xi$. The parameter ξ takes values between zero and two and measures the spatial "roughness" of the velocity statistics. We observe that the scaling behavior of the correlation function is completely encoded in the pole structure of Mellin transform, with e.g. the pole at $z' = \xi$ corresponding to the leading scaling behavior of the velocity structure function.

B. Decomposition in basis tensor functions

Being a rank two tensor field, the pair correlation function may be decomposed in hyperspherical basis tensor functions as in [14, 23]. Such a decomposition is also an important tool in analyzing the data from numerical simulations, as witnessed e.g. in [24]. We shall be concerned only with the axial anisotropy, and apply this decomposition on the Fourier transform of the pair correlation function. This has the advantage of making the incompressibility condition very easy to solve, among other things. We consider only the case of even parity and symmetry in indices, which leaves us with a basis of four tensors:

$$\begin{cases} B^1_{ij}(\hat{\boldsymbol{p}}) &= |\boldsymbol{p}|^{-l}\delta_{ij}\Phi^l(\boldsymbol{p}) \\ B^2_{ij}(\hat{\boldsymbol{p}}) &= |\boldsymbol{p}|^{2-l}\partial_i\partial_j\Phi^l(\boldsymbol{p}) \\ B^3_{ij}(\hat{\boldsymbol{p}}) &= |\boldsymbol{p}|^{-l}(p_i\partial_j + p_j\partial_i)\Phi^l(\boldsymbol{p}) \\ B^4_{ij}(\hat{\boldsymbol{p}}) &= |\boldsymbol{p}|^{-l-2}p_ip_j\Phi^l(\boldsymbol{p}) \end{cases} \tag{15}$$

with the actual decomposition

$$\widehat{G}_{ij}(\boldsymbol{p}) := \sum_{b,l} B^{b,l}_{ij}(\hat{\boldsymbol{p}})\widehat{G}^b_l(\boldsymbol{p}). \tag{16}$$

Here $\Phi^l(\boldsymbol{p})$ is defined as $\Phi^l(\boldsymbol{p}) := |\boldsymbol{p}|^l Y^l(\hat{\boldsymbol{p}})$, where Y^l is the hyperspherical harmonic function (with the multi-index $m = 0$). It satisfies the properties

$$\begin{aligned} \Delta\Phi^l(\boldsymbol{p}) &= 0 \\ \boldsymbol{p}\cdot\nabla\Phi^l(\boldsymbol{p}) &= l\Phi^l(\boldsymbol{p}). \end{aligned} \tag{17}$$

The same decomposition will naturally be applied to the forcing correlation function as well.

C. The forcing correlation function

We require the forcing correlation function to decay faster than a power law for large momenta and to behave as $C_{ij}(p) \propto L^d(Lp)^{2N}$ for small momenta with positive integer N. The $N = 0$ case corresponds to the usual large scale forcing with a nonzero "charge" $q_0 = \int d\boldsymbol{r} C_L(\boldsymbol{r})$ and is responsible for the canonical scaling behavior of the passive scalar at large scales[6], whereas any $N > 0$ corresponds to a vanishing charge[6]. Applying the Mellin transform to such a tensor (decomposed as above) yields

$$\widehat{C}^z_{ij}(\boldsymbol{p}) = \int_0^\infty \frac{dw}{w} w^{d+z}\widehat{C}_{ij}(w\boldsymbol{p}) = |\boldsymbol{p}|^{-d-z}\sum_b B^b_{ij}(\hat{\boldsymbol{p}})\bar{c}^N_b(z), \tag{18}$$

with

$$\bar{c}^N_b(z) = \frac{C^*_b L^{-z}}{z+d+2N}, \quad \mathcal{R}e(z) > -d-2N, \tag{19}$$

and the strip of analyticity $-d-2N < \mathcal{R}e(z)$. The details of the actual cutoff function are absorbed in the constants C^*_b and play no role in the leading scaling behavior. All the interesting phenomena can be classified by using only the cases $N = 0$ and $N = 1$. We will mostly be concerned with the latter type of forcing which is also of the type considered in [6, 7]. By inverting the Mellin transform we would obtain an expression for the forcing correlation function

$$C_{ij}(t,\boldsymbol{r}) = \int đz|\boldsymbol{r}|^z \bar{c}^N_a(z)\mathrm{K}^{ab}(z)B^b_{ij}(\hat{\boldsymbol{r}}) \tag{20}$$

where the matrix $\mathbf{K}$ is defined in appendix D. We note that $\bar{c}^N_a$ determines the large scaling behavior of the above quantity as r^{-d} or r^{-2-d}, depending on the forcing, while the matrix K is responsible for the small scale behavior $\propto r^l$, where l is the angular momentum variable.

D. Mellin transformed equation and overview of calculations

As mentioned earlier in this section, equation (6) is much too unwieldy for actual computations. In appendix A we perform a more careful derivation of the equation in Fourier variables and by using the Itô formula. The resulting equation (A9) still has an inconvenient convolution integral. By applying the Mellin transform, we obtain an equation

$$\begin{aligned} &-Dm_v^{-\xi}\bar{g}_b(z) - D_0\widetilde{\lambda}\bar{g}_b(z-\xi) + \int đz' \bar{d}_{m_v}(z')\mathrm{T}^{bc}_{d+z',d+z-z'}\bar{g}_c(z-z') \\ &= \bar{c}_b(z-2). \end{aligned} \tag{21}$$

for the Mellin transformed coefficients $\bar{g}_b$ of the tensor decomposition (16) (defined explicitly in eq. (A11)). The matrix $\mathbf{T}$ is defined in eq. (A13) and involves rather difficult but manageable integrals, and $\widetilde{\lambda}$ is defined in eq. (A7). The integration contour with respect to z' lies inside the strip of analyticity $\mathcal{R}e(z) < \mathcal{R}e(z') < 0$, determined from eq. (A14). For small values of m_v the contour may (and must) be completed from the right. The reason for performing the Mellin transform becomes evident when one studies the pole structure of the functions $\bar{d}_{m_v}(z')$ and $\mathbf{T}$: first two (positive) poles occur at $z' = 0$ (from $\mathbf{T}$) and at $z' = \xi$ (from $\bar{d}_{m_v}(z')$) and correspond to a term $\propto m_v^{-\xi}$ and a constant in m_v, respectively. The former of these cancels out from the equation, hence one is free to take the limit $m_v \to 0$. This leaves us with a simple equation

$$-\widetilde{\lambda}\bar{g}_b(z-\xi) - \mathrm{T}^{bc}_{d+\xi,d+z-\xi}\bar{g}_c(z-\xi) = \frac{1}{D_0}\bar{c}_b(z-2). \tag{22}$$

From now on we absorb D_0 in the functions $\bar{c}_b$. In appendix B we have applied the incompressibility condition to the correlation function $\widehat{G}_{ij}(\boldsymbol{p})$ and the equation, which has the effect of leaving us only with two independent functions to be solved, $\bar{g}_1$ and $\bar{g}_2$. Applying also a translation $z \to z + \xi$ in eq. (23), we have

$$-\left(\widetilde{\lambda}\mathbf{1} + \mathbf{A} + \mathbf{B}\cdot\mathbf{X}\right)\bar{\mathbf{h}}(z) = \bar{\mathbf{f}}(z+\xi-2), \tag{23}$$

with the definitions

$$\begin{aligned} \bar{\mathbf{h}} &= (\bar{g}_1, \bar{g}_2)^{\mathrm{T}} \\ \bar{\mathbf{f}} &= (\bar{c}_1, \bar{c}_2)^{\mathrm{T}}, \end{aligned} \tag{24}$$

and

$$\mathbf{T}_{d+\xi,d+z} = \begin{pmatrix} \mathbf{A} & \mathbf{B} \\ \mathbf{C} & \mathbf{D} \end{pmatrix} \quad , \quad \mathbf{X} = \begin{pmatrix} 0 & -(l-1) \\ -1 & l(l-1) \end{pmatrix}. \tag{25}$$

All that remains now is to invert the matrix equation, although in the isotropic sector and in two dimensions it reduces to a scalar equation.

III. THE SOLUTION

Inverting the Mellin and Fourier transforms enables us to write the full solution as

$$G_{ij}(\boldsymbol{r}) = -\int \!\!\!\!\!\!- dz |\boldsymbol{r}|^z \bar{\mathbf{h}}^{\mathrm{T}}(z) \widehat{\mathbf{P}}^{\mathrm{T}} \mathbf{K} \cdot B_{ij}(\hat{\boldsymbol{r}}), \tag{26}$$

where we now have a projected version of the matrix $\mathbf{K}$ due to the incompressibility condition (see appendix D), and

$$\bar{\mathbf{h}}(z) = -\left(\widetilde{\lambda}\mathbf{1} + \mathbf{A} + \mathbf{B}\cdot\mathbf{X}\right)^{-1} \bar{\mathbf{f}}(z+\xi-2). \tag{27}$$

The strip of analyticity is now

$$2 - d - \xi - 2N < \mathcal{R}e(z) < 0, \tag{28}$$

where $N = 0$ for the traditional nonzero charge forcing and $N = 1$ for the zero charge forcing. We should note that there may in fact be poles inside the strip of analyticity due to the solution $\bar{\mathbf{h}}$, which is just a reflection of one's choice of boundary conditions.

A. Isotropic sector

In the isotropic case when $l = 0$, we have $B^1_{ij} = \delta_{ij}$, $B^4_{ij} = \widehat{\mathbf{r}}_i\widehat{\mathbf{r}}_j$ and the other B's are zero. The equation of motion (23) is now a scalar equation, hence we only need the $(1,1)$ -component of the matrix,

$$\begin{aligned}\left(\widetilde{\lambda}\mathbf{1} + \mathbf{A} + \mathbf{B}\cdot\mathbf{X}\right)_{11} &= 2(a-1)(a\xi - 1 - a - d)\Gamma\left(1+\xi/2\right)\Gamma\left(1+d/2\right) \\ -p_a(z)\frac{\Gamma\left(-z/2\right)\Gamma\left(\frac{d+z+\xi}{2}\right)\Gamma\left(\frac{4+d-\xi}{2}\right)}{2\Gamma\left(\frac{2+d+z}{2}\right)\Gamma\left(\frac{4-z-\xi}{2}\right)} &\doteq 1/\gamma_a(z),\end{aligned} \tag{29}$$

where the equality applies up to a constant term that will be absorbed in the forcing, and we have defined the polynomial

$$\begin{aligned}p_a(z) &= -(a-1)^2(d+1)\xi(2-\xi) \\ &+(z+\xi-2)\left((d-1)z^2 + \left(d(d-1)+2a\xi\right)z + \right. \\ &\left.\xi\left(-d-1+2a(d+1) - a^2(1+2d-d^2+\xi-d\xi)\right)\right)\end{aligned} \tag{30}$$

This is the same expression (only in a slightly different form) as in [11]. The expression (26) for the inhomogeneous part of the correlation function becomes

$$G_{ij}(\boldsymbol{r}) = \int \!\!\!\!\!\!- dz |\boldsymbol{r}|^z \gamma_a(z) c_1(z+\xi-2) \mathcal{P}_{ij}(z) \frac{\Gamma(-z/2)}{\Gamma\left(\frac{2+d+z}{2}\right)}, \tag{31}$$

where we have introduced the incompressibility tensor

$$\mathcal{P}_{ij}(z) = [(z+d-1)\delta_{ij} - z\hat{\mathbf{r}}_i\hat{\mathbf{r}}_j] \tag{32}$$

and irrelevant constant terms were absorbed in the forcing c_1.Henceforth such an assumption will always be implied unless stated otherwise.

B. Anisotropic sectors

Now the task is to find the poles of the inverse matrix of $\left(\widetilde{\lambda}\mathbf{1} + \mathbf{A} + \mathbf{B}\cdot\mathbf{X}\right)$, that are completely determined by the zeros of its determinant. Denoting

$$\mathbf{M} := \mathbf{A} + \mathbf{B}\cdot\mathbf{X} = \frac{\lambda_{l+d+z,d+\xi}}{d+\xi} \begin{pmatrix} \tau_{11} - \tau_{41} & \tau_{21} - (l-1)\tau_{31} + (l-1)l\tau_{41} \\ \tau_{12} - \tau_{42} & \tau_{22} - (l-1)\tau_{32} + (l-1)l\tau_{42} \end{pmatrix}, \tag{33}$$

where τ and λ are defined in appendix C, we may write

$$\det\left(\widetilde{\lambda}\mathbf{1} + \mathbf{M}\right) = \widetilde{\lambda}^2 + \widetilde{\lambda}\ \mathrm{tr}\mathbf{M} + \det\mathbf{M}. \tag{34}$$

We refrain from explicitly writing down the determinant, since the full expression is rather cumbersome and not very illuminating. It may however be easily reproduced by using the components τ_{ij} given in appendix C.

C. Two dimensions

The two dimensional case deserves some special attention. From the incompressibility requirement in eq. (B1) and by direct computation using the two dimensional spherical harmonics $\propto e^{\imath\theta}$, one can see that the correlation function satisfies the propotionality

$$\widehat{G}_{ij}(\boldsymbol{p}) \propto \left(\bar{g}^1 - l(l-1)\bar{g}^2\right) P_{ij}(\boldsymbol{p}). \tag{35}$$

Therefore in two dimensions the equation is a scalar one also in the anisotropic sectors. A formula for the solution then becomes

$$G_{ij}(\boldsymbol{r}) = -\int \!\!\!\!\!\!- dz |\boldsymbol{r}|^z \frac{\bar{c}^1 - l(l-1)\bar{c}^2}{\mathrm{F}_{11} - l(l-1)\mathrm{F}_{21}} (\widehat{\mathbf{P}}^{\mathrm{T}}\mathbf{K})^{1b} B^b_{ij}(\hat{\boldsymbol{r}}), \tag{36}$$

where $\mathbf{F} = \widetilde{\lambda}\mathbf{1} + \mathbf{A} + \mathbf{B}\cdot\mathbf{X}$.

D. Example: Passive Scalar

As one of the main themes of the present work is to consider the effect of a forcing localized around some finite wavenumber $m_f \propto 1/L$ instead of zero, it is useful to review the case in [7] by the present method (see e.g. [3, 9, 21] for more on the passive scalar problem), even more so as the magnetohydrodynamic case in two dimensions bears close resemblance to the passive scalar (indeed the two dimensional case can be completely described as a passive scalar problem with the stream function taking place of the scalar). Using the methods above, we arrive at an expression similar to (26),

$$G(\mathbf{r}) = \sum_l Y_l(\mathbf{r}) \int đz\, |\boldsymbol{r}|^z \, \frac{c^N(z+\xi-2)}{\psi_l(z)} \frac{\Gamma\left(\frac{l-z-\xi+2}{2}\right)}{\Gamma\left(\frac{l+z+d+\xi-2}{2}\right)}, \tag{37}$$

where we have again written the generic constant C' in which we will absorb finite constants. In the above equation, N equals zero or one corresponding to the nonzero and zero charge forcings and

$$\psi_l(z) = (d-1)(l-z)(l+z+d+\xi-2) + \xi l(l-1). \tag{38}$$

The strip of analyticity is now $-d-\xi < \mathcal{R}e(z) < 0$. Consider now the isotropic sector $l=0$ with the nonzero charge forcing, i.e. $N=0$. We then have (neglecting the zero modes)

$$G_{l=0}(\mathbf{x}) = C' L^{2-\xi} \int đz\, |\mathbf{r}/L|^z \, \frac{\Gamma\left(\frac{2-z-\xi}{2}\right)}{z\,(z+d+\xi-2)}. \tag{39}$$

For $r \ll L$ the integration contour must be completed from the right, thus capturing the poles $z = 0, z = 2-\xi, \ldots$. The small scale leading order behavior is therefore

$$G_{l=0} = C' \frac{\Gamma\,(1-\xi/2)}{d+\xi-2} L^{2-\xi} - C' \frac{1}{d(2-\xi)} r^{2-\xi} + \ldots \tag{40}$$

where the dots refer to higher order powers of r. The large scales $r \gg L$ require a left hand contour, resulting in another scaling regime,

$$G_{l=0} = C' \frac{\Gamma(d/2)}{d+\xi-2} L^d r^{2-d-\xi} + \ldots \tag{41}$$

We note that the above solution is constant at $r=0$ and zero at $r=\infty$, thus satisfying the boundary conditions. We conclude that the solution is completely nonanomalous, i.e.

respecting the canonical scaling.

Consider now instead the zero charge forcing with $N = 1$ that is localized around $p = 1/L$ instead of $p = 0$. The large scale pole due to the forcing at $z = -d - \xi + 2$ cancels out and we are left with

$$G_{l=0} = C' \int đz \, |\boldsymbol{r}/L|^z \, \frac{1}{z} \Gamma\left(\frac{2 - z - \xi}{2}\right). \tag{42}$$

There is now no large scale scaling behavior (the decay is faster than a power law). By looking at the $l = 2$ sector,

$$G_{l=2} = C'' L^{2-\xi} \int đz \frac{|\boldsymbol{r}/L|^z \, \Gamma\left(\frac{4-z-\xi}{2}\right)}{\psi_2(z)(z + \xi + d)\Gamma\left(z + d + \xi\right)}, \tag{43}$$

(with a different generic constant C''), we see that the relevant scaling behaviors are obtained from a solution of the equation

$$\psi_2(z) = d^2(-2 + z) - z(-2 + z + \xi) + d(-2 + z)(-1 + z + \xi) = 0, \tag{44}$$

giving the large scale behaviour of the $l = 2$ sector with the exponent

$$z_- = \frac{1}{2}\left(2 - d - \xi - \sqrt{(d - 2 + \xi)^2 + \frac{8d(d + \xi - 1)}{d - 1}}\right). \tag{45}$$

Therefore we conclude that the large scale behavior is dominated by the anisotropic modes. Note that the anisotropic modes are also anomalous in that they are not obtainable by dimensional analysis.

IV. MAGNETOHYDRODYNAMIC TURBULENCE

Setting $a = 1$ in eq. (1) yields the equations of magnetohydrodynamic turbulence (see e.g. [8, 15] and references therein). This is a special case in that the problem is completely local due to the vanishing of the pressure term. In practical terms, the quantity $\widetilde{\lambda}$ is zero, hence we only need to consider the zeros of the determinant of $\mathbf{M}$ in eq. (34).

A. Isotropic sector

The isotropic part of the correlation function becomes

$$G_{ij}(\boldsymbol{r}) = C' \int đz |\boldsymbol{r}|^z \frac{c_L^N(z + \xi - 2)}{p_0(z)} \mathcal{P}_{ij}(z) \frac{\Gamma\left(\frac{2-z-\xi}{2}\right)}{\Gamma\left(\frac{d+z+\xi}{2}\right)}, \tag{46}$$

where

$$p_0(z) = (d-1)z(d+z) + ((d-1)d+2z)\xi + (d-1)\xi^2 \tag{47}$$

with another generic constant C'. We find the usual poles at

$$\begin{aligned} z_n &= 2-\xi+2n, \\ z_\pm &= \frac{1}{2}\left(-d-\frac{2\xi}{d-1}\right) \pm \frac{\sqrt{d}}{2}\sqrt{d-\frac{4(d-2)\xi}{(d-1)}-\frac{4(d-2)\xi^2}{(d-1)^2}}, \end{aligned} \tag{48}$$

where n is a nonnegative integer. For the nonzero charge type forcing we have $c_L^0(z+\xi-2) \propto 1/(z+d+\xi-2)$, which presents another pole. On the other hand, for the zero charge forcing we have $c_L^1(z+\xi-2) \propto 1/(z+d+\xi)$, which cancels with a zero of the gamma function. It turns out that this sort of cancelation occurs for each model, rendering the large scale behavior anomalous. We will postpone the arbitrary dimensional case until the end of the present sector and instead consider first the three and two dimensional cases.

B. Anisotropic sectors

Note that since $\det \mathbf{M} \propto \lambda^2_{l+d+z,d+\xi}$, the inverse of $\mathbf{M}$ is only proportional to $\lambda^{-1}_{l+d+z,d+\xi}$, so the correct form to look at is actually $\det M/\lambda_{l+d+z,d+\xi}$. Dropping z -independent terms we have

$$\frac{\det \mathbf{M}}{\lambda_{l+d+z,d+\xi}} = C\frac{\Gamma\left(\frac{l-z-2}{2}\right)\Gamma\left(\frac{l+z+d+\xi-2}{2}\right)}{\Gamma\left(\frac{l+z+d+2}{2}\right)\Gamma\left(\frac{l-z-\xi+2}{2}\right)}\Psi_l(z), \tag{49}$$

where $\Psi_l(z)$ is a fourth order polynomial in z and C is a z -independent constant. Due to its rather lengthy expression, we shall consider the whole problem in three and two dimensions only. We note immediately that there's also an infinite number of solutions due to one of the gamma functions, namely at

$$z = l+2-\xi+2n \tag{50}$$

for nonnegative integers n and even l. The other gamma function cancels with the terms from (D2).

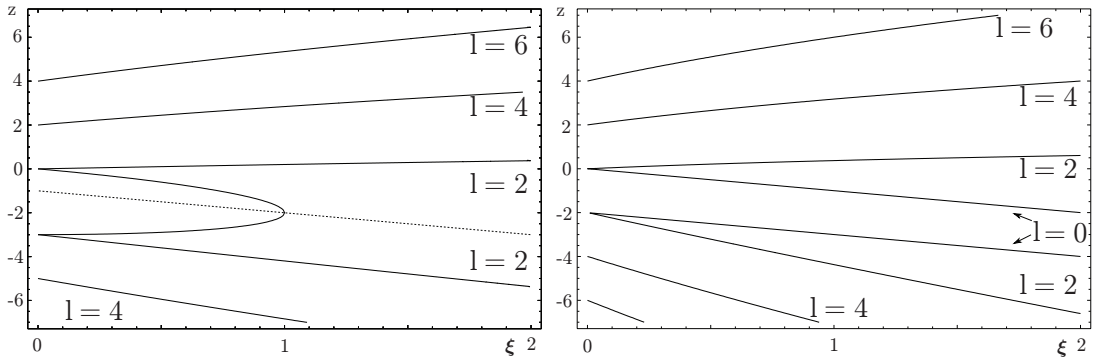

(a) d=3 (b) d=2

FIG. 1: The MHD scaling exponents of the isotropic, $l = 2$, $l = 4$ and $l = 6$. In (a) The isotropic poles $z_+ \geq z-$ are adjoined at $\xi = 1$. The dashed line in (a) corresponds to the forcing with nonzero charge with a pole at $-1 - \xi$, whereas for the zero charge forcing there are no poles. In (b) the zero modes are never adjoined.

C. d=3

We have the four solutions to $\Psi_l(z) = 0$ of which the following two are dominant in the small and large scales,

$$z_l^{\pm} = -\frac{3+\xi}{2} \pm \frac{1}{2}\sqrt{A \mp 2(2-\xi)\sqrt{B}}, \tag{51}$$

where

$$\begin{aligned} A &= (2+\xi)\,(2l(l+1) - 6 - \xi) + 17, \\ B &= (2+\xi)\,(2l(l+1) + \xi) + 1, \end{aligned} \tag{52}$$

which match exactly to the results obtained in [14, 17], after some convenient simplifications. The isotropic zero modes are

$$z_{\pm} = \frac{1}{2}\left(3 - \xi \pm \sqrt{3(1-\xi)(3+\xi)}\right). \tag{53}$$

We have plotted the leading poles in Fig. (1) from $l = 0$ to $l = 6$ together with the pole due to the nonzero charge. We note that the isotropic exponents become complex valued for

$\xi > 1$, implying an oscillating behavior and therefore a positive Lyapunov exponent for the time evolution [8, 15]. The above steady state assumption therefore applies for $0 \leq \xi \leq 1$ only in the isotropic sector. The fact that the anisotropic exponents are continuous curves for all $0 \leq \xi \leq 2$ seems to imply that the steady state exists for all ξ in the anisotropic sectors. Indeed, in [14] this was shown to be the case by preforming a more careful eigenvalue analysis.

1. Nonzero forcing charge

In the isotropic sector for the forcing with nonzero charge $N = 0$ we have

$$G_{ij}(\boldsymbol{r})|_{l=0} \quad = -C' L^{2-\xi} \int \!\!\!\!\!\!- dz \frac{|\boldsymbol{r}/L|^z \mathcal{P}_{ij}(z) \Gamma\left(\frac{2-z-\xi}{2}\right)}{(z-z_-)(z-z_+)(z+1+\xi)\Gamma\left(\frac{3+z+\xi}{2}\right)} \tag{54}$$

with the contour bound $-1-\xi < \mathcal{R}e(z) < 0$ and $z_- < -1-\xi < z_+ < 0$. C' again denotes some generic finite (and positive) constant. The pole z_+ divides the strip of analyticity in two parts, which correspond to different boundary conditions. Small scale behavior corresponds to picking up the poles to the right of the contour and large scale behavior corresponds to left hand side poles. We note that both the zero modes $z_\pm$ are negative, except that $z_+ = 0$ at $\xi = 0$. Therefore z_+ cannot be a large scale exponent, as the solution has to decay at infinity. The real strip of analyticity is then in fact $-1-\xi < \mathcal{R}e(z) < z_+$, thus resulting in the small scale behavior

$$G_{ij}^{<} = C_1 r^{z_+} \mathcal{P}_{ij}(z_+) \tag{55}$$

and the large scale behavior

$$G_{ij}^{>} = C_2 r^{-1-\xi} \mathcal{P}_{ij}(-1-\xi) \tag{56}$$

We note that the large scale behavior is determined by the forcing and therefore respects canonical scaling.

2. Zero charge forcing

Because of the pole cancelation we now have a similar expression,

$$G_{ij}(\boldsymbol{r})|_{l=0} \quad = C' L^{2-\xi} \int \!\!\!\!\!\!- dz \frac{|\boldsymbol{r}/L|^z \mathcal{P}_{ij}(z) \Gamma\left(\frac{2-z-\xi}{2}\right)}{(z-z_-)(z-z_+)\Gamma\left(\frac{5+z+\xi}{2}\right)} \tag{57}$$

with the strip of analyticity is now $-3-\xi < \mathcal{R}e(z) < 0$. The contour bound now encloses both the zero modes (see again Fig. (1)). In addition to the above considerations with a forcing of nonzero charge, we conclude that z_- cannot be present at small scales due to regularity conditions at $\xi = 0$, so the real strip of analyticity is in fact $z_- < \mathcal{R}e(z) < z_+$. This gives rise to the small scale behavior

$$G_{ij}^{<} = C_1 r^{z_+} \mathcal{P}_{ij}(z_+) \tag{58}$$

for the small scales and

$$G_{ij}^{>} = C_2 r^{z_-} \mathcal{P}_{ij}(z_-) \tag{59}$$

for the large scales. The large scales are therefore dominated by the smaller zero mode z_- instead of the exponent $-1-\xi$ as with the nonzero charge forcing and is therefore anomalous. However, unlike in the passive scalar case, the anisotropic exponents are subdominant at both small and large scales (see Fig. (1)) and we therefore conclude that there is isotropization at both scales.

D. d=2

The (dominant) zero modes in two dimensions are

$$\begin{aligned} z_l^+ &= -4-\xi+\sqrt{4l^2(1+\xi)+\xi^2} \\ z_l^- &= -3\xi-\sqrt{4l^2(1+\xi)+\xi^2} \end{aligned} \tag{60}$$

of which we separately mention the isotropic zero modes,

$$\begin{aligned} z_+ &= -\xi \\ z_- &= -2-\xi. \end{aligned} \tag{61}$$

The expression for the inhomogeneous part of the correlation function is

$$G_{ij}(\boldsymbol{r})|_{l=0} = C' L^{2-\xi} \int \mathrm{d}z |\boldsymbol{r}/L|^z c_L(z+\xi-2) \mathcal{P}_{ij}(z) \frac{\Gamma\left(\frac{-z-\xi}{2}\right)}{\Gamma\left(\frac{4+z+\xi}{2}\right)} \tag{62}$$

with contour bound is $-2-\xi < z < 0$ together with the bound from the forcing.

1. Nonzero charge forcing

Because $c_L \propto 1/(z+\xi)$, the expression for the isotropic sector of the correlation function simplifies to

$$G_{ij}(\boldsymbol{r})|_{l=0} \quad = C' L^{2-\xi} \int đz |\boldsymbol{r}/L|^z \mathcal{P}_{ij}(z) \frac{\Gamma\left(\frac{-z-\xi}{2}\right)}{(z+\xi)\Gamma\left(\frac{4+z+\xi}{2}\right)} \tag{63}$$

where the bound is now $-\xi < \mathcal{R}e(z) < 0$. Note the appearance of a double pole at $z = -\xi$ giving rise to logarithmic behavior. There are now no poles inside the contour bound, so finding the asymptotics is easy. We observe that there are no small scale poles and therefore the correlation function decays faster than any power at small scales, whereas at large scales we have

$$G_{ij}^{>} \quad = C' \log(r/L) L^{2-\xi} |r/L|^{-\xi} \mathcal{P}_{ij}(-\xi) + C' L^{2-\xi} |r/L|^{-\xi} \mathcal{P}'_{ij}(-\xi), \tag{64}$$

where $\mathcal{P}'_{ij}(-\xi) = \delta_{ij} - \hat{\mathbf{r}}_i \hat{\mathbf{r}}_j$ to ensure incompressibility and other next to leading order nonlogarithmic terms were discarded. By looking at Fig. (1) we see that there is a hierarchy of small scale exponents in the anisotropic sectors. We therefore make the conclusion that in two dimensions the anisotropic effects in the MHD model are dominant at small scales for a forcing of nonvanishing charge, conversely to the passive scalar case. Note that setting $\xi = 0$ in the above equation reproduces correctly the usual logarithmic behavior of the diffusion equation steady state with an infrared finite large scale forcing.

2. Zero charge forcing

We now have $c_L \propto 1/(z+\xi+2)$ and the isotropic correlation function becomes

$$G_{ij}(\boldsymbol{r})|_{l=0} \quad = -C' L^{2-\xi} \int đz |\boldsymbol{r}/L|^z \mathcal{P}_{ij}(z) \frac{\Gamma\left(-1-\frac{z+\xi}{2}\right)}{\Gamma\left(\frac{4+z+\xi}{2}\right)} \tag{65}$$

with the usual strip $-2-\xi < \mathcal{R}e(z) < 0$. There are no double poles and the leading simple poles are just at $z = -\xi$ and $z = -2-\xi$, so the asymptotic behaviours at small and large scales are simply

$$\begin{aligned} G_{ij}^{<} \quad &= C' |r/L|^{-\xi} \mathcal{P}_{ij}(-\xi) \\ G_{ij}^{>} \quad &= C' |r/L|^{-2-\xi} \mathcal{P}_{ij}(-2-\xi). \end{aligned} \tag{66}$$

As in the three dimensional case, all the anisotropic exponents are now subleading at both small and large scales (see Fig. (1)), so we conclude that there is again isotropization at both regimes. Note also that the large scale behavior is due to the forcing and therefore nonanomalous.

3. Any dimension, zero charge forcing

For the sake of completeness, we write explicitly the solutions in any dimension $d > 2$ in the isotropic sector for the zero charge forcing:

$$\begin{aligned} G_{ij}^{<} &= \frac{C'}{2} L^{2-\xi} |r/L|^{z_+} \frac{\mathcal{P}_{ij}(z_+)}{z_+ - z_-} \frac{\Gamma\left(\frac{2-z_+-\xi}{2}\right)}{\Gamma\left(\frac{2+d+z_++\xi}{2}\right)} \\ &\quad - C' r^{2-\xi} \frac{\mathcal{P}_{ij}(2-\xi)}{(2-\xi-z_-)(2-\xi-z_+)} \frac{1}{\Gamma\left(2+d/2\right)} + \mathcal{O}(r^{4-\xi}), \\ G_{ij}^{>} &= \frac{C'}{2} L^{2-\xi} |r/L|^{z_-} \frac{\mathcal{P}_{ij}(z_-)}{z_+ - z_-} \frac{\Gamma\left(\frac{2-z_--\xi}{2}\right)}{\Gamma\left(\frac{2+d+z_-+\xi}{2}\right)} \end{aligned} \tag{67}$$

where we have neglected the possible exponentially decaying terms. The anisotropic sectors produce rather cumbersome expressions and we will be satisfied with only the numerical results in the figures. We observe that the large scale behavior is always dominated by the negative zero mode exponent z_- and is therefore always anomalous (except in two dimensions). It is also fairly easy to see that the anisotropic exponents are always subdominant, so that there is isotropization at both small and large scales.

V. LINEAR PRESSURE MODEL

Setting $a = 0$ in eq. (1) produces the equation known as the Linear Pressure Model (LPM) (see e.g. [11, 12, 18] and references therein; sometimes this model is just called the passive vector model) By looking at equation (A9), we see that when $\widehat{G} \propto \delta^{(d)}(\boldsymbol{p})$, the left hand side evaluates to $\propto a^2 |\boldsymbol{p}|^{2-d-\xi} P_{ij}(\boldsymbol{p})$. Therefore for $a = 0$ there is a constant zero mode analogously to the passive scalar case. This is true for the anisotropic sectors as well ([12, 18]). This constant zero mode however vanishes for the structure function, so in the present case we also consider the next to leading order term. The first thing to note in the

isotropic sector is that when $a = 0$, $z = -d$ is a solution of the equation

$$\frac{1}{\gamma_0(z)} = 2(d+1)\Gamma\left(1+\xi/2\right)\Gamma\left(1+d/2\right) + p_0(z)\frac{\Gamma\left(1-z/2\right)\Gamma\left(\frac{d+z+\xi}{2}\right)\Gamma\left(\frac{4+d-\xi}{2}\right)}{\Gamma\left(\frac{2+d+z}{2}\right)\Gamma\left(\frac{4-z-\xi}{2}\right)} = 0, \tag{68}$$

where

$$p_0(z) = (d^2 - z)(z + \xi - 2) + d(z-2)(z+\xi-1) - \xi. \tag{69}$$

However, as we see from the definition of the incompressibility tensor in eq. (32), for the trace (in indices) we have

$$\mathcal{P}_{ii}(z) = (d-1)(d+z), \tag{70}$$

which produces a canceling $z+d$ term in the numerator. A physically more realistic quantity would however be a contraction with $\widehat{\boldsymbol{x}}^i\widehat{\boldsymbol{x}}^j$ than the trace, since we are more interested in the structure functions of the model. Another exact solution is $z = 2-\xi$. Other nonperturbative solutions can only be obtained numerically.

A. Any dimension

We have plotted some of the poles in Fig. (2) in three dimensions. Remembering the $z = -3$ solution, we see that the anisotropic exponents are less dominant with increasing l (a behavior repeated for higher l as well).

1. Nonzero charge forcing

The contour bound is now $2-d-\xi < \mathcal{R}e(z) < 0$, so there is no controversy in the choice of which poles to include. The small and large scale behaviors are similar to the passive scalar, and for completeness, we give the results in any dimension:

$$\begin{aligned} G^{<}_{ij} &= AL^{2-\xi}\delta_{ij} - Br^{2-\xi}\mathcal{P}_{ij}(2-\xi) \\ G^{>}_{ij} &= A'L^{2-\xi}|r/L|^{2-d-\xi}\mathcal{P}_{ij}(2-d-\xi). \end{aligned} \tag{71}$$

The A, B and A' are somewhat complicated transcendental functions of d and ξ.

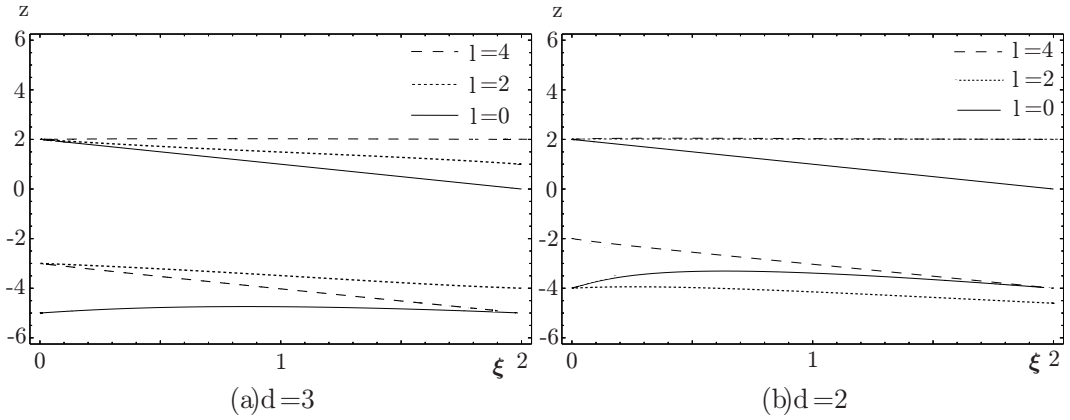

FIG. 2: The Linear Pressure Model scaling exponents of the sectors $l = 0$, $l = 2$ and $l = 4$ in three (a) and two (b) dimensions. The $z = 0$ and $z = -d$ are omitted for the sake of clarity. We note that in two dimensions, there is a $z = 2$ exponent in the $l = 2$ sector but the $l = 4$ sector's exponent goes slightly above $z = 2$.

2. Zero charge forcing

Now the forcing contributes a pole $\propto 1/(z + \xi + d)$ and the contour bound is $-d - \xi < \mathcal{R}e(z) < 0$. The quantity γ_0 in eq. (68) has a zero there that cancels with the pole from the forcing. Therefore we again conclude that the forcing doesn't contribute in the scaling. The small scale behavior is therefore same as above, but the large scale isotropic sector of the correlation function behaves as

$$G_{ij}^{>} = C'|L|^{2-\xi}\left(A'|r/L|^{-d}\mathcal{P}_{ij}(-d) + B'|r/L|^{z_-}\mathcal{P}_{ij}(z_-)\right), \tag{72}$$

where A' and B' are again some nonzero constants (depending of d and ξ), z_- is the $l = 2$ large scale mode (see Fig. (2)) and we have the traceless tensor

$$\mathcal{P}_{ij}(-d) = d\hat{\boldsymbol{r}}_i\hat{\boldsymbol{r}}_j - \delta_{ij}. \tag{73}$$

By looking at Fig. (2) we observe that the subleading exponent z_- is smaller than the anisotropic exponent $l = 2$ in three dimensions and $l = 4$ at two dimensions (except when ξ is close to two, when the $l = 2$ exponent is larger than the $l = 4$ exponent). Therefore the *trace* of the correlation function is dominated by the anisotropic modes.

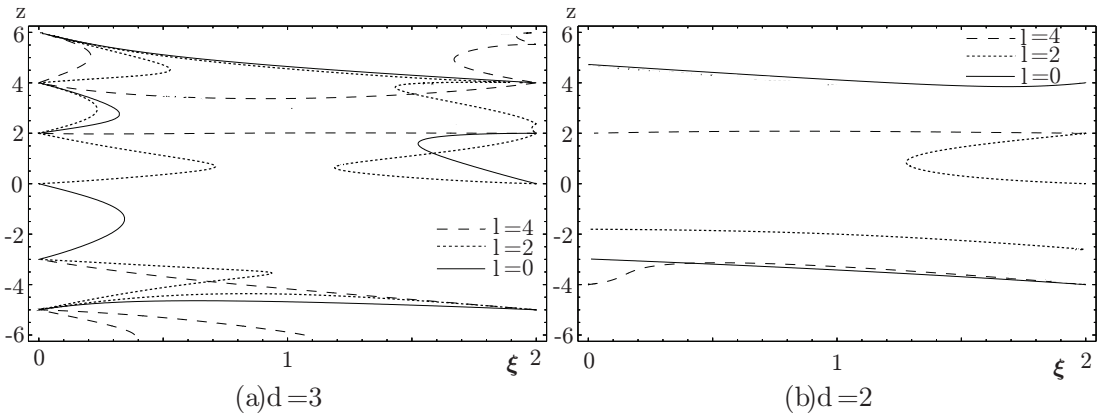

FIG. 3: The Linearized Navier-Stokes equation exponents for sectors $l = 0$, $l = 2$ and $l = 4$ (the legend applies to both figures) at three and two dimensions. In (a) the $l = 4$ curves run slightly below and above the curves $z = -3 - \xi$ and $z = 2$, respectively. Other than leading exponents are also displayed.

VI. LINEARIZED NAVIER-STOKES EQUATION

Setting $a = -1$ in eq. (1) yields the Linearized Navier-Stokes equation (see e.g. [1, 25, 26]). The equation may be considered as zeroth order perturbation theory of the full Navier-Stokes turbulence problem, from which one can at least in principle proceed to higher orders in perturbation theory. It will also serve as a stability problem where the background flow is determined by the Kraichnan ensemble instead of a solution to the Navier-Stokes equation (see chapter III of [26]). Not much is known of this case, except for the perturbative results in [11, 12]. The eq. (29) becomes

$$\begin{aligned}\frac{1}{\gamma_{-1}(z)} &= 4(d+\xi)\Gamma\left(1+\xi/2\right)\Gamma\left(1+d/2\right) \\ &-p_{-1}(z)\frac{\Gamma\left(-z/2\right)\Gamma\left(\frac{d+z+\xi}{2}\right)\Gamma\left(\frac{4+d-\xi}{2}\right)}{2\Gamma\left(\frac{2+d+z}{2}\right)\Gamma\left(\frac{4-z-\xi}{2}\right)},\end{aligned} \tag{74}$$

with

$$\begin{aligned}p_{-1}(z) &= (z+\xi)\left(-2z+2\xi+d^2(z+\xi-2)\right. \\ &\left.-(z+\xi)^2+d(2+(z-3)z-(3-\xi)\xi)\right)+4z^2.\end{aligned} \tag{75}$$

We choose to save space by not writing down explicitly the determinant for the anisotropic sectors. The expression may be reproduced by using the results of appendix C. We will also

refrain from explicitly writing down expressions for the correlation functions, as it turns out that whichever sector has the leading exponents varies quite a bit with different values of ξ.

A. d=3 with zero charge forcing

The contour bound is, as usual, $-3-\xi < \mathcal{R}e(z) < 0$ and again one observes a cancelation of the corresponding pole. Inspecting Fig. (3) one observes quite wild behavior of the various scaling exponents at a first few sectors. A notable similarity to the three dimensional MHD case ($a = 1$) are the exponents starting at 0 and -3 and joining at $\xi \approx 0,35$. However in the LNS case one also sees similar behavior near $\xi = 2$. Indeed one is tempted to assume the existence of a steady state only for ξ near zero and two. The same conclusion could be drawn for the anisotropic sectors as well. We will further discuss this at the end of the paper. We will be satisfied with only reporting the scaling behaviors as the procedure for finding them is close to above cases. Assuming the steady state exists for ξ close enough to zero and two, we conclude that for ξ near zero, the small and large scale are dominated by the isotropic exponents starting at 0 and -3, respectively. For ξ near 2, one instead observes $l = 2$ dominance at small scales and $l = 4$ dominance at large scales. We have deliberately neglected the nonzero charge forcing, as that would only bring about the familiar nonanomalous $-1 - \xi$ scaling at large scales.

B. $d = 2$ with zero charge forcing

The behavior of the scaling exponents are much nicer, as can be seen by looking at Fig. (3). For $0 \leq \xi \lesssim 1,3$, we see the small scales dominated by the $l = 4$ anisotropic sector, and the large scale by the $l = 2$ sector. For other values of ξ the $l = 2$ anisotropic sector dominates the small scales as well. The $l > 4$ anisotropic exponents are all subleading with respect to the ones in the figure, and indeed respect the usual hierarchy of exponents [11]. In any case, the isotropic exponent is subleading.

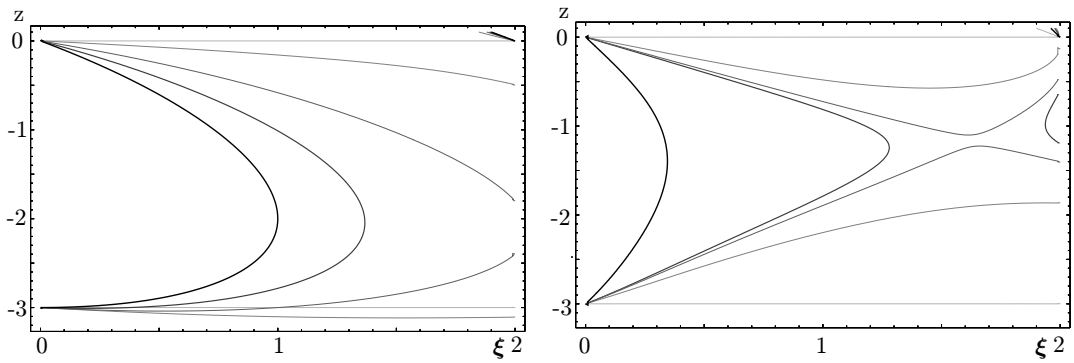

(a) (b)

FIG. 4: The leading isotropic exponents as a is varied from 1 to 0 (a) and from -1 to 0 (b) in three dimensions. The darkest curves correspond to $a = 1$ and $a = -1$.

VII. THE EFFECT OF VARYING THE PARAMETER a

It is useful to discuss also other values of a beside the discrete values $a = 1, 0, -1$. More specifically, looking at Fig. (4) we see how the closed contour determining the leading scaling exponents is deformed as a varies from $a = 1$ and $a = -1$ to 0. Both end up as curves $z = 0$ and $z = -3$. Also, as we know that when $a = 1$ the steady state exists for $\xi < 1$ in the isotropic sector [8] (and for all ξ in the anisotropic sectors [14]), it now seems even more reasonable to expect the steady state to exist for all ξ in the $a = 0$ case.

VIII. CONCLUSION

The purpose of the present paper was to present an exact solution for the two point function of the so-called a -model in the small and large scaling regimes, which incorporates the magnetohydrodynamic equations, the linear pressure model and the linearized Navier-Stokes equations. The phenomena of anomalous scaling and anisotropy dominance was investigated in each model with emphasis placed in the zero charge forcing concentrated at a finite wavenumber $\sim 1/L$ as in [6]. Below we briefly summarize the findings in each model.

For the magnetohydrodynamic equations with $a = 1$ the leading scaling behavior was observed to be anomalous and isotropic at both small and large scales in three

dimensions for the zero charge forcing, in accordance with previous small scale results [13, 14, 17]. In two dimensions with nonzero charge forcing one observes anomalous and anisotropic behavior at small scales, while the large scales are dominated by logarithmic behavior. The mechanism of the small scale anisotropy dominance is strikingly similar to the passive scalar *large* scale anisotropy dominance, except that in the MHD case the phenomenon results from the *nonzero* charge forcing. The zero charge forcing case in two dimensions is in agreement with the results in [8].

For the linear pressure model with $a = 0$ and zero charge we recovered the small scale exponents of [18]. The small scale behavior is now dominated by the isotropic and canonical scaling exponent $z = 2 - \xi$ (neglecting the constant mode by considering the structure function). The large scale behavior was seen to be dominated by a curious isotropic zero mode $z = -d$, although the *trace* of the structure function exhibits anomalous and anisotropic behavior at large scales. The nonzero charge forcing simply renders the large scale behavior canonical. The existence of the steady state is nevertheless controversial in two dimensions and requires further study.

The linearized Navier-Stokes equations corresponding to $a = -1$ seem to be the most interesting of the models considered, even more so because it is also the least well known. There still remains the question of the existence of the steady state, without which one cannot claim to have completely solved the problem. One may however conjecture it's existence at least for small enough ξ (at least in the isotropic sector), in which case the small and large scales are dominated by the isotropic anomalous scaling exponents in three dimensions. In two dimensions, the small scale exponents coincide with the somewhat rough numerical estimates of [20], the difference now being the absence of the scaling $\propto r^{-\xi}$ due to the forcing. Indeed, it was observed that both the small and large scales were dominated by anomalous *anisotropic* scaling exponents.

Although the linear equations above with the somewhat crude Kraichnan model are certainly some distance from the real problem of turbulence, similar scaling behavior has been observed in real and numerical simulations (see e.g. [24, 27] and references therein), namely implying that the scaling exponents in each anisotropic sector are universal as

outlined above. Probably the closest case to the real Navier-Stokes turbulence is the linearized Navier-Stokes equation. The equation arises usually as one tries to verify the stability of a given stationary flow by decomposing the velocity field as $v + u$, where v is the stationary, time independent term and u is a small perturbation [26]. If one can show that u decays in time, the velocity field v is indeed a laminar, stable flow. In our case v is determined by the Kraichnan model and we are now concerned with the stability of the statistical steady state. It has been pointed out in [12] that in such a case one might be able to show that higher order perturbative terms are irrelevant in the sense of the renormalization group, thus implying that the steady state is in fact in the same universality class as the full NS turbulence. This would mean that the anomalous scaling exponent of the linear model is equal to the NS turbulence exponent. All this would of course depend on the existence of the steady state for u. Unfortunately it seems that such a steady state does not exist for the exponent $\xi = 2/3$, which could be a sign of incompleteness of the Kraichnan model or a symptom of the general complexity of the problem of turbulence. The stability and existence problem will be studied more carefully in a future paper by the present author.

Acknowledgments

The author wishes to thank P. Muratore-Ginanneschi, A. Kupiainen and I. Fouxon for useful discussions, suggestions and help on the matter. This work was supported by the Academy of Finland "*Centre of excellence in Analysis and Dynamics Research*" and TEKES project n. 40289/05 "*From Discrete to Continuous models for Multiphase Flows*".

APPENDIX A: EQUATION OF MOTION FOR THE PAIR CORRELATION FUNCTION

We take the Fourier transform of equation (1) and rewrite it as a stochastic partial differential equation of Stratonovich type as

$$d\widehat{u}_i(\boldsymbol{p}) = -\nu p^2 \widehat{u}_i(\boldsymbol{p})dt - \widehat{\mathcal{D}}^p_{i\mu\nu} \int \!\!\!\!\!\!- d^d\boldsymbol{q} d\widehat{V}_\nu(\boldsymbol{q}) \circ \widehat{u}_\mu(\boldsymbol{p}-\boldsymbol{q}) + d\widehat{F}_i(\boldsymbol{p}), \tag{A1}$$

where we have dropped the t -dependence and denoted

$$\widehat{\mathcal{D}}^p_{iab} = i\left(\delta_{ia}p_b - a\delta_{ib}p_a\right) + i(a-1)p_i p_a p_b/p^2 \tag{A2}$$

and defined the Stratonovich product

$$d\widehat{V}_\nu(\boldsymbol{q}) \circ \widehat{u}_\mu(\boldsymbol{p}-\boldsymbol{q}) = d\widehat{V}_\nu(t,\boldsymbol{q})\widehat{u}_\mu(t+\frac{dt}{2},\boldsymbol{p}-\boldsymbol{q}). \tag{A3}$$

As argued in [28] by physical grounds, the symmetric prescription $\theta(0) = 1/2$, corresponding to the Stratonovich definition of the SPDE, is the correct way of defining the equation. We will however use the relation $\widehat{u}_\mu(t+\frac{dt}{2},\boldsymbol{p}) = \widehat{u}_\mu(t,\boldsymbol{p}) + \frac{1}{2}d\widehat{u}_\mu(t,\boldsymbol{p})$ to transform the equation into a following Itô SPDE,

$$\begin{aligned} d\widehat{u}_i(\boldsymbol{p}) = &-\nu p^2\widehat{u}_i(\boldsymbol{p})dt + \frac{1}{2}\widehat{\mathcal{D}}^p_{i\mu\nu}\int\!\!d^d\boldsymbol{q}\,\widehat{D}_{\nu\sigma}(\boldsymbol{q})\widehat{\mathcal{D}}^{p-q}_{\mu\rho\sigma}\widehat{u}_\rho(\boldsymbol{p}) \\ &\ldots - \widehat{\mathcal{D}}^p_{i\mu\nu}\int\!\!d^d\boldsymbol{q}\,d\widehat{V}_\nu(\boldsymbol{q})\widehat{u}_\mu(\boldsymbol{p}-\boldsymbol{q}) + d\widehat{F}_i(\boldsymbol{p}), \end{aligned} \tag{A4}$$

where we have used the relation

$$d\widehat{V}_i(t,\boldsymbol{p})d\widehat{V}_j(t,\boldsymbol{p}') = \widehat{D}_{ij}(\boldsymbol{p})\delta^d(\boldsymbol{p}+\boldsymbol{p}')dt. \tag{A5}$$

The first integral on the right hand side of the Itô SPDE can be done explicitly, resulting in

$$-\frac{1}{2}\widehat{\mathcal{D}}^p_{i\mu\nu}\int\!\!d^d\boldsymbol{q}\,\widehat{D}_{\nu\sigma}(\boldsymbol{q})\widehat{\mathcal{D}}^{p-q}_{\mu\rho\sigma}\widehat{u}_\rho(\boldsymbol{p}) = Dm_v^{-\xi}p^2\widehat{u}_i(\boldsymbol{p}) + \widetilde{\lambda}p^{2-\xi}\widehat{u}_i(\boldsymbol{p}) + \mathcal{O}(m_v^+), \tag{A6}$$

where the incompressibility condition $p_i\widehat{u}_i(\boldsymbol{p}) = 0$ was used, and denoting

$$\widetilde{\lambda} = (a-1)\left(d+1+a(1-\xi)\right)\frac{d\pi\xi\csc(\pi\xi/2)\Gamma(d/2)c_d}{16\Gamma\left(\frac{d-\xi}{2}+2\right)\Gamma\left(\frac{d+\xi}{2}+1\right)}. \tag{A7}$$

Applying the Itô formula to the quantity

$$\langle\widehat{u}_i(t,\boldsymbol{p})\widehat{u}_j(t,\boldsymbol{p}')\rangle \doteq \widehat{G}_{ij}(t,\boldsymbol{p})\delta^d(\boldsymbol{p}+\boldsymbol{p}') \tag{A8}$$

and by assuming stationarity, one obtains the nonlocal PDE (with obvious $\boldsymbol{p}$ dependence omitted)

$$\left[2\nu - Dm_v^{-\xi}\right]|\boldsymbol{p}|^2\widehat{G}_{ij} - \widetilde{\lambda}D_0|\boldsymbol{p}|^{2-\xi}\widehat{G}_{ij} + \widehat{\mathcal{D}}^p_{i\mu\nu}\widehat{\mathcal{D}}^{-p}_{j\rho\sigma}\int\!\!d^d\boldsymbol{q}\,\widehat{D}_{\nu\sigma}(\boldsymbol{q})\widehat{G}_{\mu\rho}(\boldsymbol{p}-\boldsymbol{q}) = \widehat{C}_{ij}. \tag{A9}$$

Using the SO(d) decomposition for $\widehat{G}$,

$$\widehat{G}_{ij}(\boldsymbol{p}) := \sum_a B^a_{ij}(\hat{\boldsymbol{p}})\widehat{G}^a(p) \tag{A10}$$

(and similarly for $\widehat{C}$), dividing the equation by p^2, and by taking the Mellin transform of the equation while remembering the definition

$$\widehat{G}^z_{ij}(\boldsymbol{p}) = \int_0^\infty \frac{dw}{w} w^{d+z} \widehat{G}_{ij}(w\boldsymbol{p}) = |\boldsymbol{p}|^{-d-z} \sum_q B^a_{ij}(\hat{\boldsymbol{p}}) \bar{g}_a(z), \tag{A11}$$

and by expressing $\widehat{D}$ in the integrand as an inverse Mellin transform, we finally obtain the equation

$$\begin{aligned}\left[2\nu - Dm_v^{-\xi}\right] \bar{g}_b(z) - \widetilde{\lambda} D_0 \bar{g}_b(z-\xi) + \int \!\!\!\!\!\!- dz' \bar{d}_{m_v}(z') \mathrm{T}^{bc}_{d+z',d+z-z'} \bar{g}_c(z-z') \\ = \bar{c}_b(z-2),\end{aligned} \tag{A12}$$

where we have defined (note the transpose in definition)

$$\sum_b \mathrm{T}^{cb}_{d+z',d+z-z'} B^c_{ij}(\hat{\boldsymbol{p}}) = |\boldsymbol{p}|^{d+z-2} \mathcal{D}^{\boldsymbol{p}}_{i\mu\nu} \mathcal{D}^{-\boldsymbol{p}}_{j\rho\sigma} \int \!\!\!\!\!\!- d^d\boldsymbol{q} \frac{P_{\nu\sigma}(\boldsymbol{p}-\boldsymbol{q}) B^b_{\mu\rho}(\boldsymbol{q})}{|\boldsymbol{p}-\boldsymbol{q}|^{d+z'} |\boldsymbol{q}|^{d+z-z'}}, \tag{A13}$$

with the strips of analyticity,

$$\begin{aligned}\mathcal{R}e(z) - \mathcal{R}e(z') &< 0 \\ \mathcal{R}e(z') &< 0 \\ d + \mathcal{R}e(z) &> 0\end{aligned} \tag{A14}$$

such that the 9×9 matrix $\mathbf{T}$ is independent of $\boldsymbol{p}$. The matrix elements T^{bc} can be determined exactly by computing the right hand side integral, which is the subject of the next appendix. As mentioned in sec. II D, the first poles on the right occur at $z' = 0$ and $z' = \xi$, which results in the equation in the limit of vanishing m_v:

$$\begin{aligned}\left[2\nu - Dm_v^{-\xi}\right] \bar{g}_b(z) - D_0 \widetilde{\lambda} \bar{g}_b(z-\xi) + \bar{d}_{m_v}(0) \mathrm{R}^{bc} \bar{g}_c(z) - D_0 \mathrm{T}^{bc}_{d+\xi,d+z-\xi}(z) \bar{g}_c(z-\xi) \\ = \bar{c}_b(z-2).\end{aligned} \tag{A15}$$

We have defined the residue matrix

$$\mathrm{R}^{bc} = \mathcal{R}\left(\mathrm{T}^{bc}_{d+z',d+z-z'}\right)|_{z'=0} \tag{A16}$$

and used the residue of the velocity correlation at $z' = \xi$:

$$\mathcal{R}_{z'=\xi}\left(\bar{d}_{m_v}(z')\right) = -D_0. \tag{A17}$$

APPENDIX B: INCOMPRESSIBILITY CONDITION

The incompressibility condition for u and f amounts to requiring that the contraction of the covariances (16) with $\boldsymbol{p}$ is zero, i.e.

$$\begin{aligned} |\boldsymbol{p}|^{d+z+l} p_i \widehat{G}^z_{ij}(\boldsymbol{p}) &= (p_j \bar{g}_1 + l p_j \bar{g}_3 + p_j \bar{g}_4)\, \Phi^l(\boldsymbol{p}) + |\boldsymbol{p}|^2 \left((l-1)\bar{g}_2 \partial_j + \bar{g}_3 \partial_j\right) \Phi^l(\boldsymbol{p}) \\ &\equiv 0, \end{aligned} \tag{B1}$$

which gives a system of equations

$$\begin{aligned} \bar{g}_1 + l\bar{g}_3 + \bar{g}_4 &= 0 \\ (l-1)\bar{g}_2 + \bar{g}_3 &= 0. \end{aligned} \tag{B2}$$

We can achieve this conveniently by defining a projection operator

$$\widehat{\mathbf{P}} = \begin{pmatrix} \mathbf{1} & 0 \\ \mathbf{X} & 0 \end{pmatrix}, \tag{B3}$$

where

$$\mathbf{X} = \begin{pmatrix} 0 & -(l-1) \\ -1 & l(l-1) \end{pmatrix}. \tag{B4}$$

The solution to eq. (B2) (and a similar one for the forcing) can then be written conveniently as

$$\bar{\mathbf{g}} := \begin{pmatrix} \bar{\mathbf{h}} \\ \mathbf{X} \cdot \bar{\mathbf{h}} \end{pmatrix}; \bar{\mathbf{c}} := \begin{pmatrix} \bar{\mathbf{f}} \\ \mathbf{X} \cdot \bar{\mathbf{f}} \end{pmatrix}. \tag{B5}$$

We also rewrite the matrices $\mathbf{R}$ and $\mathbf{T}$ in block form as

$$\mathbf{R} = \begin{pmatrix} \mathbf{R}_1 & \mathbf{R}_2 \\ \mathbf{R}_3 & \mathbf{R}_4 \end{pmatrix}; \mathbf{T}_{d+\xi, d+z} = \begin{pmatrix} \mathbf{A} & \mathbf{B} \\ \mathbf{C} & \mathbf{D} \end{pmatrix}. \tag{B6}$$

Note the above definition of $\mathbf{T}$ with a translation $z \to z + \xi$. $\mathbf{R}$ is independent of z. By operating with $\widehat{\mathbf{P}}$ on eq. (23), we obtain the equations (after translation $z \to z + \xi$),

$$\begin{aligned} &\left[2\nu - D m_v^{-\xi}\right] \bar{\mathbf{h}}(z+\xi) + \bar{d}_{m_v}(0)\, (\mathbf{R}_1 + \mathbf{R}_2 \cdot \mathbf{X}) \bar{\mathbf{h}}(z+\xi) - \widetilde{\lambda} D_0 \bar{\mathbf{h}}(z) - D_0\, (\mathbf{A} + \mathbf{B} \cdot \mathbf{X})\, \bar{\mathbf{h}}(z) \\ &= \bar{\mathbf{f}}(z + \xi - 2) \end{aligned} \tag{B7}$$

and an identical one but multiplied by $\mathbf{X}$ from the left. Thus we see that we only need the upper 2 by 2 matrices from $\mathbf{T}$. By using the definition eq. (A16) and the results for T^{ab} in appendix C, we obtain

$$\mathbf{R}_1 + \mathbf{R}_2 \cdot \mathbf{X} = -\frac{d-1}{\Gamma(d/2+1)} c_d \mathbf{1}, \tag{B8}$$

which results in a cancellation of the remaining mass dependent terms. The remaining equation depends now only on the physical diffusivity ν. Solving the equation iteratively would amount to a series expansion in powers of ν or ν^{-1}, but we shall only consider the $\nu \to 0$ limit, which produces the solution in eq. (23).

APPENDIX C: NECESSARY COMPONENTS OF THE MATRIX T

Due to incompressibility, only some of the components of $\mathbf{T}$ will be needed. Computing the integrals of the type in (A13) can be performed by using the result

$$\int d^d \boldsymbol{q} \frac{\Phi^l(\widehat{\boldsymbol{q}} \cdot \widehat{e})}{|\boldsymbol{q}|^{2\alpha} |\boldsymbol{p}-\boldsymbol{q}|^{2\beta}} =: \lambda_{2\alpha,2\beta} |\boldsymbol{p}|^{d-2(\alpha+\beta)} \Phi^l(\widehat{\boldsymbol{p}} \cdot \widehat{e}), \tag{C1}$$

where we have denoted by $\widehat{\boldsymbol{q}} \cdot \widehat{e}$ the angle between $\boldsymbol{q}$ and the z -axis and defined

$$\lambda_{2\alpha,2\beta} := \frac{\Gamma(d/2+l-\alpha)\Gamma(d/2-\beta)\Gamma(\alpha+\beta-d/2)}{\Gamma(\alpha)\Gamma(\beta)\Gamma(d+l-\alpha-\beta)}. \tag{C2}$$

The tensorial structure can be obtained by partial integrations and by taking derivatives in $\boldsymbol{p}$. We will further define (note the transpose in the definition)

$$\mathrm{T}^{ab}_{d+\xi,d+z} := \frac{\lambda_{l+d+z,d+\xi}}{d+\xi} \tau^{ab}(z). \tag{C3}$$

The necessary components of τ are (others do not contribute due to the incompressibility condition):

$$\begin{aligned}
\tau^{11} &= \frac{(1+a^2)(d-1)(l-z) - a^2\xi(z+d+\xi-l)}{(l-z-\xi)} + \frac{l(l-1)\xi}{(l-z-\xi)(l+z+d+\xi-2)} \\
\tau^{12} &= \frac{a^2\xi}{(l-z-\xi)(l+z+d+\xi-2)}
\end{aligned}$$

$$
\begin{aligned}
\tau^{21} &= a^2 l(l-1)\frac{l+z+d-2}{l+z+d+\xi-2}\left(d-1+\xi\frac{z-l+d+\xi+2}{z-l+2}\right)\\
\tau^{22} &= \frac{(d-1)(l+z+d-2)}{l+z+d+\xi-2}+\frac{(l-2)\xi\left(a^2(l-3)+2a(z+d+1)+l-3\right)}{(l-z-2)(l+z+d+\xi-2)}\\
&+\frac{(a-1)^2(2-\xi)\xi(l^2-5l+6)}{(l-z-2)(l+z+d+\xi-2)(l+z+d+\xi-4)}
\end{aligned}
$$

$$
\begin{aligned}
\tau^{31} &= \frac{2al\xi(z+d+\xi-1)}{(l-z-\xi)(l+z+d+\xi-2)}+2a^2 l\left(\frac{z+l(d+\xi-1)-(d+\xi)(z+\xi)}{l-z-\xi}\right.\\
&\left.-\frac{(l-1)\xi(d+\xi-1)}{(l-z-\xi)(l+z+d+\xi-2)}-\frac{(l-1)(2-\xi)(d+\xi)\xi}{(l-z-2)(l-z-\xi)(l+z+d+\xi-2)}\right)\\
\tau^{32} &= 2\xi\frac{a\left(d-1+a(l-2)+z+\xi\right)-d-1}{(l-z-\xi)(l+z+d+\xi-2)}+\frac{4a(l-2)(2-\xi)\xi}{(l-z-2)(l-z-\xi)(l+z+d+\xi-2)}\\
&+\frac{2\xi(a-1)^2\left(l^2-5l+6\right)(2-\xi)}{(l-z-2)(l-z-\xi)(l+z+d+\xi-4)(l+z+d+\xi-2)}
\end{aligned}
$$

$$
\begin{aligned}
\tau^{41} &= \frac{a^2\left((d+\xi)(z+\xi)-l(d+\xi-1)-z\right)-2a\xi}{l-z-\xi}\\
&+\xi\frac{d+1+2a(l-1)+a^2(1+2d-d^2-\xi(d-1))}{(l+z+d)(l-z-\xi)}\\
&+\frac{(a-1)^2(d+1)(2-\xi)\xi}{(l+z+d)(l-z-\xi)(l+z+d+\xi-2)}\\
&-(2-\xi)\xi\frac{(a-1)^2\left(d^2+l(l+1)\right)+d\left((1+2l)(1-2a)+a^2(1+3l-l^2)\right)}{(l-z-2)(l+z+d)(l-z-\xi)(l+z+d+\xi-2)}\\
&+\frac{2(a-1)^2(d+l)(d+1+l)\xi(\xi^2-6\xi+8)}{(l-z-2)(l+z+d)(l-z-\xi+2)(l-z-\xi)(l+z+d+\xi-2)}
\end{aligned}
$$

$$
\begin{aligned}
\tau^{42} &= \frac{a\xi\left(a(l+z+d)-2(2-\xi)\right)}{(l+z+d)(l-z-\xi)(l+z+d+\xi-2)}\\
&-\frac{(2-\xi)\xi\left(d+3-2a(d+1+l)+a^2(d+3)\right)}{(l-z-2)(l+z+d)(l-z-\xi)(l+z+d+\xi-2)}\\
&+\frac{(a-1)^2\xi(d+3)(8-6\xi+\xi^2)}{(l-z-2)(l+z+d)(l-z-\xi)(l-z-\xi+2)(l+z+d+\xi-2)}\\
&+\frac{(a-1)^2\xi(6-5l+l^2)(8-6\xi+\xi^2)}{(l-z-2)(l+z+d)(l-z-\xi)(l-z-\xi+2)(l+z+d+\xi-4)(l+z+d+\xi-2)}.
\end{aligned}
$$

APPENDIX D: THE MATRIX $\widehat{\mathbf{P}}^{\mathbf{T}}\mathbf{K}$

We defined the matrix $\mathbf{K}$ as

$$\mathrm{K}^{ab}B^{b}_{ij}(\hat{\boldsymbol{r}}) = \int d^{d}\boldsymbol{p} e^{i\boldsymbol{p}\cdot\boldsymbol{r}} \frac{B^{a,l}_{ij}(\hat{\boldsymbol{p}})}{|\boldsymbol{p}|^{d+z}}, \tag{D1}$$

where the elements are obtained by direct computation. Multiplication with the transpose of the projector (B3) yields

$$\mathbf{P}^{\mathrm{T}}\mathbf{K} = \imath 2^{-z} \frac{\Gamma\left(\frac{l-z}{2}\right)}{\Gamma\left(\frac{d+l+z}{2}\right)} \kappa, \tag{D2}$$

where κ is now a 2×4 matrix,

$$\kappa = \begin{pmatrix} 1 - \frac{1}{z+d+l} & \frac{-1}{(z+2-l)(z+d+l)} & \frac{-1}{z+d+l} & -\frac{z-l}{z+d+l} \\ \frac{l(l-1)}{z+d+l} & \frac{(z+d)^2-l}{(z+d+l)(z+2-l)} & z+d-1+\frac{l(l-1)}{z+d+l} & 2(z-l)(z+d+l-2)+\frac{l(l-1)}{z+d+l} \end{pmatrix}. \tag{D3}$$

[1] U. Frisch. *Turbulence: The Legacy of A. N. Kolmogorov*. Cambridge University Press, 1995.

[2] G. Falkovich, K. Gawędzki, and M. Vergassola. Particles and fields in fluid turbulence. *Rev. Mod. Phys.*, 73(4):913–975, Nov 2001.

[3] K. Gawędzki and A. Kupiainen. Anomalous scaling of the passive scalar. *Phys. Rev. Lett.*, 75(21):3834–3837, Nov 1995.

[4] Robert H. Kraichnan. Anomalous scaling of a randomly advected passive scalar. *Phys. Rev. Lett.*, 72(7):1016–1019, Feb 1994.

[5] V. Hakulinen. Passive advection and the degenerate elliptic operators m_n. *Communications in Mathematical Physics*, 235(1):1, 2003.

[6] G. Falkovich and A. Fouxon. Anomalous scaling of a passive scalar in turbulence and in equilibrium. *Physical Review Letters*, 94(21):214502, 2005.

[7] A. Celani and A. Seminara. Large-scale anisotropy in scalar turbulence. *Physical Review Letters*, 96(18):184501, 2006.

[8] M. Vergassola. Anomalous scaling for passively advected magnetic fields. *Phys. Rev. E*, 53(4):R3021–R3024, Apr 1996.

[9] A. Kupiainen and P. Muratore-Ginanneschi. Scaling, renormalization and statistical conservation laws in the kraichnan model of turbulent advection. *J. Stat. Phys.*, 126(3):669–724, Feb 2007.

[10] Luiza Angheluta, Roberto Benzi, Luca Biferale, Itamar Procaccia, and Federico Toschi. Anomalous scaling exponents in nonlinear models of turbulence. *Physical Review Letters*, 97(16):160601, 2006.

[11] L. Ts. Adzhemyan, N. V. Antonov, A. Mazzino, P. Muratore-Ginanneschi, and A. V. Runov. Pressure and intermittency in passive vector turbulence. *EPL (Europhysics Letters)*, 55(6):801–806, 2001.

[12] N. V. Antonov, Michal Hnatich, Juha Honkonen, and Marian Jurčišin. Turbulence with pressure: Anomalous scaling of a passive vector field. *Phys. Rev. E*, 68(4):046306, Oct 2003.

[13] N. V. Antonov, A. Lanotte, and A. Mazzino. Persistence of small-scale anisotropies and anomalous scaling in a model of magnetohydrodynamics turbulence. *Phys. Rev. E*, 61(6):6586–6605, Jun 2000.

[14] I. Arad, L. Biferale, and I. Procaccia. Nonperturbative spectrum of anomalous scaling exponents in the anisotropic sectors of passively advected magnetic fields. *Phys. Rev. E*, 61(3):2654–2662, Mar 2000.

[15] H. Arponen and P. Horvai. Dynamo effect in the kraichnan magnetohydrodynamic turbulence. *J. Stat. Phys.*, 129(2):205–239, Oct 2007.

[16] M. Hnatich, J. Honkonen, M. Jurcisin, A. Mazzino, and S. Sprinc. Anomalous scaling of passively advected magnetic field in the presence of strong anisotropy. *Physical Review E (Statistical, Nonlinear, and Soft Matter Physics)*, 71(6):066312, 2005.

[17] Alessandra Lanotte and Andrea Mazzino. Anisotropic nonperturbative zero modes for passively advected magnetic fields. *Phys. Rev. E*, 60(4):R3483–R3486, Oct 1999.

[18] L. Ts. Adzhemyan, N. V. Antonov, and A. V. Runov. Anomalous scaling, nonlocality, and anisotropy in a model of the passively advected vector field. *Phys. Rev. E*, 64(4):046310, Sep 2001.

[19] R. Benzi, L. Biferale, and F. Toschi. Universality in passively advected hydrodynamic fields: the case of a passive vector with pressure. *The European Physical Journal B*, 24:125, 2001.

[20] K. Yoshida and Y. Kaneda. Anomalous scaling of anisotropy of second-order moments in a model of a randomly advected solenoidal vector field. *Phys. Rev. E*, 63(1):016308, Dec 2000.

[21] D. Bernard, K. Gawędzki, and A. Kupiainen. Slow modes in passive advection. *J. Stat. Phys.*, 90(3):519–569, Feb 1998.

[22] J. Bertrand, P. Bertrand, and J. Ovarlez. *The Mellin Transform. The Transforms and Applications Handbook: Second Edition.* CRC Press LLC, 2000.

[23] Itai Arad, Victor S. L'vov, and Itamar Procaccia. Correlation functions in isotropic and anisotropic turbulence: The role of the symmetry group. *Phys. Rev. E*, 59(6):6753–6765, Jun 1999.

[24] Itai Arad, Luca Biferale, Irene Mazzitelli, and Itamar Procaccia. Disentangling scaling properties in anisotropic and inhomogeneous turbulence. *Phys. Rev. Lett.*, 82(25):5040–5043, Jun 1999.

[25] U. Frisch, Z. S. She, and P. L. Sulem. Large-scale flow driven by the anisotropic kinetic alpha effect. *Physica D: Nonlinear Phenomena*, 28(3):382–392, 1987.

[26] L. D. Landau. *Fluid Mechanics, 2nd. edition, Volume 6.* Elsevier, 1987.

[27] Itai Arad, Brindesh Dhruva, Susan Kurien, Victor S. L'vov, Itamar Procaccia, and K. R. Sreenivasan. Extraction of anisotropic contributions in turbulent flows. *Phys. Rev. Lett.*, 81(24):5330–5333, Dec 1998.

[28] J. Zinn-Justin. *Quantum Field Theory and Critical Phenomena, 3rd ed.* Oxford University Press, 1996.

4. Steady state existence of passive vector fields under the Kraichnan model

Steady state existence of passive vector fields under the Kraichnan model

Heikki Arponen

Helsinki University, Department of Mathematics and Statistics,

P.O. Box 68, 00014 Helsinki (Finland)[*]

(Dated: April 28, 2009)

Abstract

The steady state existence problem for Kraichnan advected passive vector models is considered for isotropic and anisotropic initial values in arbitrary dimension. The model includes the magnetohydrodynamic (MHD) equations, linear pressure model (LPM) and linearized Navier-Stokes (LNS) equations. In addition to reproducing the previously known results for the MHD and linear pressure model, we obtain the values of the Kraichnan model roughness parameter ξ for which the LNS steady state exists.

PACS numbers: 47.27.E-, 47.27.-i

[*]Electronic address: heikki.arponen@helsinki.fi

I. INTRODUCTION

This is a companion paper to a previous work by the present author [1], wherein the phenomenon of anisotropic anomalous scaling was studied in the context of passive vector fields. The work was in part incomplete, as the main assumption was the existence of a steady state solution for the pair correlation function. We aim here to find exactly the preconditions under which this assumption is valid. Much of the technical material is from the above paper, to which we often refer for details. We study the stability of an equal time pair correlation function of a field $\mathbf{u}(t,x)$ determined by the equation

$$\dot{u}_i - \nu\Delta u_i + \mathbf{v}\cdot\nabla u_i - a\mathbf{u}\cdot\nabla v_i + \nabla_i P = 0, \tag{1}$$

where the vector field $\mathbf{v}(t,x)$ is determined by the Kraichnan model [2] and all vector quantities are divergence free.

The model was introduced in [3] as the most general linear passive vector model respecting galilean invariance. The parameter $a = -1, 0$ or 1 corresponds respectively to the linearized Navier-Stokes equations [3] (abbreviated henceforth as LNS), the so called linear pressure model[3–8] (LPM) and the magnetohydrodynamic (MHD) equations [3, 9–17]. In the context of the magnetohydrodynamic case, the inexistence of the steady state is known as the "dynamo effect", where the dynamo refers to exponential growth in time of the pair correlation function (see e.g. [9–11] and references therein). This problem is by far the easiest of the three due to the vanishing of the nonlocal pressure effects. In [4] it was shown that for the linearized pressure model (corresponding to $a = 0$) the steady state always exists by showing that the semi-group involved with the time evolution is always positive. The analysis for the linearized Navier-Stokes case with $a = -1$ is considerably more difficult than the above two cases since unlike in the MHD case, the nonlocal effects are present and contribute strongly to the dynamics, and because unlike in the LPM case, the semigroup is not always positive.

The present goal is therefore to find the values of ξ for which the LNS steady state exists, where ξ is the roughness exponent of the Kraichnan velocity field $v \sim r^{\xi}$. The method by which this is accomplished involves applying a Mellin transform on the equation for the two point correlation function, and by solving a resulting recursion relation.

II. THE MODEL

We sketch here the derivation of the equation in Mellin transformed form and refer to the previous paper [1] for further details. All vector quantities in eq. (1) being divergence free results in an expression for the pressure,

$$P = (1-a)\left(-\Delta\right)^{-1}\partial_i v_j \partial_j u_i. \tag{2}$$

One may then rewrite the equation compactly as

$$\dot{u}_i - \nu\Delta u_i + \mathcal{D}_{ijk}\left(u_j v_k\right) = 0, \tag{3}$$

with an integro-differential operator

$$\mathcal{D}_{ijk} = \delta_{ij}\partial_k - a\delta_{ik}\partial_j + (a-1)\partial_i\partial_j\partial_k\Delta^{-1}, \tag{4}$$

where Δ^{-1} is the inverse laplacian. The equal time pair correlation is defined as

$$G_{ij}(t,\boldsymbol{r}) = \langle u_i(t,\boldsymbol{x}+\boldsymbol{r})u_j(t,\boldsymbol{x})\rangle, \tag{5}$$

where the angular brackets denote an ensemble average with respect to the velocity field, which in turn is defined by the Kraichnan model as

$$\begin{aligned}\left\langle v_i(t,\boldsymbol{r})v_j(0,0)\right\rangle &= \delta(t)D_{ij}(\boldsymbol{r}) \\ &= \delta(t)D_1\int \mathrm{d}\!\!^{-d}\boldsymbol{q}\frac{e^{i\boldsymbol{q}\cdot\boldsymbol{r}}}{\left(\boldsymbol{q}^2+m_v^2\right)^{d/2+\xi/2}}P_{ij}(\boldsymbol{q})\end{aligned} \tag{6}$$

where we have defined the incompressibility tensor $P_{ij}(\boldsymbol{q}) = \delta_{ij} - \widehat{\boldsymbol{q}}_i\widehat{\boldsymbol{q}}_j$ and denoted $\mathrm{d}\!\!^{-d}\boldsymbol{q} := \frac{d^dq}{(2\pi)^d}$.

We note a subtle difference from [9] in that we have defined

$$D_1 = \frac{4\xi\Gamma\left(\frac{2+d+\xi}{2}\right)}{\Gamma\left(1-\xi/2\right)}D_0. \tag{7}$$

The reason for this is that the velocity correlation and structure functions would otherwise diverge at $\xi = 0$ and $\xi = 2$ as the mass cutoff is removed. The equation for the pair correlation function is then

$$\partial_t G_{ij} - 2\nu\Delta G_{ij} - \mathcal{D}_{i\mu\nu}\mathcal{D}_{i\rho\sigma}\left(D_{\nu\sigma}G_{\mu\rho}\right) = 0. \tag{8}$$

The Fourier transform of the correlation function will then be decomposed in terms of hyperspherical tensor basis according to the prescription in [18] as

$$\widehat{G}_{ij}(t,\boldsymbol{p}) := \sum_{a,l} B^{a,l}_{ij}(\hat{\boldsymbol{p}})\widehat{G}_{a,l}(t,p), \tag{9}$$

where the tensor basis components are

$$\begin{cases} B^{1,l}_{ij}(\hat{\boldsymbol{p}}) &= |\boldsymbol{p}|^{-l}\delta_{ij}\Phi^l(\boldsymbol{p}) \\ B^{2,l}_{ij}(\hat{\boldsymbol{p}}) &= |\boldsymbol{p}|^{2-l}\partial_i\partial_j\Phi^l(\boldsymbol{p}) \\ B^{3,l}_{ij}(\hat{\boldsymbol{p}}) &= |\boldsymbol{p}|^{-l}(p_i\partial_j + p_j\partial_i)\Phi^l(\boldsymbol{p}) \\ B^{4,l}_{ij}(\hat{\boldsymbol{p}}) &= |\boldsymbol{p}|^{-l-2}p_ip_j\Phi^l(\boldsymbol{p}) \end{cases} \tag{10}$$

and where $\Phi^l(\boldsymbol{p})$ is defined as $\Phi^l(\boldsymbol{p}) := |\boldsymbol{p}|^l Y^l(\hat{\boldsymbol{p}})$, where Y^l is the hyperspherical harmonic function (with the multi-index $m = 0$). It satisfies the properties

$$\begin{aligned} \Delta\Phi^l(\boldsymbol{p}) &= 0 \\ \boldsymbol{p}\cdot\nabla\Phi^l(\boldsymbol{p}) &= l\Phi^l(\boldsymbol{p}). \end{aligned} \tag{11}$$

Note that we are concerned only with even parity and axial anisotropy. We now introduce the Mellin transform (the anisotropy index l will usually be omitted)

$$\bar{g}_a(t,z) = \int_0^\infty \frac{dw}{w} w^{d+z}\widehat{G}_a(t,w) \tag{12}$$

and the inversion formula to provide an expression for the correlation function,

$$G_a(t,\boldsymbol{r}) = \int_{z\in S} đz|\boldsymbol{r}|^z\mathcal{A}_z\bar{g}_a(t,z), \tag{13}$$

where S refers to the strip of analyticity, which is determined from the boundary conditions and the equation, and $\mathcal{A}_z = \frac{\Omega_d}{(2\pi)^d}\frac{\Gamma(d/2)\Gamma(-z/2)}{2^{z+1}\Gamma\left(\frac{d+z}{2}\right)}$ originates from the inversion of the fourier integral (with volume of the unit sphere Ω_d).

Applying the Fourier transform, dividing by p^2, applying the Mellin transform and finally setting the cutoff parameter m_v to zero in eq. (1) (see [1] for details), we obtain the complex recurrence/differential equation

$$\partial_t\bar{g}_a(t,z-2) + 2\nu\bar{g}_a(t,z) - \widetilde{\lambda}\bar{g}_a(t,z-\xi) - \mathrm{T}^{ab}_{d+\xi,d+z-\xi}\bar{g}_b(t,z-\xi) = 0, \tag{14}$$

with the definitions

$$\widetilde{\lambda} = (a-1)\left(d+1+a(1-\xi)\right)\frac{d\pi\xi\csc(\pi\xi/2)\Gamma(d/2)c_d}{16\Gamma\left(\frac{d-\xi}{2}+2\right)\Gamma\left(\frac{d+\xi}{2}+1\right)} \tag{15}$$

and

$$\mathrm{T}^{ab}_{2\alpha,2\beta} = \frac{4\xi\Gamma\left(\frac{d+\xi}{2}\right)}{\Gamma\left(1-\xi/2\right)}\frac{\Gamma(d/2+l-\alpha)\Gamma(d/2-\beta)\Gamma(\alpha+\beta-d/2)}{\Gamma(\alpha)\Gamma(\beta)\Gamma(d+l-\alpha-\beta)}\tau^{ab}(z), \tag{16}$$

where the matrix coefficients $\tau^{ab}(z)$ are listed in the appendix of [1]. We have also effectively set $D_0 = 1$ by redefining time and viscosity. Requiring the correlation function (9) to be divergence free, i.e. zero when contracted with p_i, results in only two of the four coefficients $\bar{g}_a$ being independent. The resulting equation may then be written in the following form,

$$\partial_t\bar{\mathbf{h}}(t,z+\xi-2) + 2\nu\bar{\mathbf{h}}(t,z+\xi) - \left(\widetilde{\lambda}\mathbf{1}+\mathbf{A}+\mathbf{B}\cdot\mathbf{X}\right)\bar{\mathbf{h}}(t,z) = 0. \tag{17}$$

Here we have performed a translation $z \to z+\xi$, defined the vector quantity $\bar{\mathbf{h}} = (\bar{g}_1, \bar{g}_2)^{\mathrm{T}}$ and the matrices by

$$\mathbf{T}_{d+\xi,d+z} = \begin{pmatrix} \mathbf{A} & \mathbf{B} \\ \mathbf{C} & \mathbf{D} \end{pmatrix} \quad , \quad \mathbf{X} = \begin{pmatrix} 0 & -(l-1) \\ -1 & l(l-1) \end{pmatrix}. \tag{18}$$

A. Isotropic sector

We will be mostly concerned with the isotropic case since much of the actual computations can be neatly performed all the way. For $l = 0$, only the tensors B^1 and B^4 are nonzero, and correspondingly in the tensor decomposition we only have the coefficients $\bar{g}_1(z)$ and $\bar{g}_4(z) = -\bar{g}_1(z)$ (due to the divergence free condition). The equation (17) then becomes a scalar equation for $\bar{g}_1(z)$ alone, hence we only need the $(1,1)$ component of the matrix $\left(\widetilde{\lambda}\mathbf{1}+\mathbf{A}+\mathbf{B}\cdot\mathbf{X}\right)$, which reads explicitly

$$\begin{aligned}\left(\widetilde{\lambda}\mathbf{1}+\mathbf{A}+\mathbf{B}\cdot\mathbf{X}\right)_{11} &= \frac{2(a-1)(a\xi-1-a-d)\Gamma\left(1+\xi/2\right)\Gamma\left(1+d/2\right)}{\Gamma\left(\frac{4+d-\xi}{2}\right)} \\ -p_a(z)\frac{\Gamma\left(-z/2\right)\Gamma\left(\frac{d+z+\xi}{2}\right)}{2\Gamma\left(\frac{2+d+z}{2}\right)\Gamma\left(\frac{4-z-\xi}{2}\right)} &\doteq \Lambda^a_\xi(z),\end{aligned} \tag{19}$$

where

$$
\begin{aligned}
&p_a(z) = -(a-1)^2(d+1)\xi(2-\xi) \\
&+(z+\xi-2)\left((d-1)z^2 + (d(d-1)+2a\xi)\,z + \right. \\
&\left.\xi\left(-d-1+2a(d+1)-a^2(1+2d-d^2+\xi-d\xi)\right)\right)
\end{aligned}
\tag{20}
$$

The equation in the isotropic sector is then

$$
\partial_t \bar{g}_1(t, z+\xi-2) + 2\nu \bar{g}_1(t, z+\xi) - \Lambda^a_\xi(z)\bar{g}_1(t,z) = 0. \tag{21}
$$

III. THE METHOD

We now consider the eigenvalue problem with $\bar{g}_1(t,z) \propto e^{-Et} g(z)$, resulting in the equation

$$
E\bar{g}(z+\xi-2) - 2\nu\bar{g}(z+\xi) + \Lambda^a_\xi(z)\bar{g}(z) = 0. \tag{22}
$$

This is analogous to the Schrödinger method in [10–12]. The steady state exists if one can show that the spectrum is nonnegative. However, for example in the magnetohydrodynamic case as in the above mentioned papers and in [9], it was shown that there exists a critical value of the parameter ξ above which one has negative energies resulting in an exponential growth in time. This phenomenon is interpreted as the dynamo effect of magnetic fields. All of the above papers resorted to some approximative or numerical schemes to find the growth rate $|E|$ as a function of ξ. Here we will settle for simply finding the values of ξ for which the energies are nonnegative. This is done by studying the *zero energy* equation, i.e. setting $E = 0$. This has the advantage of providing us with an exact solution, up to a numerical solution of a transcendental equation. Such equations have been studied before, usually in the context of special functions (see e.g. [19] and references therein).

A. Comparison to the Schrödinger equation

For motivational purposes, consider the "node theorem" for the Scrhödinger boundary value problem on $\mathbb{R}_+$ [20] with

$$\begin{cases} -u''(r) + V(r)u(r) \ = Eu(r) \\ u(0) = 1 \\ u(R) = 0 \end{cases} \tag{23}$$

for a potential $V(r)$ bounded from below and R tending to infinity. By rewriting this as $u''(r)/u(r) = V(r) - E$, we see that for small enough E both u'' and u are of the same sign due to positivity of the right hand side. If both u and u'' are positive at zero, they will thus remain so for all $r \geq 0$, hence u is never zero. Suppose now that for $E = 0$ u crosses zero at least once as in Fig. (1). We then know that as E is decreased, the nodes move to the right and eventually reach R. The values of E at which a node hits R are the discrete eigenvalues, since only then the boundary condition is satisfied. Most importantly, the ground state energy is therefore the value of E for which the last node hits R.

The present approach taken here will be closely analogous to the Schrödinger case except that we consider the zero energy equation only but for different values of ξ. It will be shown that in each case $a = \pm 1$ the $\xi = 2$ solution has an infinite number of nodes, hence the steady state does not exist (the spectrum is nonnegative for $a = 0$ [4]). On the other hand, the $\xi = 0$ case is pure diffusion for which the steady state does exist. Analogously to the Schrödinger equation, we infer that by decreasing ξ from two has the same effect of the nodes going to infinity, and that there must be a critical value ξ_c for which the zero energy solution is the ground state. Thus as we cross the critical value from $\xi > \xi_c$, we also pass from the phase of exponential growth to the steady state phase.

B. Isotropic equation for $\xi = 2$

For $\xi = 2$ the problem becomes simple enough to be solved exactly even for nonzero energies. We have now

$$\Lambda_2^a(z) = (d-1)z^2 + (4a + d(d-1))\, z + 2a\left(d + a(d^2-2)\right) \tag{24}$$

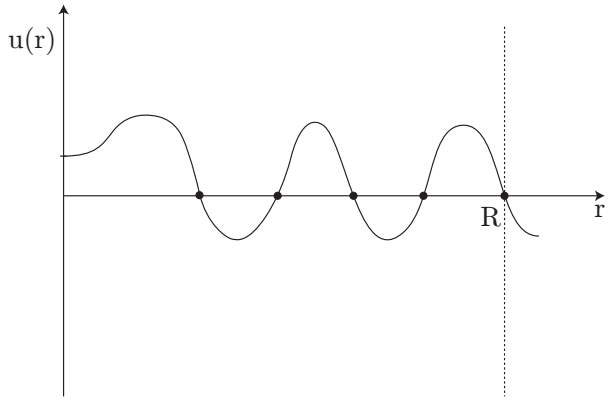

FIG. 1: A sketch of a solution to the Schrödinger equation with five nodes. As energy is decreased the nodes eventually hit R. The energy at which the last node reaches R is the ground state energy.

and the equation (22) can now be written as

$$(z - z_+)\,(z - z_-)\,\bar{g}(z) = 2\nu\bar{g}(z+2), \tag{25}$$

where we have defined the roots

$$z_\pm = \frac{-4a - d(d-1) \pm \sqrt{D_E}}{2(d-1)} \tag{26}$$

with the discriminant

$$D_E = -4(d-1)E + d^2 + d(d-2)\left(d^2 - 8(d+1)a^2\right). \tag{27}$$

We note that the most general solution of eq. (25) is

$$\bar{g}(z) = \sigma_2(z)\left(\frac{\nu}{2}\right)^{-z/2}\Gamma\left(\frac{z-z_+}{2}\right)\Gamma\left(\frac{z-z_-}{2}\right), \tag{28}$$

where $\sigma_2(z+2) = \sigma_2(z)$ is a so far arbitrary periodic function (with the subscript denoting the period). Note that we could equally well have written e.g. $1/\Gamma\left(\frac{2-z+z_+}{2}\right)$ instead of the gamma function in the numerator. This can however be brought to the above form by use of the Euler reflection formula by absorbing the sin term in $\sigma_2(z)$. Which gamma function is to be used, depends on the existence of the inverse transform, as will be shown below. To be able to use the inversion formula (13), we multiply by $\mathcal{A}_z$ and obtain

$$\bar{f}(z) = \sigma_2(z)\left(\frac{\nu}{2}\right)^{-z/2}\frac{\Gamma\left(\frac{-z}{2}\right)\Gamma\left(\frac{z-z_+}{2}\right)\Gamma\left(\frac{z-z_-}{2}\right)}{\Gamma\left(\frac{z+d}{2}\right)}. \tag{29}$$

So far we have only been able to state that one end of the strip of analyticity is at zero due to requiring $G_a(0) = \text{const.}$, i.e. that $\bar{f}(z)$ has a simple pole at $z = 0$. This is indeed satisfied by the above solution due to the gamma function $\Gamma(-z/2)$. To be able to identify eq. (25) with the equation if the coordinate space, we also need to *assume* that the width of the strip is at least 2 [23]. Because the boundary condition is already satisfied, $\sigma_2(z)$ must also be analytic at $z = 0$, whence we conclude that it is an entire function in the whole complex plane. We still need to consider the possibility that the function $\sigma_2(z)$ has zeros that cancel with some of the poles in the solution. This will be clarified by the existence of the inversion integral (13), i.e. by studying the properties of the solution at $\pm\imath\infty$. Using the formula $\Gamma(-z/2)\Gamma(1 + z/2) = -\pi/\sin(\pi z/2)$, we infer that the part with the gamma functions behave asymptotically as $\propto |y|^{\frac{a}{d-1}} e^{-\frac{\pi}{2}|y|}$ with $z = x + \imath y$. Since $\sigma_2(z)$ is periodic, we can expand it as Fourier series in the x -direction in terms of the trigonometric functions $\sin(\pi n x)$ and $\cos(\pi n x)$. By analyticity, we can replace $x \to z$, and infer that the integrability is violated for each $n \neq 0$. Therefore only the constant term in the Fourier series survives and we conclude that $\sigma_2(z) = \text{const.}$

For $E = 0$ and $a = \pm 1$ we have

$$z_\pm = \frac{-4 - d(d-1) \pm \sqrt{d\,(d^3 - 10d^2 + 9d + 16)}}{2(d-1)}, \tag{30}$$

from which we see that $z_\pm$ has a nonzero imaginary part in space dimensions $3 \leq d \leq 8$. The imaginary part leads to an oscillating behavior $\propto \cos \log r$ after preforming the inverse Mellin transform, which amounts to existence of zeros of the correlation function at large scales. As we learned from the Schrödinger equation, this means that there must be negative energy states below the zero energy state, and that the time evolution is therefore unstable. This result was previously discovered for the magnetohydrodynamic case $a = 1$ in [9]. As with the Schrödinger equation, decreasing the energy has the effect of moving the zeros to the right, until we reach the ground state energy at which the last zero disappears to infinity. This happens exactly when the roots $z_\pm$ become real, hence the ground state energy for $\xi = 2$, $a = \pm 1$ is

$$E_0 = \frac{d\,(d^3 - 10d^2 + 9d + 16)}{4(d-1)}. \tag{31}$$

For $a = 0$ the roots are always real, hence the flow is is stable. We now turn to other values of ξ in the magnetohydrodynamic and linearized Navier-Stokes models and determine the critical value ξ_c below which the flow becomes stable.

IV. ISOTROPIC SECTOR

A. Magnetohydrodynamics: a = 1

The magnetohydrodynamic model has been studied before numerically in e.g. [11] and by an approximative scheme in [9] (see either one for further references). Although the dynamo problem can be considered to be more or less solved in the present context, it will still be useful to review the problem using the technology as explained above. This is because the results to be given below for the existence problem are exact, which provides some much needed evidence in favor of the approximation scheme in the paper [9] and of course for the numerics as well. The magnetohydrodynamic case will also shed some light on the much more difficult problem of the linearized Navier-Stokes problem, which will be discussed in the next section. For $a = 1$ we have

$$\Lambda^1_\xi(z) = (d-1)\,(z-z_+)\,(z-z_-)\,\frac{\Gamma\left(-z/2\right)\Gamma\left(\frac{z+d+\xi}{2}\right)}{\Gamma\left(\frac{2-z-\xi}{2}\right)\Gamma\left(\frac{z+d+2}{2}\right)}, \tag{32}$$

where the roots are

$$z_\pm = -\frac{d(d-1)+2\xi}{2(d-1)} \pm \frac{\sqrt{d}}{2}\sqrt{d - 4\frac{d-2}{d-1}\xi - 4\frac{d-2}{(d-1)^2}\xi^2}. \tag{33}$$

We recognize them immediately as the anomalous scaling exponents of the magnetohydrodynamic steady state [1]. The zero energy equation is then

$$\bar{g}(z) = \frac{2\nu}{d-1}\frac{\Gamma\left(\frac{z+d+2}{2}\right)\Gamma\left(\frac{2-\xi-z}{2}\right)}{\Gamma\left(\frac{z+d+\xi}{2}\right)\Gamma\left(\frac{-z}{2}\right)}\frac{\bar{g}(z+\xi)}{(z-z_+)\,(z-z_-)}. \tag{34}$$

By performing a substitution

$$\bar{g}(z) = \frac{\Gamma\left(\frac{z+d}{2}\right)}{\Gamma\left(-\frac{z}{2}\right)}\bar{f}(z) \tag{35}$$

(the gamma functions are the same as in the definition of $\mathcal{A}_z$ on p. 3), the equation simplifies to

$$\bar{f}(z) = \frac{-\nu}{2(d-1)}\frac{(z+d)\,(z+\xi)}{(z-z_+)\,(z-z_-)}\bar{f}(z+\xi). \tag{36}$$

As in the previous section, we observe that the general solution is

$$\bar{f}(z) = \alpha_\xi(z)\left(\frac{\nu}{2(d-1)}\right)^{-z/\xi}\frac{\Gamma\left(\frac{z-z_+}{\xi}\right)\Gamma\left(\frac{z-z_-}{\xi}\right)}{\Gamma\left(\frac{z+d}{\xi}\right)\Gamma\left(\frac{z+\xi}{\xi}\right)}, \tag{37}$$

where we have now defined an antiperiodic function $\alpha_\xi(z+\xi) = -\alpha_\xi(z)$ (note that we have absorbed in it the minus sign of ν). Due to the boundary condition, we require a behavior $\sim -1/z$ as $z \to 0$, so we define

$$\alpha_\xi(z) = \frac{-\xi\sigma_\xi(z)}{\pi \sin\left(\frac{\pi}{\xi}z\right)}, \tag{38}$$

with a periodic function $\sigma_\xi(z)$. We can deduce that it is in fact a constant, and therefore does not cancel any of the poles, using exactly the same lines of thought as in the $\xi = 2$ case, albeit again with the consistency assumption that the strip of analyticity is *at least* $-\xi < \mathcal{R}e(z) < 0$. We also employ the Euler reflection formula $\Gamma(1-z)\Gamma(z) = \pi/\sin(\pi z)$ to simplify the final solution into

$$\bar{f}(z) = \xi\left(\frac{\nu}{2(d-1)}\right)^{-z/\xi} \frac{\Gamma\left(\frac{z-z_+}{\xi}\right)\Gamma\left(\frac{z-z_-}{\xi}\right)\Gamma\left(-\frac{z}{\xi}\right)}{\Gamma\left(\frac{z+d}{\xi}\right)}. \tag{39}$$

For values of $\rho := r/\nu^{1/\xi} > 1$ and ξ close to two and $d > 2$, the integration contour must be closed from the left, hence the leading poles are the roots $z_\pm = -\frac{d}{2} - \frac{\xi}{d-1} \pm \imath\chi$ (that lie to the left of $-\xi$) with the real valued quantity

$$\chi \doteq \frac{\sqrt{d}}{2}\sqrt{4\frac{d-2}{(d-1)^2}\xi^2 + 4\frac{d-2}{d-1}\xi - d}. \tag{40}$$

Hence we obtain the large scale behavior

$$G_1(\rho) \propto \rho^{-\frac{d}{2}-\frac{\xi}{d-1}} \cos(\chi \log\rho). \tag{41}$$

The zeros disappear exactly when χ is zero, which happens at a critical value

$$\xi_c = -\frac{d-1}{2} + \sqrt{\frac{(d-1)^3}{2(d-2)}}. \tag{42}$$

This is the same result as in [9]. We therefore conclude that the flow is stable only below the critical value ξ_c, which we have plotted in Fig.(3).

B. Linearized Navier-Stokes equation: $\mathbf{a} = -1$

The stability problem in the linearized Navier-Stokes case is closely related to the laminar flow stability problem as described in §26 of [21]. The equation is derived from the Navier-Stokes equation by decomposing the velocity field into $\mathbf{v}(\boldsymbol{r}) + \mathbf{u}(t, \boldsymbol{r})$, where $\mathbf{v}$ is a stationary

solution and $\mathbf{u}$ is a small perturbation, resulting in the equation

$$\dot{u}_i - \nu\Delta u_i + \mathbf{v}\cdot\nabla u_i + \mathbf{u}\cdot\nabla v_i + \nabla_i P = 0. \tag{43}$$

The question is then whether or not the laminar flow is stable under such perturbations. Here instead the field $\mathbf{v}$ is supposed to model a *statistical steady state* solution of the full Navier-Stokes turbulence, as prescribed by the Kraichnan model. We are therefore studying whether or not the Kraichnan model is an adequate steady state description of turbulence in terms of stability. We now have

$$\Lambda^-_\xi(z) = \frac{4(d+\xi)\Gamma\left(1+\xi/2\right)\Gamma\left(1+d/2\right)}{\Gamma\left(\frac{4+d-\xi}{2}\right)} - p_{-1}(z)\frac{\Gamma\left(-z/2\right)\Gamma\left(\frac{z+d+\xi}{2}\right)}{2\Gamma\left(\frac{z+d+2}{2}\right)\Gamma\left(\frac{4-\xi-z}{2}\right)}, \tag{44}$$

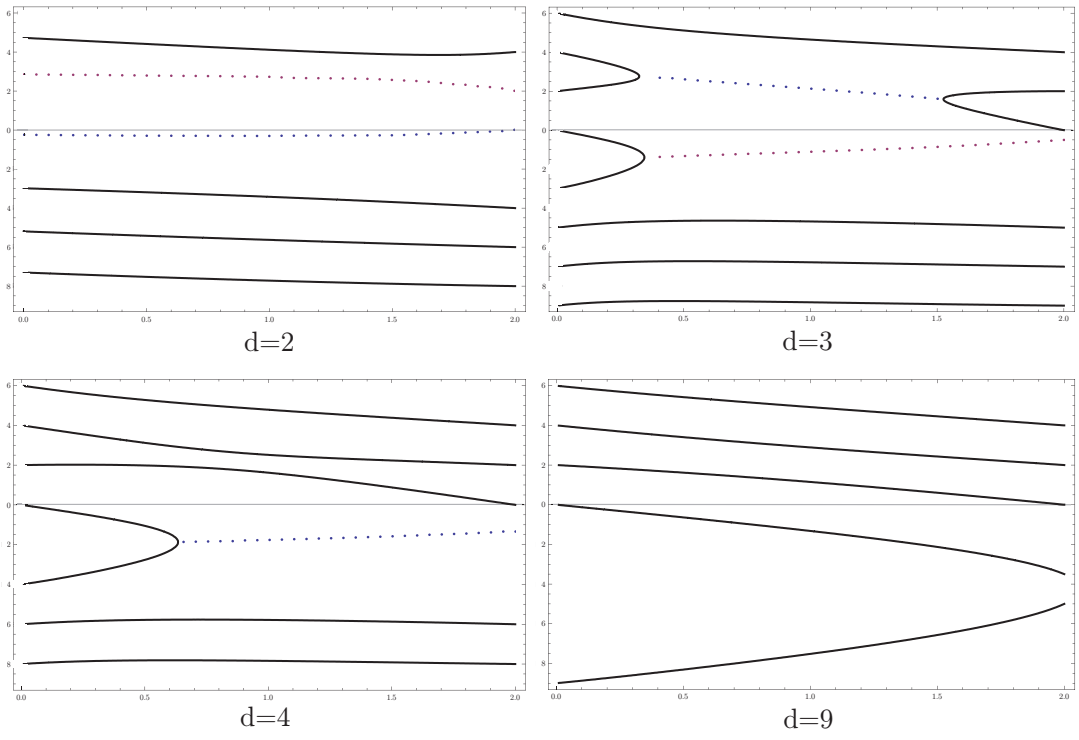

FIG. 2: A plot of the $a = -1$ poles of the solution $\bar{g}(z)$ in the isotropic sector versus ξ in various dimensions. The dashed curves denote the real parts of complex valued poles. There is an infinity of poles, but all the others not displayed here are real. Also, all the poles in dimensions $d \geq 9$ are real in $0 \leq \xi \leq 2$.

where

$$\begin{aligned} p_{-1}(z) &= (z+\xi)\left(-2z+2\xi+d^2(z+\xi-2)\right. \\ &\quad \left.-(z+\xi)^2+d(2+(z-3)z-(3-\xi)\xi)\right)+4z^2. \end{aligned} \tag{45}$$

The problem is obviously now much more difficult because of the transcendental nature of the function Λ_ξ^-. We can however expand the function as an infinite product of zeros and poles according to the Weierstrass factorization theorem (see e.g. [22]). We may then rewrite the function Λ_ξ^- as

$$\Lambda_\xi^-(z) = e^{s(z)} \prod_{k=1}^{\infty} \frac{\left(z-a_k^+\right)\left(z-a_k^-\right)}{\left(z-b_k^+\right)\left(z-b_k^-\right)} e^{\delta/k}, \tag{46}$$

where the $+$ and $-$ signs refer to zeros or poles that are respectively positive (or zero) or negative, see Fig. (3). We also have the poles $b_k^+ = 2k$, $b_k^- = -d-\xi-2k$ and $s(z)$ is some unknown entire function on the complex plane and δ is a z -independent Weierstrass factor that enforces convergence of the infinite product. It can be derived by showing that asymptotically as $z \to \pm\infty$, the poles and zeros of eq. (44) behave respectively as $\pm 2k + \text{const.}$ where the constant term depends on ξ and d. It may certainly be possible to derive bounds for $s(z)$ by asymptotic analysis of eq. (44), but since it can not contribute to the pole or zero structure of the solution, we refrain from doing so. We can also neglect the explicit form of the constant δ for the same reason. The zero energy equation from (22), rewritten here as

$$\bar{g}(z) = \frac{2\nu}{\Lambda_\xi^-(z)} \bar{g}(z+\xi), \tag{47}$$

can then be solved by the now familiar methods (again with the strip of analyticity assumption $-\xi < \mathcal{R}e(z) < 0$), resulting in

$$\begin{aligned} \bar{g}(z) &= \sigma_\xi(z)\Psi(z)(2\nu)^{-z/\xi} \\ &\quad \times \prod_{k>0} e^{z\delta/\xi k} \frac{\Gamma\left(\frac{z-a_k^-}{\xi}\right)\Gamma\left(\frac{2k+\xi-2-z}{\xi}\right)}{\Gamma\left(\frac{a_k^++\xi-z}{\xi}\right)\Gamma\left(\frac{2k+z+d+\xi-2}{\xi}\right)} \end{aligned} \tag{48}$$

where $\Psi(z)$ satisfies the equation $\Psi(z) = e^{-s(z)}\Psi(z+\xi)$, whose solution is again an exponential of an entire function. The following subtlety concerning the above formula should be observed: we deliberately chose to use the form $\sim 1/\Gamma(1-x)$ instead of $\Gamma(x)$. The

reason is that only in this form the strip of analyticity remains pole free. For example using $\Gamma\left(\frac{z-a_k^+}{\xi}\right)$ in the above result would introduce poles at $z = a_k^+ - \xi n$ for positive integers n, that would eventually permeate the strip of analyticity. It seems quite impossible to deduce the asymptotic behavior at imaginary infinities from the above formula for the solution, but we can study that by an asymptotic expansion of the exact form of eq. (44). The function $\Lambda_\xi^-(z)$ behaves asymptotically as $\sim z^\xi$ at imaginary infinities, so the asymptotic version of the difference equation (47) reads

$$\bar{g}(z) = z^{-\xi}\bar{g}(z+\xi) \tag{49}$$

up to some irrelevant constant term. The asymptotic solution is then $\bar{g}(z) = \sigma_\xi(z)\Gamma(z)^\xi$. Multiplication by $\Gamma(-z/2)/\Gamma\left((z+d)/2\right)$ in defining $\bar{f}$ introduces a pole at $z = 0$, which takes care of the boundary condition. Then we have asymptotically $\bar{f}(z) \sim \sigma_\xi(z)e^{-\frac{\pi}{\xi}y}y^{(\xi-1)(x-1/2)}$, where $z = x+\imath y$. Fourier expansion of σ_ξ would then contain terms such as $\sin\left(\frac{2\pi}{\xi}nz\right)$, which would spoil integrability for $0 < \xi < 2$, unless $n = 0$. Therefore $\sigma_\xi(z)$ has to be a constant. We see now that the poles of $\bar{f}(z)$ occur for non-negative integers n at $z = \xi - 2 + 2k + \xi n$, $z = 2(k-1)$ (with $k > 0$) and at $z = a_k^- - \xi n$, where only the latter affects the large scale behavior. We draw the especially important conclusion that the small scale poles a_k^+ have no effect on the steady state existence problem. By looking at Fig. (2) we can see how the first few large scale poles a_k^- behave in various dimensions. In two dimensions the leading pole a_1^- is complex for all ξ, which implies that there is no steady state at all in the isotropic sector [24]. In three dimensions the poles a_1^- and a_2^- become complex at around $\xi_c \approx 0.345$. Similar behavior occurs with different ξ_c in higher dimensions, until at $d = 9$ the poles stay real for all $0 \leq \xi \leq 2$. We have plotted the value of ξ_c in Fig. (3) in dimensions $2 \ldots 9$ together with the magnetohydrodynamic case.

We should point out a worrying aspect about the strip of analyticity assumption, $-\xi < \mathcal{R}e(z) < 0$. By looking at Fig. (2), we see that for sufficiently large values of ξ the complex values leading exponents lie inside the strip. It is presently unclear to the author why this happens, and one is therefore forced to disregard the results corresponding to this situation. Nevertheless, below the critical ξ everything is under control, and we are still able to conclude the existence of the steady state below ξ_c

One important lesson of the present section is that the "complexification" hypothesis of [1, 9] is indeed an indication of instability of the flow, in the sense that the imaginary parts of

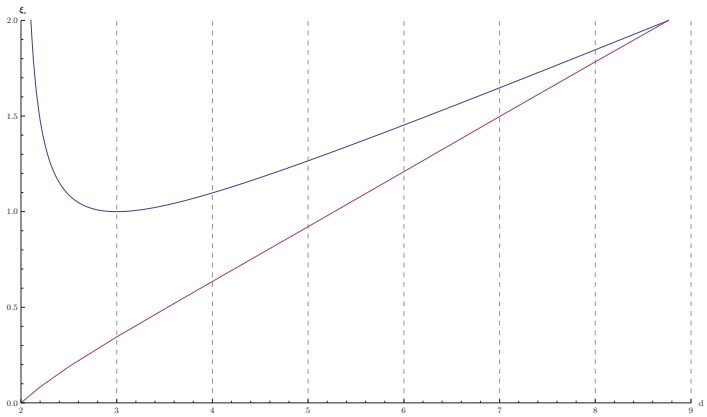

FIG. 3: A plot of the critical value ξ_c, above which the flow becomes unstable, versus the space dimension d. The upper curve refers to the magnetohydrodynamic case with $a = 1$ and the lower to the linearized Navier-Stokes case with $a = -1$.

the scaling exponents correspond to oscillations of the correlation function and are therefore responsible for the instability. The second lesson is that one only needs to be concerned with the *negative* zeros a_k^- of $\Lambda_\xi^a(z)$ when considering the stability problem, since they become the poles in the solution $\bar{f}(z)$. The positive zeros a_k^+ appear only as zeros in $\bar{f}(z)$.

V. ANISOTROPIC SECTORS OF LNS

The anisotropic sectors can be studied with the same methods as above. We will however refrain from performing the actual computations and simply extend what we have learned from the isotropic sector to the anisotropic case, namely that one simply needs to study the complexification of the negative poles of the solution $\bar{f}_a(z)$ (we now have a matrix equation). The role of Λ_ξ will now be taken by the determinant of the matrix in eq. (17), instead of just the $(1, 1)$ component. Since we already know that the flow is stable in the anisotropic sectors for $a = 1$ and $a = 0$ (see e.g. [4, 18]), we concentrate only on the $a = -1$ case in various dimensions. The anisotropic linearized Navier-Stokes exponents differ from the magnetohydrodynamic ones in that even if the leading exponent is real, the next to leading exponent may be complex valued, resulting in oscillating behavior at intermediate scales. These exponents however have no effect on the existence problem. This is because the

boundary condition at R tending to infinity can only be satisfied by the leading *oscillating* exponent. Suppose that at some ξ_c the leading exponent becomes real, but some subleading exponents are still complex. Decreasing ξ further cannot bring the nodes corresponding to the subleading exponents to R, since the large scale behavior is always dominated by the now real leading exponent as R tends to infinity. For finite R the situation might be completely different, although we do not consider that case here. We also need to make sure that the periodic function $\sigma_\xi(z)$ is again required to be a constant due to integrability, so that it will not cancel with any of the poles. This results from the fact that *all* matrix coefficients beside the (1,1) coefficient in eq. (19) behave asymptotically as $\sim z^\xi$ irrespectively of l [25], and therefore so does the determinant. Hence the same conclusions will be drawn as in the isotropic case, i.e. that σ_ξ is indeed a constant.

We have plotted some leading negative exponents in various anisotropic sectors in two and three dimensions in fig. (4). In two dimensions the leading anisotropic exponent is real, except (strangely enough) for $\xi \lesssim 0.15$. The anisotropic sectors are therefore quite stable in comparison to the completely unstable isotropic sector. In three dimensions the $l = 2$ anisotropic leading exponent becomes complex at $\xi_c^{(2)} \approx 0.937$ and all the higher sectors have purely real leading exponents. The anisotropic sectors are therefore much more stable in comparison to the isotropic sector critical value $\xi_c^{(0)} \approx 0.345$, somewhat similarly to the magnetohydrodynamic case. We also note that none of the poles lie inside the strip of analyticity, so the results should in fact be more reliable than in the isotropic sector. In dimensions $d \geq 4$ the anisotropic exponents are always real.

VI. CONCLUSION

The stability analysis of the passive vector models previously considered in a companion paper [1] was successfully completed. The critical value ξ_c below which the steady state exists was found in all dimensions, although the possibility of a steady state for an even larger region could not be excluded in the isotropic sector. The reason for flow unstability was show to be caused by the complexification of the largest negative pole of the solution, corresponding to large scale behavior of the correlation function. It was observed that in two dimensions the linearized Navier-Stokes problem is not stable for any ξ in the isotropic sector, but relatively stable in the anisotropic sectors. In three dimensions the isotropic

sector was observed to be stable for $\xi \lesssim 0.345$, the $l = 2$ anisotropic sector for $\xi \lesssim 0.937$ and higher anisotropic sectors for all ξ. In dimensions from four to eight, the isotropic sector is stable below the critical values plotted in Fig. (3) and the anisotropic sectors are stable for all ξ. In dimensions $d \geq 9$, all sectors are stable for all ξ. The results rely on the assumption of the strip of analyticity, which was required to make sense of the equations. At present time, it is not known to the author if such requirement can be proven.

Acknowledgments

The author wishes to thank P. Muratore-Ginanneschi and A. Kupiainen for useful discussions, suggestions and help on the matter. This work was supported by the Academy of Finland "*Centre of excellence in Analysis and Dynamics Research*" and TEKES project n. 40289/05 "*From Discrete to Continuous models for Multiphase Flows*".

---

[1] H. Arponen. Anomalous scaling and anisotropy in models of passively advected vector fields (to be published). *Phys. Rev. E*, 2009.

[2] Robert H. Kraichnan. Anomalous scaling of a randomly advected passive scalar. *Phys. Rev. Lett.*, 72(7):1016–1019, Feb 1994.

[3] L. Ts. Adzhemyan, N. V. Antonov, A. Mazzino, P. Muratore-Ginanneschi, and A. V. Runov. Pressure and intermittency in passive vector turbulence. *EPL (Europhysics Letters)*, 55(6):801–806, 2001.

[4] Itai Arad and Itamar Procaccia. Spectrum of anisotropic exponents in hydrodynamic systems with pressure. *Phys. Rev. E*, 63(5):056302, Apr 2001.

[5] L. Ts. Adzhemyan, N. V. Antonov, and A. V. Runov. Anomalous scaling, nonlocality, and anisotropy in a model of the passively advected vector field. *Phys. Rev. E*, 64(4):046310, Sep 2001.

[6] R. Benzi, L. Biferale, and F. Toschi. Universality in passively advected hydrodynamic fields: the case of a passive vector with pressure. *The European Physical Journal B*, 24:125, 2001.

[7] N. V. Antonov, Michal Hnatich, Juha Honkonen, and Marian Jurčišin. Turbulence with pressure: Anomalous scaling of a passive vector field. *Phys. Rev. E*, 68(4):046306, Oct 2003.

[8] L. Ts. Adzhemyan, N. V. Antonov, and A. V. Runov. Anomalous scaling, nonlocality, and anisotropy in a model of the passively advected vector field. *Phys. Rev. E*, 64(4):046310, Sep 2001.

[9] H. Arponen and P. Horvai. Dynamo effect in the kraichnan magnetohydrodynamic turbulence. *J. Stat. Phys.*, 129(2):205–239, Oct 2007.

[10] A. P. Kazantsev. Enhancement of a magnetic field by a conducting fluid flow. *Sov. Phys. JETP*, 26:1031, 1968.

[11] D. Vincenzi. The Kraichnan-Kazantsev dynamo. *J. Stat. Phys.*, 106(5–6):1073–1091, March 2002.

[12] M. Vergassola. Anomalous scaling for passively advected magnetic fields. *Phys. Rev. E*, 53(4):R3021–R3024, Apr 1996.

[13] I. Arad, L. Biferale, and I. Procaccia. Nonperturbative spectrum of anomalous scaling exponents in the anisotropic sectors of passively advected magnetic fields. *Phys. Rev. E*, 61(3):2654–2662, Mar 2000.

[14] N. V. Antonov, A. Lanotte, and A. Mazzino. Persistence of small-scale anisotropies and anomalous scaling in a model of magnetohydrodynamics turbulence. *Phys. Rev. E*, 61(6):6586–6605, Jun 2000.

[15] M. Hnatich, J. Honkonen, M. Jurcisin, A. Mazzino, and S. Sprinc. Anomalous scaling of passively advected magnetic field in the presence of strong anisotropy. *Physical Review E (Statistical, Nonlinear, and Soft Matter Physics)*, 71(6):066312, 2005.

[16] Alessandra Lanotte and Andrea Mazzino. Anisotropic nonperturbative zero modes for passively advected magnetic fields. *Phys. Rev. E*, 60(4):R3483–R3486, Oct 1999.

[17] N. V. Antonov, A. Lanotte, and A. Mazzino. Persistence of small-scale anisotropies and anomalous scaling in a model of magnetohydrodynamics turbulence. *Phys. Rev. E*, 61(6):6586–6605, Jun 2000.

[18] Itai Arad, Victor S. L'vov, and Itamar Procaccia. Correlation functions in isotropic and anisotropic turbulence: The role of the symmetry group. *Phys. Rev. E*, 59(6):6753–6765, Jun 1999.

[19] E. W. Barnes. The Linear Difference Equation of the First Order. *Proc. London Math. Soc.*, s2-2(1):438–469, 1905.

[20] M. Reed and B. Simon. *Methods of modern mathematical physics IV: Analysis of operators.*

Academic press, 1978.

[21] L. D. Landau. *Fluid Mechanics, 2nd. edition, Volume 6.* Elsevier, 1987.

[22] J.B. Conway. *Functions of one complex variable I.* Springer, 1978.

[23] At present time the author is unaware of a possible proof for the minimum width of the strip, except that minimum width of 2 is required for the formulae to make sense.

[24] The previous paper [1] by the present author failed to address this complex valued pole. This led to an incorrect hypothesis about the existence of the steady state

[25] This can easily be verified by studying the asymptotics of the matrix coefficients T^{ab} in appendix C of [1].

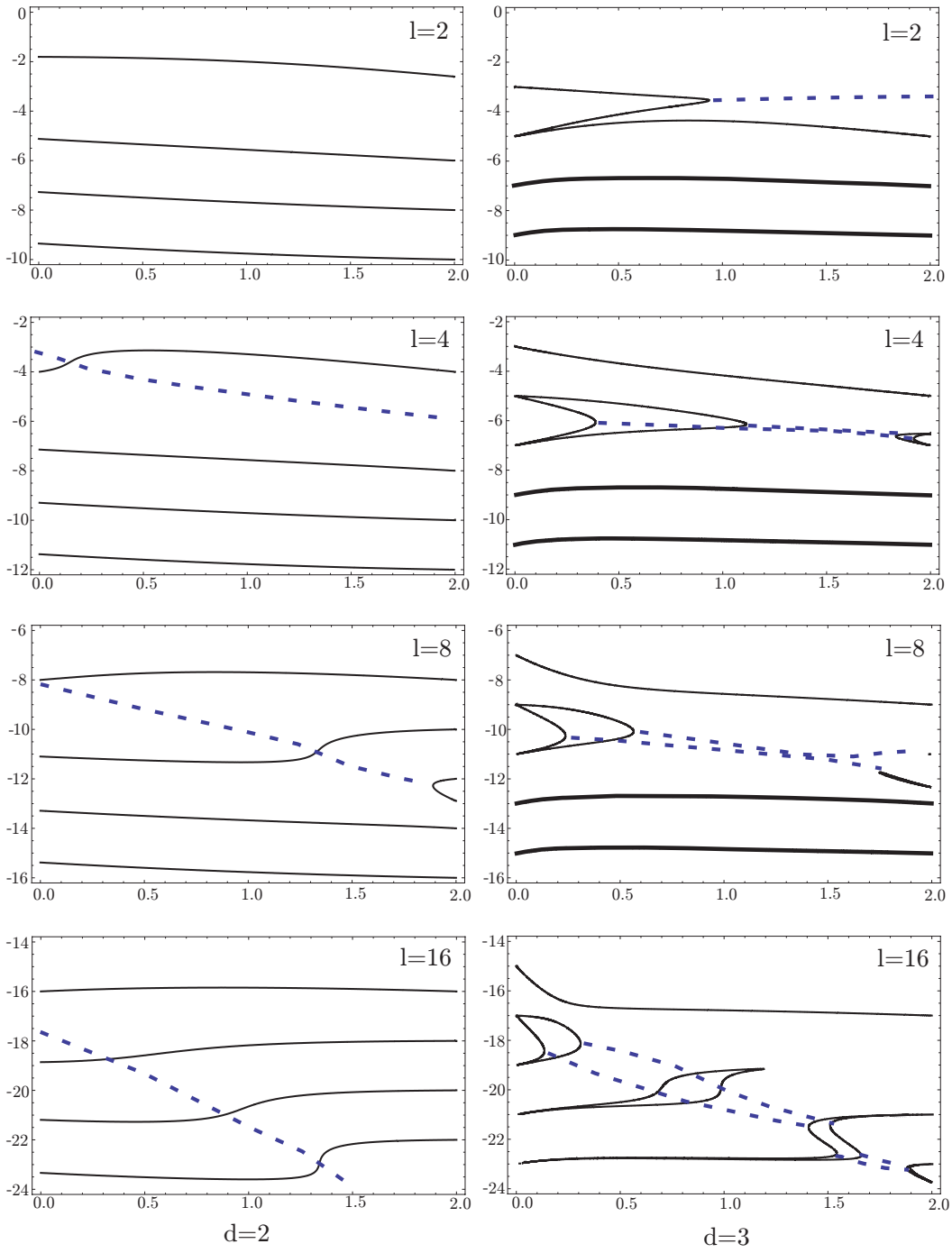

FIG. 4: A figure showing the leading large scale poles a_k^- in various anisotropic sectors in two and three dimensions. The dashed lines denote the real parts of complex valued poles. The thick curves denote two poles very close to each other. All the poles beyond what are shown here are real for $0 < \xi < 2$.